PAX7 DEFINES GERMLINE STEM CELLS IN THE ADULT TESTIS

APPROVED BY SUPERVISORY COMMITTEE

_____

Diego Castrillon, MD, PhD

_____

James Amatruda, MD, PhD

_____

F. Kent Hamra, PhD

_____

Andrew Zinn, MD, PhD

DEDICATION

To Rosalind Franklin.

PAX7 DEFINES GERMLINE STEM CELLS IN THE ADULT TESTIS

by

GINA M. ALOISIO

DISSERTATION

Presented to the Faculty of the Graduate School of Cancer Biology

The University of Texas Southwestern Medical Center at Dallas

In Partial Fulfillment of the Requirements

For the Degree of

DOCTOR OF PHILOSOPHY

The University of Texas Southwestern Medical Center at Dallas

Dallas, TX

May 8, 2015

ACKNOWLEDGMENTS

It is hard to list all the people who I want to thank. So many have had a positive impact on this project or have been a positive influence on me that this hardly seems like this thesis should be mine alone. First and foremost of course is Diego Castrillon. His support is tireless; his mentorship invaluable; and his patience endless. Its your guidance that took me from a naïve graduate student looking to cure cancer to where I am now, and started me on the path to who I'll become in the future. Your enthusiasm for knowledge is truly infectious, and I know you will continue to be the catalyst in the career of many young scientists.

My thesis committee also needs special thanks. Drs. Amatruda, Cleaver, Hamra, and Zinn, have been there for both scientific and life advice. What's more, I actually *enjoyed* my committee meetings. Not many graduate students can say that.

The Castrillon lab has always been a source of good science and good friends. In that vein, I would like to thank, Ileana Cuevas, Duygu Saatcioglu, Chris Peña, Qing Yun Mai, Yuji Nakada, Mohammad "Max" Ezzati, Jishnu Mukherjee, Eddie Tarnawa, Michael Baker, Ru Wu, and Meredith Goertz. The lab was always a great place to be, day or night, and I hope our paths will cross again soon.

I certainly would not be as sane as I am if it weren't for my friends. Thanks to Mariam Ashmawy, for bringing me food, Rachel Thomas for coffee breaks, Alex Ghaben for sectioning everything, Leila Zuo for making me be social, and Hema Manjunath for Tuesdays. That is not to forget contributions of George Wendt, Ying Li, Tom Morley, Ehsan Sayed, Barrett Updegraff, Laura Yuan, Pedro Salinas, Austin Reece, and Miles Black. Y'all best keep in touch. Last but certainly not least, I have

to thank my family for their love and support. Mom, you've been there for me on my highs and my lows. You have cheered me on when I am succeeding, and you've offered to "call up reviewer three and give him a piece of your mind." Dad, you've taught me to always have a backup plan, and to be self-sufficient, both of which have helped a great deal in graduate school. Finally, John, you have been a real source of inspiration. Follow your dreams and the rest will follow.

PAX7 DEFINES GERMLINE STEM CELLS IN THE ADULT TESTIS

GINA M. ALOISIO

The University of Texas Southwestern Medical Center at Dallas, 2015

DIEGO H. CASTRILLON, M.D., Ph.D.

ABSTRACT

Spermatogenesis is a complex, multistep process that maintains male fertility and is sustained by rare germline stem cells. Spermatogenic progression begins with spermatogonia, populations of which express distinct markers. The identity of the spermatogonial stem cell population in the undisturbed testis is controversial due to a lack of reliable and specific markers and a full understanding of spermatogonial stem cell biology. Here we identified the transcription factor Pax7 as a specific marker of a rare subpopulation of A_{single} spermatogonia in mice. $Pax7^{+}$ cells were present in the testis at birth. Compared with the adult testis, $Pax7^{+}$ cells constituted a much higher percentage of neonatal germ cells. Lineage tracing in healthy adult mice revealed that $Pax7^{+}$ spermatogonia self-maintained and produced expanding

clones that gave rise to mature spermatozoa. Interestingly, in mice subjected to chemotherapy and radiotherapy, treatments which damage the vast majority of germ cells and can result in sterility, Pax7^{+} spermatogonia selectively survived, and their subsequent expansion contributed to the recovery of spermatogenesis. Finally, Pax7^{+} spermatogonia were present in the testes of a diverse set of mammals. Our data indicate that the Pax7^{+} subset of A_{single} spermatogonia functions as robust testis stem cells that maintain fertility in normal spermatogenesis in healthy mice and mediate recovery after severe germline injury, such as occurs after cancer therapy.

TABLE OF CONTENTS

PRIOR PUBLICATIONS

Tarnawa ED, Baker MD, Aloisio GM, Carr BR, Castrillon DH (2013). Gonadal expression of Foxo1, but not Foxo3, is conserved in diverse Mammalian species. *Biology of Reproduction* 88(4):1-11.

Baker MD, Ezzati M, Aloisio GM, Tarnawa ED, Cuevas I, Nakada Y, Castrillon DH (2014). The small GTPase Rheb is required for spermatogenesis but not oogenesis. *Reproduction.* 147(5):615-25.

Aloisio GM, Nakada Y, Saatcioglu HD, Peña CG, Baker MD, Tarnawa ED, Mukherjee J, Manjunath H, Bugde A, Sengupta AL, Amatruda JF, Cuevas I, Hamra FK, Castrillon DH (2014). Pax7 expression defines germline stem cells in the adult testis. *Journal of Clinical Investigation* 124(9):3929-44.

LIST OF FIGURES

LIST OF TABLES

LIST OF ABBREVIATIONS

BSA: bovine serum albumin

BTB: blood-testis barrier

Bu: Busulfan

cKO: conditional knock out

cDNA: complementary deoxyribonucleic acid

CTX: chemotherapy

DMEM: Dulbecco's modified eagle's medium

DNA: deoxyribonucleic acid

dpc: days post-coitum

E: embryonic day

FBS: fetal bovine serum

FGF: fibroblast growth factor

FSH: follicle-stimulating hormone

GCNA: germ cell nuclear antigen

GDNF: glial-derived neurotrophic factor

GSC: germline stem cell

H&E: hematoxylin & eosin

IF: immunofluorescence

IGF2: insulin-like growth factor 2

IHC: immunohistochemistry

LCM: laser-capture microdissection

LH: luteinizing hormone

MEF: mouse embryonic fibroblast

PBS: phosphate buffered saline

PCR: polymerase chain reaction

PD: post-natal day

PFA: paraformaldehyde

pH3: phospho-histone H3

Plzf: promyelocytic leukemia zinc finger protein

PTEN: phosphatase and tensin homologue deleted on chromosome 10

RA: retinoic acid

RNA: ribonucleic acid

RT: Radiotherapy

Sall4: sal-like protein 4

SCF: stem cell factor

SFM: spermatogonial stem cell culture media

SSC: spermatogonial stem cell

Stra8: stimulated by retinoic acid gene 8

TAM: tamoxifen

TUNEL: terminal deoxynucleotidyl transferase dUTP nick end labeling

WT: wild-type

Introduction

The ultimate drivers of tissue regeneration—adult stem cells—lie are the crux of both normal tissue maintenance and disease. As cells are lost during normal growth and development, stem cells must both differentiate to replace the lost cell types, and divide to self-maintain, creating a precarious balance. If stem cells favor differentiation over self-maintenance, they will eventually become exhausted and disease will ensue due to loss of normal tissue. On the other hand, tipping the balance of stem cells towards self-maintenance could be harmful as well, in that insufficient numbers of differentiated cells would not allow for normal tissue function. In this vein, some cancers are thought to result from an exaggeration of stem cell self-renewal, resulting in a pileup of non-committed cells which can subsequently accumulate genetic mutations. Finally, after injury to an organ system, it is the adult stem cells which must expand to restore the tissue, and the extent to which resident stem cells of distinct tissues can divide and differentiate helps to determine how much regeneration can occur. Thus, adult stem cells play a significant role in tissue homeostasis as well as recovery from injury or disease.

Although the existence of adult stem cells is inferred in most tissues, the precise identity of these cells in many organs is not yet known. As such, though a testicular stem cell has long been implicated in the maintenance of male fertility, the identity of this cell has remained somewhat controversial. This thesis will describe to the identification of the testis stem cell by the protein marker Pax7, and then to describe the contribution of these cells to normal spermatogenesis as well as during injury to the germline.

CHAPTER 1: MALE REPRODUCTION

Organization of the testis

Spermatogenesis is necessary for the passage of genetic information from one generation to the next, and thus is essential to the evolution and survival of a species. The overall importance and complexity of this process is reflected in the organization of the testis, which can be divided into two parts: germ cells, and the somatic compartment consisting of Sertoli cells, and the interstitium, which consists of the Leydig cells, vasculature, and lymphatics (**Figure 1.1,** (1)). All of these parts must function together to maintain spermatogenesis, the process by which mature spermatozoa is formed.

The blood supply of the testis passes through the interstitium via many small coursing blood vessels, which do not penetrate the seminiferous tubules, but rather run alongside them amid interstitial Leydig cells. These vessels can be readily seen in cross sections through the testis. The interstitium also contains lymphatics, run alongside these testicular arteries and veins and eventually drain to the inguinal lymph nodes (1). Thus, the germline receives its oxygen supply via diffusion of molecules across the basement membrane. In fact, tight junctions between the cells inside the seminiferous tubules create the blood-testis-barrier (BTB), which prevents the passage of large molecules into the lumen of the tubules. Early in development, the immune system must learn how to recognize “self” from “not-self” to avoid an autoimmune reaction. However, since sperm are not made until after puberty, this immune tolerance, or learning to recognize “self”, has already occurred, leaving the possibility that circulating antibodies might react to normal spermatozoa. Thus, the BTB is essential to preserving the germline.

Also located in the interstitium are the Leydig cells, which are essential for male reproduction as they the source of local testosterone. Testosterone is both necessary for spermatogenesis as well as for the development of secondary sex characteristics. Leydig cells are located in the periphery of the seminiferous tubules, and can be identified in H&E stains by their eosinophilic cytoplasm (1). However, many of the fixation processes used to prepare tissue samples give rise to an artifact known as Leydig cell retraction, in which the cells seem to pull away from the tubules, whereas *in vivo* they are in direct contact. During testicular development, there are two distinct sets of Leydig cells, termed fetal and adult. Fetal Leydig cells are proliferative during embryonic development, but do not make testosterone and are eventually lost during adulthood. At the onset of puberty, adult Leydig cells under the influence of luteinizing hormone from the pituitary gland begin to make testosterone and other androgens, which serve as a major source of testosterone for the body (1).

The functional unit of the mammalian testis is the seminiferous tubule, which serves as the "home base" for the male germline, with the majority of cells in the testis being located here. These tubules are tightly wound; although one cross section through the testis may contain what appears to be hundreds of seminiferous tubules, estimates of the total number of tubules are 8-10 (2). All the tubules connect at the rete testis, an anastomosis between the epididymis and the testis, which serves as an emptying duct before mature sperm enter into the epididymis. Aiding mature sperm in their path to the epididymis are extratubular myoid cells, muscle-like cells which squeeze the tubules to force sperm along to the rete testis and also serve as trophic support, contributing to the overall levels of intratubular GDNF and other factors (**Figure 1.1**).

Though the seminiferous tubules are composed of mostly germline cells, the Sertoli cells are of upmost importance in maintaining male fertility. These cells are often called the “nurse cells” as they provide essential nutrients and growth factors for the germline, and dysfunction of these cells can completely ablate the germline. Sertoli cells also are interconnected via tight junctions to form the blood testis barrier discussed previously, which separates the germline into a basal (progenitor testis cells) and adluminal (more differentiated cells) compartment. Sertoli cells can then control the microenvironment of the most immature germline cells, located on the basement membrane. They also serve important roles in elimination of cellular debris (phagocytosis).

Prepubertal germline

Three distinct cell lineages are formed very early in embryonic development: the epiblast, from which the fetus will be derived, the trophoectoderm and the extraembryonic endoderm. Even at this early stage, formation of the germline is set in motion. A very small number, approximately 40-50, of the precursors to primordial germ cells, or PGCs, can first identified by their location in the early embryo at E6.0 (3, 4), even prior to gastrulation, or the formation of the gut tube. At E7.5, PGCs can be reliably identified by their expression of alkaline phosphatase and other factors, such as Fragilis and Stella (3, 5). At this time, PGCs, which express the cell surface tyrosine kinase Kit, begin their long and complicated migration under the influence of Kit ligand through first the primitive streak and then the hindgut to reach their final destination in the genital ridges at E11.0 (3, 4, 6). Once the cell has become resident in the genital ridges,

expression of the pan-germ cell marker GCNA begins (3). At this point, the PGCs begin to acquire sex-specific differences (7), and undergo extensive epigenetic reprogramming to lock in their fate as the precursors to sperm or oocytes (8). At e13.5 male PGCs begin to proliferate. At this time, they cease expression of alkaline phosphatase, and are termed gonocytes, or prospermatogonia (3, 9, 10).

As noted above, at e13.5 prospermatogonia divide to expand the germline. These cells that go from PGCs directly to mitosis are termed “M prospermatogonia” for multiplying prospermatogonia (10, 11). After mitosis, prospermatogonia enter two transitional stages, termed “T_1 prospermatagonia” and “T_2 prospermatagonia,” to demark how close a cell is to transitioning into mature spermatogonia (10, 11). M spermatogonia are mitotic and are located in the center of cords until about e16.5 (12), when they become T_1 spermatogonia. They then enter G0 arrest, until soon after birth, upon which mitosis is resumed. The germ cells migrate to the basement membrane and are termed T_2 prospermatagonia (3, 9, 12, 13). However, this summary belies the complexity of this process as these phases can overlap and exist concurrently, and histologic identification of the subtypes is difficult at best (9, 11). Many questions still remain as to the mechanisms which determine the on and off of how these cells divide. During neonatal development, germ cells migrate to the basement membrane so that by PD6, all germ cells are basal. At this point, prospermatogonia have completed the transition into spermatogonia.

Important differences have been noted in expression of prospermatogonial markers during neonatal development. For instance, Foxo1 is localized in the cytoplasm at birth, but relocates to being predominately nuclear during adulthood (14). Furthermore,

Oct4 is located only in a subset of prospermatogonia (15). Collectively, these differences point to distinct subsets of prospermatogonia, although these cells have historically been treated as a homogenous population. Additionally, since the very first wave of spermatogenesis is a separate program than subsequent rounds of spermatogenesis, it has been postulated that a certain subset of prospermatogonia are responsible for the first wave and do not self-renew. A second set of cells then consists of transit-amplifying cells, while a third set are the cells which are responsible for establishing the stem cell pool in the testis.

Spermatogenesis

Spermatogenesis is a dynamic process that serves to maintain male fertility throughout the life of the organism, producing mature spermatozoa from immature precursor cells, through a process of mitosis and meiosis. Classically, A_{single} spermatogonia have been identified as the earliest morphological precursor cells through careful histologic analyses (16, 17). Type A spermatogonia refers to small, oval cells located on the basement membrane with little to no visible heterochromatin. A_{single} spermatogonia divide, and through incomplete dissolution of cytokinetic bridges, form a pair of cells (A_{paired}) which are interconnected (**Figure 1.2**). A_{paired} cells divide to form chains of 4, 8 16, and sometimes 32 interconnected ($A_{aligned}$) cells. These bridges between cells serve as a primitive developmental history of an individual cell. Together, A_{single} through $A_{aligned}$ are termed undifferentiated spermatogonia.

There are few markers that are expressed in distinct subsets of undifferentiated spermatogonia. Id4, Erbb3, and Pax7 have been reported to be expressed in a subset of

A_{single} spermatogonia (18-20). To date, there are no proteins expressed specifically in A_{paired} or only $A_{aligned.}$ Markers that span multiple types of undifferentiated spermatogonia include Ret and Gfrα1, which form a heterodimer on the cell surface that acts as the receptor for the growth factor GDNF, and are expressed predominately in A_{single} and A_{paired} cells, with a few $A_{aligned.4}$ retaining expression. GDNF is essential for the survival of spermatogonia, and mutations in Ret cause infertility in the mouse (21). The forkhead transcription factor Foxo1 and the zinc finger transcription factor Plzf both mark all undifferentiated spermatogonia, and are required for normal SSC homeostasis (14, 22). Upon expression of kit, the cells are committed to differentiation, and are therefore called differentiating spermatogonia (A_{1-4}). These cells mature and without dividing, become Intermediate spermatogonia, with a moderate amount of visible heterochromatin, and then become Type B spermatogonia, which are easily identified by their condensed chromatin.

Type B spermatogonia divide to form primary spermatocytes, larger, round cells committed to meiosis. Primary spermatocyte staging refers to the five stages of prophase in which homologous recombination occurs. Preleptotene cells are the two daughter cells of Type B spermatogonia, and are the last stage in which cells reside on the basement membrane. Leptotene cells have condensed chromatin, but are unpaired. Pairing of chromosomes first occurs in the zygotene stage, and pairing is complete in the pachytene phase. Chromatin chiasmata appear in the diplotene phase, and the nuclear membrane breaks down in diakinesis. Primary spermatocytes progress through meiosis I, including metaphase, anaphase, and telophase to produce secondary spermatocytes, which proceed through meiosis II to form haploid spermatids. Spermatids undergo a huge structural

remodeling process to change from small round cells to mature spermatozoa, which are released in the tubular lumen.

Spermatogonial stem cells

Clearly the continued production of mature spermatozoa requires a testis stem cell to maintain cell numbers. However, the identity of this cell has been somewhat controversial. Using intracellular bridges between undifferentiated spermatogonia as a primitive lineage trace, some had postulated early on that all A_{single} spermatogonia could function as stem cells. The advent of spermatogonial stem cell transplantation allowed for more precise testing of the idea that spermatogonia were able to reconstitute spermatogenesis in an infertile recipient.

Transplantation is achieved by creating a single cell suspension of testicular cells and injecting them directly into the rete testis of a mouse which has been treated to eliminate endogenous spermatogenesis. Using this method, Nagano (23) et al demonstrated that only a fraction of A_{single} spermatogonia can function as stem cells via transplantation studies. SSC transplantation quickly became a method commonly employed to determine whether or not a cell could function as a stem cell, but this methodology still has not pinpointed the exact identity of stem cells in the testis. While new sorting strategies to enrich the portion of stem cells injected have demonstrated which cell fractions are likely to contain stem cells, the interpretation of such analyses is not usually straightforward. For example, although sorting spermatogonia by Kit cell surface expression has confirmed that Kit^{+} spermatogonia are not stem cells, and are committed to differentiation, a few

Kit$^+$ spermatogonia can in fact form function colonies in transplantation (24), calling into question whether transplantation tests stemness itself, or merely the potential for stemness. Furthermore, the markers used to sort cells for transplantation do not always carry over to the *in vivo* setting. Using Thy1$^+$ sorted cells, one can achieve a 30% enrichment of SSCs (18). However, locating Thy1$^+$ cells in sections and therefore identifying which cells can function as stem cells via transplantation has proven difficult. Moreover, it is unclear whether the harsh treatments used to create single cell suspension can affect the behavior of the cells themselves. Does breaking up an intercellular bridge between two A_{paired} cells create two new functional $A_{singles}$? Furthermore, elimination of endogenous spermatogenesis in the recipient mouse could increase the number of available "niches". The treatments used to sterilize recipient mice for transplantation are highly toxic to the germline, but also injure somatic cells (25). Therefore, the environment in which potential SSCs begin to engraft may not accurately reflect the environment in which they function as stem cells in the undisturbed testis.

Another assay to study SSCs is *in vitro* culture, as SSCs can be passaged continuously in the presence of GDNF and other growth factors. SSCs are grown in a mix of stem and non-stem cells on top of a feeder layer of mouse embryonic fibroblasts (MEFs). SSCs in culture have many of the same characteristics as they do *in vivo*. Cells uniformly express Gfrα1, Foxo1, and Plzf, which are exclusively expressed in undifferentiated spermatogonia, although some Kit expression has been detected via western blot (unpublished data, Castrillon lab). SSCs in culture form clusters which have intercellular bridges akin to the chains seen *in vitro*. It is

also known via transplantation that only a fraction of these cultured cells function as stem cells. Therefore, SSC cultures are thought to be a mix of stem, undifferentiated, and differentiating cells, although the media is not sufficient for spermatogonia to complete differentiation and these cells eventually die (26, 27). It is known that even in these cultures, RA can induce differentiation. Cells can also be genetically manipulated through lentivrial and shRNA knockdown as well as CRISPR (28, 29), and SSC lines can be derived from mice with distinct genetic backgrounds. Thus, SSC cultures can serve a good means to answer basic questions of stem cell maintenance and differentiation that may not be possible *in vivo.*

Although transplantation and SSC cultures are useful experimental tools, the precise identification of the SSC (i.e. *in vivo*) has been limited by the lack of reliable and specific markers. Many genes have been discovered to be essential for normal spermatogenesis, and some have even been implicated in the maintenance and/or differentiation of the SSC, but are expressed in all undifferentiated spermatogonia and thus are not restricted to the stem cell itself. At the start of this project, the most restricted marker known was Id4, expressed in A_{single} spermatogonia. Subsequently, Id4 was reported to be expressed in only a subset of A_{single} spermatogonia, demonstrating heterogeneity in this cell population. Knockout of Id4 moderately effected spermatogenesis, with more males becoming infertile over time than control animals (18). Using an Id4-GFP mouse, $Id4^{+}$ vs. $Id4^{-}$ cell were sorted and transplanted into recipient mice, and stem cell activity was almost exclusively contained in the $Id4^{+}$ fraction (26). While this remains a major advancement in the

field, many questions still exist as to the behavior of these cells. How do $Id4^+$ SSCs contribute to normal spermatogenesis? What is the role of these cells during injury?

Infertility during cancer treatment

Cancer therapy works by targeting highly proliferative cells, which clearly include cancer cells, but also organs with a high rate of turnover: skin, hair, gut, and the male germline. Male infertility after cancer therapy is a detrimental side effect that can affect a patient's life long after their cancer has been treated. For males, the current clinical practice is to use semen cryopreservation for assisted reproductive techniques, but this is not an option for young boys with cancer due to the lack of motile spermatozoa before the onset of puberty (30). After cessation of cancer treatment, fertility sometimes recovers—but not always—and infertility represents a potentially lifelong side effect (30, 31). Although most germ cells are ablated after cancer therapy, a few stem cells must survive in order to restore fertility. It is not known which cells survive through these toxic insults, nor the mechanisms by which they expand to repopulate the testis.

The recovery of spermatogenesis after cancer therapy has been previously studied in mouse models using busulfan, cyclophosphamide and radiation (32-34). Thus, good tools and model systems are available to answer these clinical questions. Busulfan, a.k.a. myleran, is an alkylating agent which is exquisitely toxic to the mouse germline (34). In fact, a single high dose of busulfan is sufficient to sterilize mice to prepare them as recipients for transplantation (35). Zohni et. al 2011 have demonstrated the extent of damage by three different single doses of busulfan of

15mg/kg, 30mg/kg or 45mg/kg and found that all three doses were sufficient to cause infertility, but the higher doses required a longer recovery period (36). Interestingly, most SSCs were lost within three days after treatment, underscoring how sensitive spermatogonia are to chemotherapeutics (36).

Although busulfan is well-suited for mouse models of infertility, it is not as commonly used in the clinic as cyclophosphamide. Cyclophosphamide is not as toxic to the germline in a single dose, and necessitates a multidose treatment to achieve a significant degree of germ cell toxicity. A 6 dose regimen of cyclophosphamide injections of 150mg/kg every 5 days eliminated nearly all differentiating cells, and the majority of tubules contained mainly Sertoli cells (32). However, most of the tubules recovered spermatogenesis after a long period (81 days), although some tubules still only contained Sertoli cells (32).

As in mouse models of infertility during chemotherapy, spermatogenesis usually recovers in male cancer patients. This poses a paradox: on the one hand, nearly all germ cells are ablated, but on the other, the recovery of fertility implies the existence of rare stem cells which serve to repopulate the testis. However, the identity of these cells is currently not known.

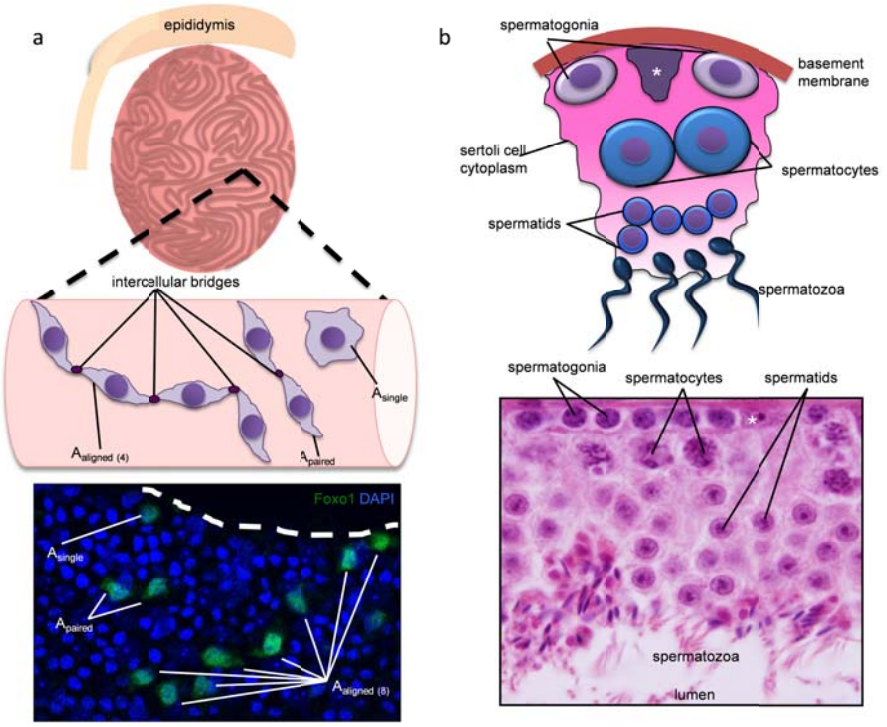

Figure 1.1: Schematic of the organization of the testis. (A) Tightly coiled seminiferous tubules make up the bulk of the testis, while the epididymis sits on top of the testis. Viewing one tubule in wholemount preparations demonstrates A_{single} spermatogonia, A_{paired}, which are connected by one intercellular bridge, and chains of $A_{aligned}$ spermatogonia from 4-16 cells in length. Below is a wholemount immunofluorescent stain using the antibody Foxo1 to delineate these undifferentiated spermatogonia. DAPI stains all cell nuclei. (B) Schematic of spermatogenesis in a cross-section of a seminiferous tubule, followed by H&E stain of the tubule, containing spermatogonia on the basement membrane, spermatocytes, spermatids, and mature spermatozoa in the tubular lumen. Asterisk indicates Sertoli cell nuclei.

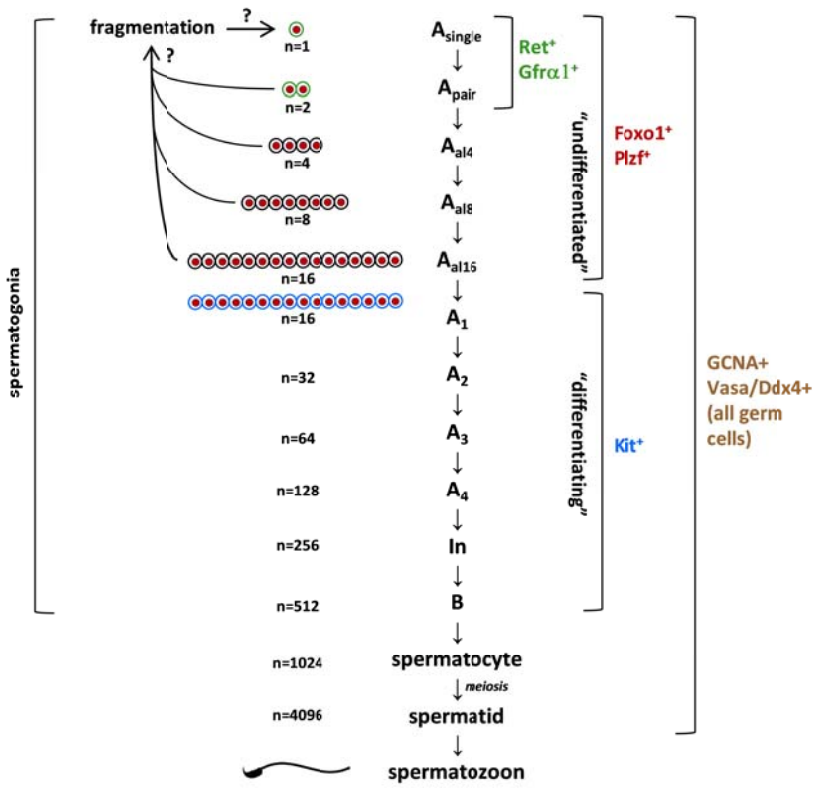

Figure 1.2: Overview of spermatogenesis. A_{single} spermatogonia are the morphological precursors of spermatogenesis. Subsequent cell divisions occur with incomplete cytokinesis, producing intercellular bridges. The number of interconnected cells in a chain serves as a record of the number of previous mitotic divisions. Ret and Gfrα1 are co-expressed in most A_{single} and A_{pair} spermatogonia. Further rounds of mitotic divisions produce longer chains of 4, 8, and 16 spermatogonia, collectively termed $A_{aligned}$. These chains can undergo fragmentation,

which may contribute to the pool of A_{single} spermatogonia, but this has not been formally established. A_{single} to $A_{aligned}$ cells are collectively called “undifferentiated” spermatogonia and express Foxo1 and Plzf. Kit+ spermatogonia (A_{1-4} to B) are termed “differentiating” spermatogonia. B spermatogonia become spermatocytes that initiate meiosis to produce round spermatids, which elongate and eventually are released as spermatozoa.

CHAPTER 2: Pax7 AND ITS ROLE IN SKELTAL MUSCLE SATELLITE CELLS

Introduction

Regeneration of skeletal muscle not only repairs damaged muscle fibers due to injury, but also helps remodel skeletal muscle after normal exercise, thus creating newer and stronger muscles. The resident adult stem cell of the muscle is the satellite cell, for its position alongside normal skeletal muscle nuclei at the periphery of myofibers. These cells, which represent a very small percentage, of adult skeletal muscle nuclei (approximately 5%) (37), lay dormant until muscle damage, when they become activated and divide to replenish lost muscle fibers. Markers of satellite cells include the transcription factors Pax7, which is expressed in all satellite cells, and Pax3, which is expressed only in a subset of these cells in certain muscle groups (38).

Organization of skeletal muscle

An individual muscle is made up of multiple, far-reaching muscle fibers, or myofibers, which can span long distances in the body. Myofibers are ensheathed in connective tissue called the epimysium. Within the epimysium are myofibers are grouped into fascicles, which are also ensheathed by the perimysium (1). The muscular blood supply, as well as nerve endings are also found within the perimysium (1). Myofibers are multinucleate cells which are formed early in development. In a cross-section of skeletal muscle, there are multiple myocyte nuclei, and the myofibers are ensheathed by the endomysium, also made of

connective tissue. The cytoplasm of myocytes is called the sarcoplasm, and the plasma membrane is the sarcolemma. The satellite cells are named such because of their position between the sarcolemma of muscle cells and the basal lamina. In H&E-stained sections, the nuclei of myofibers and satellite cells cannot be distinguished, but they can be identified by electron microscopy (39). Other cells that can be readily visualized in H&E sections include those that form the vasculature, by which $Pax7^+$ satellite cells tend to be located, and interstitial cells, which include connective tissue fibroblasts, which help support the basal lamina, nerve fibers, and cells with adipogenic potential. All in all, the interstitium is a source of important growth factors, which aid the muscle in regeneration after injury.

Pax7 during myogenesis

The Pax proteins are a family of nine transcription factors that function during early embryogenesis and play roles in development. Pax7 and Pax3 play roles in skeletal muscle development. One of the earliest steps in making muscle is the specification of somites, or segments of the embryo, which go on to become sclerotomes (bone), dermomyotomes (dermatomes and muscle), and sclerotomes (cartilage). The dermomytome expresses both Pax3 and Pax7 (40), and gives rise to mulipotent muscle progenitor cells, (MPCs), which are restricted to the muscle lineage, which give rise to myoblasts, which are highly proliferative and will go on to form the basis of skeletal muscle.

The formation of muscles in the trunk depends on both Pax3 and Pax7 (40). Without these two proteins, myogenic progression halts in embryonic development,

with practically a complete loss of muscle fibers observed by e11.5 (41). In late fetal development, Pax7 is expressed in most all of the myoblasts, but Pax3 expression starts to become more restricted. Pax3 and Pax7 expression levels fall throughout birth to adulthood such that by 6wks of age, Pax3 is very rarely expressed in satellite cells in the hindlimb muscles, expressed in approximately 50% of forelimb muscles, and is abundant in satellite cells in the diaphragm (42, 43). There are many different engineered mouse Pax3 mutants, all of which exhibit various degrees of skeletal muscle hypoplasia, and demonstrate a requirement for Pax3 in the development of the diaphragm (44). One of these mutants is a Pax3-Cre line, which does not encode a functional copy of the Pax3 gene. Homozygosing these mice results in defects early in embryogenesis, including neural tube deformities and cardiac abnormalities (45). Crossing these Pax3-Cre mice with a Cre reporter line showed that Pax3 derivatives contribute to skeletal muscle, the aorta, the kidneys, and some of the colonic epithelium. However, there were no Pax3 descendants in the testis, although the entire epididymis seemed to be labeled.

In a similar vein, the loss of Pax7 causes neonatal lethality in 90% of Pax7 null mice. Pax7 null mice are smaller than their littermates, and this size difference persists into adulthood in the surviving fraction (46, 47). It was originally thought that these mice have a complete loss of satellite cells suggesting a role of Pax7 during satellite cell specification (37), but further analysis demonstrated that in fact satellite cells are present at reduced numbers, and further decline during development, leading to hypothesis that Pax7 is involved in maintenance of satellite

cells (47). Using a Pax7 Cre line, Pax7-derived cells were detected in the skeletal muscle, eye, pancreas, gut, skin, olfactory system, and neural crest cells (48, 49).

In summary, Pax3 is required for embryonic myogenesis and is expressed mainly during embryogenesis but is down-regulated after birth in many satellite cells. On the other hand, Pax7 is not necessary during embryonic myogenesis but is indispensable in neonatal myogenesis. Thus these transcription factors play overlapping, but separate, roles in myogenesis (38).

The role of Pax7 in adult satellite cells

Adult satellite cells lie dormant until muscle injury, whereupon they are activated and begin to divide to replace lost muscle. In fact, satellite cells are indispensable for muscle regeneration. Using a tamoxifen-inducible Pax7-Cre crossed with a lox-stop-lox diphtheria toxin mouse, satellite cells can be completely ablated temporally. In the adult, loss of these cells in conjunction with injury with a myotoxin leads to complete absence of muscle repair. Furthermore, satellite cells from these mice can no longer engraft by transplantation (50). These findings were confirmed independently by the use of a diphtheria toxin receptor under the control of the Pax7 promoter. No muscle regeneration occurred over a period of 7wks, and the injured muscle was instead infiltrated by adipocytes. Even more striking was the finding that with strenuous exercise, the muscles fail to repair themselves, and get progressively smaller over time (51). Both sets of experiments concluded that Pax7+ satellite cells are absolutely required for muscle generation, and challenged other hypotheses that non-satellite cells could contribute to muscle repair (50, 51).

The role of Pax7 itself in muscle repair has been controversial. Initially it was reported that Pax7 was dispensable for muscle regeneration (52). Using a short pulse of tamoxifen, *Pax7* homozygous floxed (*f/f*); *Pax7 Cre ERT2* mice challenged with a myotoxin and muscle repair seemed to proceed as normally. In fact, using this same scheme, Pax3 and Pax7 were eliminated concurrently, again with no ill effects on muscle regeneration. However, when these same experiments were repeated with very young mice, loss of Pax7 resulted in a severe decrease in muscle regeneration. It was concluded from these results that Pax7 must only be important in juvenile muscle development and repair (52).

More recently, however, these same mice in the experiments above have yielded different results when exposed to a continuous source of tamoxifen. When examining histologic sections through *Pax7* $^{f/f}$*; Pax7-Cre* ^{ERT2} skeletal muscle treated with a short course of tamoxifen, an increase in infiltrating adipocytes was noted, suggesting that there was a partial phenotype in these mice. To explore this possibility, tamoxifen chow was used instead of the three dose intraperitoneal injection regimen. After myotoxic injury, there is significantly less regeneration of muscle when compared to control mice. This longer dose regimen is thought to prevent cells that do not have efficient Cre recombination ("escaper cells") from dividing and essential repopulating the tissue with normal satellite cells (53). These results have taken Pax7 from its previous status as merely a maker of satellite cells to a protein whose targets are essential to normal muscle function.

CHAPTER 3: MOUSE MODELS AND RELATED METHODS

A brief history of mouse models

The use of animals for medical research dates back even as far as the ancient Greeks (54). Breeding of *Mus musculus* for specific traits most likely had its origins in China, where selection for different color of fur or traits such as "waltzing" (spinning in circles) was popular with mouse enthusiasts (55). To ensure the heritability of the trait of interest, mice would be crossed to siblings multiple times, which caused the mice to be homozygous on nearly every loci on each chromosome (56). This trend of color and trait selection caught on in Victorian England, where "fancy" mice were bred as pets, and these mice can be traced back as the ancestors to inbred strains used in the laboratory today (55).

Even in the early 1900s, mice were being used as model organisms, a species which is increasingly being studied to gain biologic insights into human disease. The choice of mice seemed easy: they were small, easy to care for and house, were relatively short-lived and bred prolifically. Compared to other model organisms such as zebrafish or fruit flies, the mouse was more closely related to humans. In the beginning, scientists were limited by discovering a phenotype, and then working backward from there to understand the disease process. However, in the 1980s and 1990s, the transgenic mouse was born; a gene of interest could be inserted or deleted from a mouse, and the phenotype could be monitored over time (57). Thus, the fates of mice and men became intertwined in the world of biomedical research.

Mouse genetics and development

It takes approximately 19-21 days from fertilization to birth. At conception, a vaginal plug is formed, made of coagulated secretions from the male. The day the plug is discovered is termed embryonic day 0.5 (e0.5), and each day following is labeled accordingly. Thus, most mice (in our lab) give birth at e19.5. Once the pup is born, the nomenclature of the age changes from embryonic to postnatal, so that a three-day-old mouse pup is termed PD3 for postnatal day 3. For the purpose of this paper, a PD0.5 mouse is one that had just been delivered and had not yet nursed (no milk spot) and a PD1 mouse has a visible milk spot. For most experiments, mice are said to be sexually mature around 3-4 wks of age. However, spermatogenesis has two waves, the first having different properties than steady-state spermatogenesis. Therefore, for this thesis, mice are considered to be mature at 6 wks of age. The lifespan of a mouse in captivity is 1.5-3yrs, depending on the strain.

Mouse genetics has progressed a great deal from simple phenotypic analyses of inbred strains. Genetic manipulations can now create a dizzying array of new mice. Some terminology is described here. One of the first of these new manipulations was the transgenic mouse, in which a viral or bacterial vector expressing the gene of interest and a gene promoter and enhancer is injected into the developing fertilized mouse egg. The gene integrates into the DNA of the fertilized oocyte at a random chromosomal location typically in multiple tandem repeats. One disadvantage to this strategy is that any phenotype observed must be shown to be from the new gene, and not due to disruption of an existing gene during integration. A knockin mouse is a mouse in which DNA has been inserted into the

genome in a targeted fashion. A vector is made that contains the gene of interest with a promoter, flanked by DNA from the site of interest, which will integrate via homologous recombination. A knockout mouse is similar to a knockin, only instead of inserted a gene, an existing gene is deleted by removing essential exons.

Another development in mouse genetics is the advent of conditional gene modification. It was found that the bacteriophage recombinase, Cre, recombines DNA between two recognition sites, called LoxP sites. These are 34bp sequences, made of 13bp palindromes which flank an 8bp sequence that determines which direction the LoxP faces (58). If the LoxP are placed in a trans orientation on either side of a gene, the gene will be excised with Cre recombination. If they are placed in a cis orientation, the gene will be inverted. Mice expressing Cre in specific tissues can be engineered via knockin. The Cre mice can be crossed to mice expressing LoxP sites flanking the gene of interest (or *floxed*), the gene will be deleted only in those specific tissues. Furthermore, Cre expression can be controlled temporally by the fusion of an estrogen receptor, or Cre^{ERT2} (59). The Cre^{ERT2} is sequestered to the cytoplasm and cannot recombine DNA until addition of tamoxifen, which binds to the estrogen receptor and allows translocation to the nucleus and Cre-mediated excision.

In addition to temporal and tissue-specific deletion of genes, Cre and Cre^{ERT2} can be combined with Cre reporter lines, which express a "STOP" codon flanked by LoxP sites in front of an indelible marker protein. When a cell that has been through recombination divides, it will pass on the recombined allele to its daughter cell, creating a temporal history of the cell's divisions. This process, called lineage

tracing, can determine how cells contribute to the overall tissue over time. For example, Pax7 is expressed in muscle precursor cells. Using a Pax7-Cre crossed with a GFP reporter, it was found that all muscle cells were labeled, showing that the muscle derived from these $Pax7^{+}$ precursors (48).

A final mouse line using this *lox-stop-lox* technology is Dtx, in which the diphtheria toxin is knocked in to the mouse Rosa locus, a nearly ubiquitously expressed locus in the mouse that seems to have no real function. If this locus is interrupted by a reporter line or, in this case diphtheria toxin, mice develop normally, even if the line is homozygosed (60). Since mice do not have a functional diphtheria receptor, expression of the toxin results in the death only of those cells expressing Cre.

Different Cre lines used in this thesis

Germline specific Cre lines have been generated by the Castrillon lab to examine the function of proteins specifically in the testis and ovaries. Vasa is expressed specifically in the germline beginning at e12.5 in both the male and female germline (61). Although the expression of Vasa is specific, *Vasa-Cre* is sometimes ectopically expressed in the kidney and ear ((61). Since Vasa is expressed in the oocyte, when *Vasa-Cre* female mice are used for breeding, global recombination will occur in the embryo (maternal-effect recombination). Thus, male mice should be employed as the carriers of the Cre allele. A counterpart to *Vasa-Cre* is *Vasa-Cre^{ERT2}*, a tamoxifen inducible Cre line that is again expressed specifically in the germline (62). In the original paper, tamoxifen was delivered via I.P. injection

for three days, and this resulted in efficient induction of Cre (62). I also tested an alternative method of delivering tamoxifen to mice: in their food (tamoxifen chow) so that mice could be continuously fed tamoxifen over long periods. However, I found that while tamoxifen chow did in fact induce Cre via Rosa26R ß gal staining (discussed below), it was not as efficient as injecting tamoxifen (**Figure 3.1**).

A counterpart to *Vasa-Cre* is *Amh-Cre*, useful for conditional knockouts in Sertoli cells, where Amh is expressed. Anti-müllerian hormone is expressed in the Sertoli cells in male mice, and in the granulosa cells in females. Thus, *Amh-Cre* is specific for the cells which directly support the germline. Expression of Amh begins at e12.5, and persists into adulthood (63). Although initial reports showed high rates of recombination via Rosa26R ß gal staining (63), attempting to eliminate these cells with a *Dt* allele led to inefficient cell death, perhaps pointing to inefficiency in the *Dt* allele rather than the *Amh-Cre* (**Figure 3.2**).

Multiple *Pax7-Cre* lines have been generated, and all are freely available through Jackson Labs. These include *Pax7*$^{tm1(cre)Mrc}$/J (B6;129-*Pax7*$^{tm1(cre)Mrc}$/J, stock #010530) made by Mario Capecchi (64), and two tamoxifen inducible lines, *Pax7*$^{tm2.1(cre/ERT2)Fan}$/J (B6;129-*Pax7*$^{tm2.1(cre/ERT2)Fan}$/J, stock #012476) made by Chen-Ming Fan (52), and *Pax7*$^{tm1(cre/ERT2)Gaka}$/J (B6.Cg-*Pax7*$^{tm1(cre/ERT2)Gaka}$/J, stock #017763) made by Gabrielle Kardon (65). In all three lines Cre expression faithfully mirror Pax7 expression in both the testis and skeletal muscle, with varying degrees of recombination efficiency as determined with diverse Cre tester lines ((20), unpublished). *Pax7*$^{tm1(cre)Mrc}$/J was made by inserting an IRES-Cre cassette into the 3' UTR after exon 10. This does not interfere with normal function of Pax7, as mice can

be maintained as a homozygous stock (64). *Pax7*$^{tm1(cre)Mrc}$/J is about 70% efficient in Pax7^{+} spermatogonia at postnatal day 7 (unpublished data), with the tamoxifen-inducible lines being less efficient (**Figure 3.3**). The structure of the *Pax7*$^{tm2.1(cre/ERT2)Fan}$/J allele is a knockin of CreERT2 followed by an IRES-DsREd inserted into exon 1, creating a hypomorphic allele. Therefore, these mice must be maintained as a heterozygous stock as *Pax7* is an essential locus (90% of homozygous offspring die before puberty) (52). Although the *Pax7*$^{tm2.1(cre/ERT2)Fan}$ allele was designed for DSred expression in Pax7^{+} cells, the signal is not detectable via immunostaining nor by FACs, likely due to inefficient ribosomal entry at the IRES ((52), and personal observations). *Pax7*$^{tm1(cre/ERT2)Gaka}$/J, was made by inserting an IRES-CreERT2 cassette 8 bp downstream of the endogenous stop codon. The IRES in this line appears to function with much greater efficiency, and gives expression of functional Pax7 protein. Thus, the allele can be homozygosed.

Cre reporter strains

Several Cre reporter strains are attractive options for lineage tracing studies of SSCs. We have tested Rosa26 LacZ (*FVB.129S4(B6)-Gt(ROSA)26Sor*^{tm1Sor}*/J*, stock #003309,(66)), TdTomato (*B6.Cg-Gt(ROSA)26Sor*$^{tm9(CAG-tdTomato)Hze}$*/J*, stock #007909, (67)), and a membrane-bound Tomato, membrane-bound eGFP line (mT/mG, *Gt(ROSA)26Sor*$^{tm4(ACTB-tdTomato-EGFP)Luo}$*/J*, stock #007576, (68)). These three lines have each proven useful in distinct ways. For unknown reasons, β-galactosidase localizes to the chromatoid body within germ cells. Thus, when a β-galactosidase Cre reporter is used, care must be taken to interpret staining patterns within germ cells

(see (61) for description). When tubules are to be visualized following formalin fixation and embedding in paraffin, steps should be taken to minimize time in xylene, which dissolves the blue product (22, 61, 66); otherwise, the blue signal is stable and permanent, facilitating histologic analyses. Since the detection of the β-galactosidase requires a special staining process, it is not ideal for colocalization with other antibodies.

The second reporter, TdTomato, yields a very bright nuclear signal that lends itself well to FACS, and is preferred when IF will be performed simultaneously. Although the endogenous TdTomato signal is strong, it is subject to significant photobleaching during lengthy microscopy sessions. Therefore, we sometimes use a dsRed antibody (Living Colors, #632496, 1:100) to detect TdTomato when doing colocalizations. This dsRed antibody does not cross-react with GFP.

Finally, the mT/mG reporter clearly delineates cell borders, as the signal is localized to the cell membrane. The reporter is bright enough to detect endogenous fluorescence in wholemount preparation of tubules, as well as in OCT sections. Many investigators have reported difficulty in the localization of fluorescent reporter signals in frozen sections of diverse mouse tissues (69-71). On one hand, fixation and processing clearly can abolish reporter protein fluorescence. A wide variety of conditions have been blamed for this quenching of signal, from the fixation method to the mounting media (69-74). On the other hand, when unfixed tissues are cryosectioned, the fluorescent proteins readily diffuse from one labeled cell to non-labeled cells, obscuring specific signals and making visualization difficult if special steps are not taken (69). To detect endogenous fluorescence, we recommend (based

on (70)) cryosectioning unfixed tissues, allowing tissues to dry, then fixing 30 min in 4% formalin, 7% picric acid and 20% sucrose at 4°. For the best resolution of labeled clones in tissue sections, we fix testes in 10% neutral-buffered formalin, and perform IF as above using a GFP antibody (Aves, #GFP-1020, 1:500) or a dsRed antibody that detects the TdTomato protein (Living Colors, #632496, 1:100). Whereas some antibodies can cross-react with diverse fluorescent protein derivatives, these antibodies are especially useful because of their specificity to GFP and DsRed, respectively (68).

Floxed alleles

With the addition of Cre, floxed alleles allow for the spatial (and sometimes temporal) deletion of a gene. Most important to this thesis are the $Pax7^{f/f}$ alleles, of which there are two. *Pax7*$^{tm1.1Fan}$*/J* (called $Pax7^{f/f}$) has loxP sites on either side of exon 2, which could contribute to the formation of a truncated Pax7 protein, although we did not detect this protein by IF or IHC (See Chapters 5 and 6). *Pax7*$^{loxP\text{-}Gu}$, on the other hand, has loxP sites flanking the start transcriptional start site and the first three exons (75); thus, no Pax7 protein is formed. *Glis3*$^{f/f}$ mice were created by flanking exon 4 with loxP sites (76).

Mouse models of male infertility

While chemotherapeutics such as busulfan or irradiation can be highly toxic to the germline (See Chapter 1), certain genetic and surgical manipulations can also lead to the complete elimination of spermatogenesis. The pituitary gland, an

important source of hormones for the body, can be surgically removed, which eventually renders the mouse sterile as luteinizing hormone (LH) and follicle stimulating hormone (FSH) are no longer produced. In males, LH causes the Leydig cells to produce testosterone which is essential for spermatogenesis, and FSH which causes spermatocytes to under the first round of meiosis. Hypophysectomized mice (Hpa, Charles River) have a gradual loss of the germline, such that by 12wks after surgery, the testis is much smaller than before, as nearly the entire germline is ablated (See Chapter 6).

Another mouse model of male infertility used in this thesis is the Kit^{W}/Kit^{W-v} in which, in addition to a range of other abnormalities in other organ systems, the germline from differentiating spermatogonia onwards has been eliminated. Importantly, this allows access of transplanted spermatogonia to niches. Finally, there are three additional models of infertility used in this thesis that bear a quick review. $Pten^{f}$, $Pdk1^{f}$ and $Foxo1^{f}/3^{f}/4^{f}$ alleles were previously generated as described (62, 77, 78). $Foxo1^{f/f}$*;Vasa-Cre* mice have complete loss of sperm in the epididymis by 25wks of age (14). Even with this extreme phenotype, the appearance of tubules in cross section is somewhat variable, with the appearance of both seemingly normal and Sertoli cell only tubules at PD21 (14). With the triple conditional knockout of $Foxo1^{f/f}/3^{f/f}/4^{f/f}$*;Vasa-Cre* mice, the phenotype become more severe, with no normal tubules at PD21, with a few tubules having a small number of germ cells on the basement membrane (14). With the cKO of Pten, 80% of tubules are empty by 4wk, and with the cKO of Pdk1, nearly all germ cells are lost by PD14 (14).

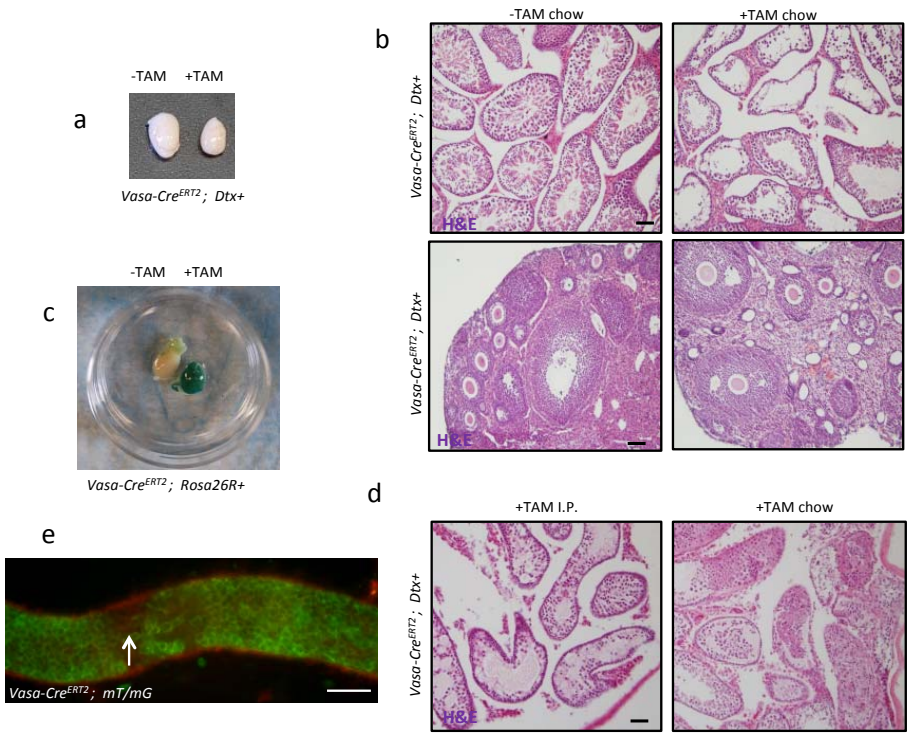

Figure 3.1: Delivery of tamoxifen in chow vs. intraperitoneal injection. a) *Vasa-Cre* ^{ERT2} *Dt*$^{+}$ testis, with and without tamoxifen injection. After delivery of tamoxifen via chow, some, but not all, germ cells are ablated. b) Histology of *Vasa-Cre* ^{ERT2} *Dt*$^{+}$ testes and ovaries with and without tamoxifen chow. While some germ cells are ablated, many still remain. c) Tamoxifen chow is sufficient to induce Cre recombination in *Vasa-Cre* ^{ERT2} *Rosa26R*$^{+}$ testes, suggesting that the fact that germ cells still remain in the *Dt* experiment could be a compound issue between chow and the *Dt* allele itself. d) Comparison of *Vasa-Cre* ^{ERT2} *Dt*$^{+}$ testes delivered tamoxifen via chow or via intraperitoneal (IP) injection. IP injection causes the ablation of far more germ cells than tamoxifen chow, though this ablation is still not 100%, suggesting that the *Dt* allele is could not be functioning properly. e) A seminiferous

tubule from *Vasa-Cre* ^{ERT2} *mT/mG*$^{+}$ testes, demonstrating that IP tamoxifen is highly efficient at inducing *Vasa-Cre* ^{ERT2} and further arguing that the *Dt* allele does not function properly in the testis. It is important to note that even IP injection is not 100% efficient, indicated by the lack of recombination (arrow). Scale bar = 50μm.

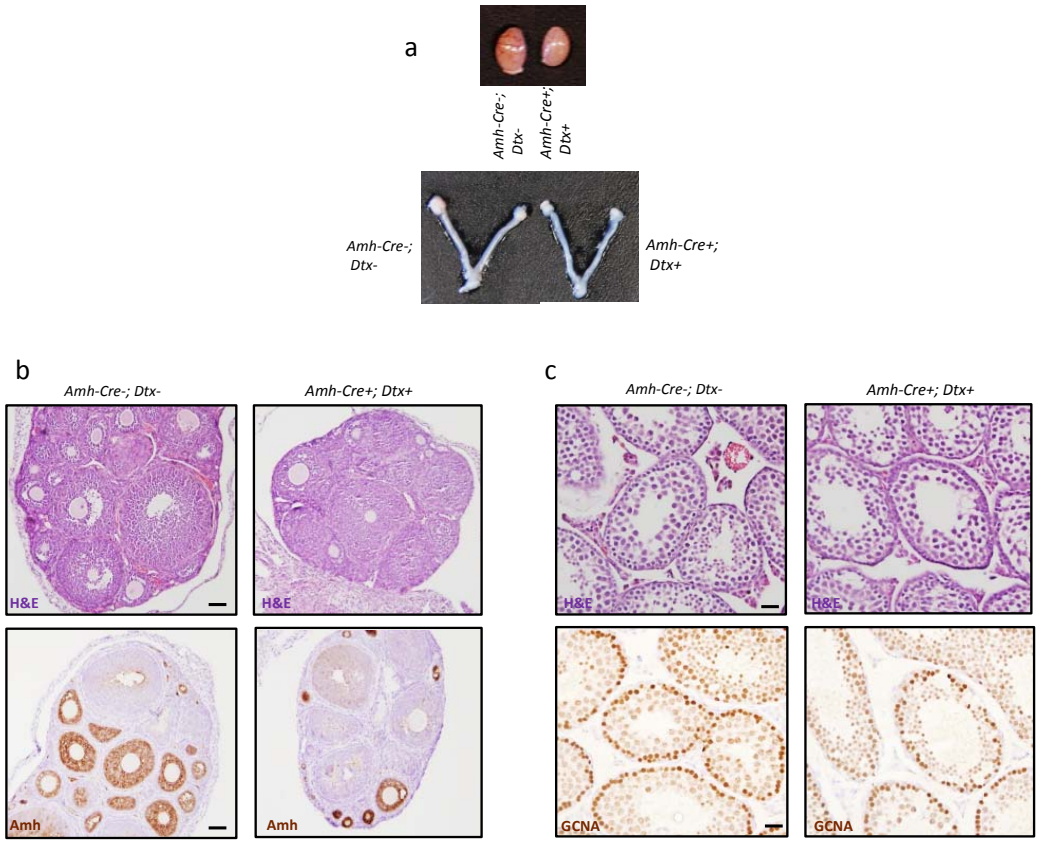

Figure 3.2: Activation of a diphtheria toxin conditional allele does not effectively eliminate Sertoli and granulosa cells. Using *Amh-Cre Dt*$^{+}$ mice, gonads were examined to determine the effect of loss of the Sertoli and granulosa cells in the testis and ovaries, respectively. (A) There was no significant difference between the sizes of the testes, ovaries, or uteri of *Amh-Cre Dt*$^{+}$ and *Amh-Cre Dt*$^{-}$ animals at 3wks. (B) Histologic examination of *Amh-Cre Dt*$^{+}$ and *Amh-Cre Dt*$^{-}$ ovaries by H&E demonstrated what appeared to be granulosa cells still present. This was confirmed by staining with Amh. Although there appeared to be fewer granulosa cells in the *Amh-Cre Dt*$^{+}$ animals, granulosa cells still remained, again suggesting that the *Dt* allele does not function properly in the gonads. (C) Histologic examination of *Amh-Cre Dt*$^{+}$ and *Amh-Cre Dt*$^{-}$ testes demonstrated relatively normal spermatogenesis at

3wks. Furthermore, GCNA staining confirmed the presence of numerous germ cells, which need functional Sertoli cells to survive. Scale bar = 50μm.

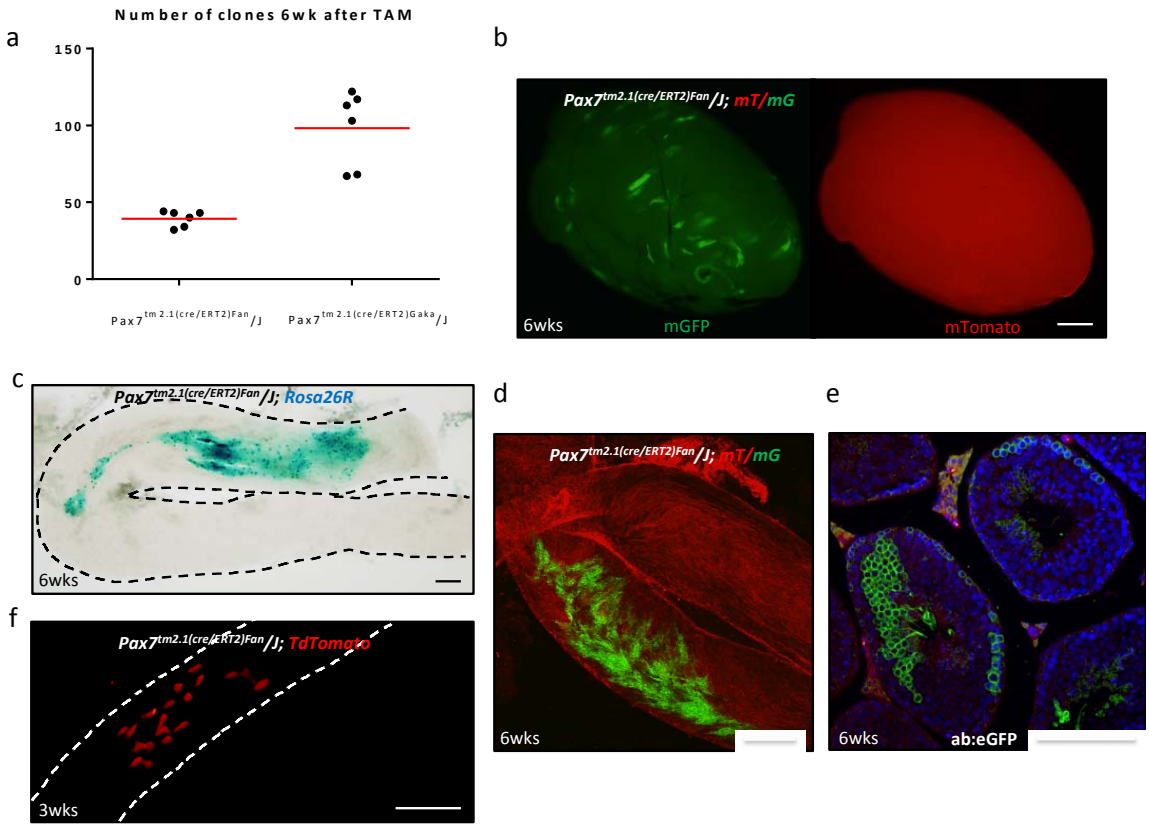

Figure 3.3: Comparison of Pax7-Cre lines. (A) Number of labeled clones 6wks after tamoxifen administration in the two CreERT2 lines. Mice were administered 2mg tamoxifen daily for 3 days at 6wks of age and aged for an additional 6wks.*The* *Pax7*$^{tm2.1(cre/ERT2)Fan}$*/J* allele had fewer labeled clones than the *Pax7*$^{tm2.1(cre/ERT2)Gaka}$*/J*, demonstrating that the latter has a higher efficiency in the germline. (B) Whole testis of a *Pax7*$^{tm2.1(cre/ERT2)Fan}$*/J; mT/mG* mouse, showing large labeled clones on the green channel, and broader (but mutually exclusive) expression on the red channel. (C) Seminiferous tubule from a *Pax7*$^{tm2.1(cre/ERT2)Fan}$*/J; Rosa26R* mouse, showing dot-like localization of β-galactosidase. Note that at this magnification, chromatoid bodies cannot be clearly resolved, but almost all of the signal within the germ cell

cytoplasm localizes to this structure. (D) Single seminiferous tubule from *Pax7*$^{tm2.1(cre/ERT2)Fan}$*/J; mT/mG* mouse, as viewed on a confocal microscope. Signal is endogenous fluorescence. (E) Testis of a *Pax7*$^{tm2.1(cre/ERT2)Fan}$*/J; mT/mG* mouse in cross-section. Individual labeled cells can be readily identified as to cell type based on cellular morphology and location. Endogenous reporter protein fluorescence can be quenched upon fixation; indirect immunofluorescence is a viable alternative. (F) Seminiferous tubule from *Pax7*$^{tm2.1(cre/ERT2)Fan}$*/J; TdTomato* mouse, showing strong endogenous nuclear signal. Tubules were isolated 6wks after tamoxifen administration except (F) 3wks after tamoxifen. Scale bars = 500μm (B) and 100μm (C) (D) (E) (F).

CHAPTER 4: METHODS

mRNA analysis and Pax7 discovery

RNA preparation, microarray hybridization, normalization, quality control, and digital Northern analysis was performed as described previously (24). Additional data sets included in this analysis were intact PD2 testes and cultured SSCs established as previously described (61), both from FVB/n mice. The embryonic stem cell, embryonic gonad, and spermatogenic cell data sets were downloaded from GEO (accession nos. GSE4193, GSE4308, and GSE6916) (62–64). Probe sets were ranked based on signal strength in SSCs as a proportion of that in the intact adult testis.

Mouse strains and procedures

Mice harboring the *Pax7-CreERT2* [B6;129-*Pax7*$^{tm2.1(cre/ERT2)Fan}$/J], *Pax7*$^{tm1(cre)Mrc}$/J B6;129-Pax7$^{tm1(cre)Mrc}$/J , and *Pax7*^{fl} [B6;129-*Pax7*$^{tm1.1Fan}$/J] and *Pax7*$^{loxP\text{-}Gu}$ alleles as well as the *R26R* [FVB.129S4(B6)-*Gt(ROSA)*^{26Sortm1Sor}/J], *mT/mG* (tdTomato/eGFP) reporter [*Gt(ROSA)26Sor*$^{tm4(ACTB–tdTomato,–EGFP)Luo}$/J], diphtheria toxin receptor B6;129-*Gt(ROSA)26Sor*$^{tm1(DTA)Mrc}$/J, *Amh-Cre*, 129S.FVB-Tg(Amh-cre)^{8815Reb}/J and nuclear tdTomato reporter [B6.Cg-*Gt(ROSA)26Sor*$^{tm9(CAG–tdTomato)Hze}$/J] alleles were purchased from Jackson Laboratories (31–33, 35). *Glis3*$^{f/f}$ mice were obtained from L. Chan (76).

Busulfan (CAS no. 55-98-1, TCI America) was dissolved in DMSO and administered as a single IP dose. EdU (catalog no. C10338, Invitrogen) was

dissolved in water and injected IP (50 mg/kg). Cyclophosphamide was dissolved in PBS and administered at 150 mg/kg IP every 5 days for 25 days. Tamoxifen (catalog no. T5648, Sigma-Aldrich) was dissolved at 100 mg/ml in 100% ethanol, then resuspended at 20 mg/ml in corn oil. 2 mg tamoxifen was delivered IP to each adult mouse daily for 3 days. Neonatal mice (PD5 or earlier) were injected IP with 0.2 mg tamoxifen daily for 3 days. Whole-body irradiation was administered (single dose) while the mice were restrained in acrylic boxes at a dose rate of 1.44 Gy/min. No specific method for randomization for animal studies was used; investigators were not blinded.

Transplantation procedure

2 testes from 1 *Pax7-CreERT2; tdTomato* (PD14) donor (mixed genetic background) were enzymatically digested with dispase (catalog no. 354235, BD) to obtain single cells that were resuspended in DMEM with 10% FBS plus 0.02% Trypan Blue (25). 5–10 μl of 9 × 103 cells/μl were transplanted by the efferent duct method into testes of 3 *KitW/KitW–v* mice (4–6 weeks old, mixed genetic background; stock no. 100410, Jackson Laboratories). Testis filling per blue dye was 50%–90% in each testis. To deplete T cells and promote engraftment, 50 μg anti-CD4 antigen (catalog no. MAB554, R&D Systems) was injected IP 3 times every other day starting on the day of transplantation. Testes were analyzed 4 weeks after transplantation.

Tissue processing, immunohistochemistry, and immunofluorescence

For IHC, tissues were fixed in 10% buffered formalin overnight, embedded in paraffin, and cut into 5-μm sections (except for the serial analysis of an entire testis and Pax7 cluster analyses, where 20-μm sections were used), with indirect detection performed as described previously (27). For whole-mount IF, seminiferous tubules were mechanically dissociated in PBS on ice and fixed overnight in 4% paraformaldehyde (PFA). Tubules were dehydrated in a series of methanol washes and stored at –20°C. To rehydrate and permeabilize, tubules were put through a series of washes with methanol and PBS plus 0.1% Tween-20, followed by incubation with 0.2% NP-40 for IF of nuclear proteins. Tubules were blocked in 2% BSA and PBS (catalog no. 37525, Thermo Scientific Blocker) for 2 hours, then in MOM block (catalog no. MKB-2213, Vector Labs), and primary antibody was added in 0.5% BSA and PBS with 0.02% sodium azide, followed by incubation at 4°C overnight. Tubules were washed 3 times for 10 minutes each in PBS at RT. Secondary antibody (Alexa Fluor 555 anti-rabbit, Alexa Fluor 488 anti-mouse, Alexa Fluor 555 anti-goat; catalog nos. A-21428, A-21121, and A-21432, respectively, Invitrogen) was added at 1:1,000 in 0.5% BSA and PBS for 2 hours at RT followed by DAPI staining (1:10,000 in PBS; catalog no. 46290, Pierce). Tubules were placed on glass slides and mounted in Vectashield (Vector Laboratories). For visualization of *mT/mG* clones in tissue sections, testes were embedded in OCT; sectioned; fixed for 30 minutes in 4% formalin, 7% picric acid, 20% and sucrose at 4°C; and then cryosectioned. Microscopy was performed with a Leica TCS SP5 confocal microscope.

Antibodies for IF and IHC

Antibodies and titers used were as follows: Pax7 (1:200 for IHC, 1:25 for IF; Developmental Studies Hybridoma Bank), Foxo1 (1:200 for IHC, 1:50 for IF; catalog no. 2880, Cell Signaling Technology), Kit (1:200 for IHC, 1:50 for IF; catalog no. 3074, Cell Signaling Technology), Plzf (1:10,000 for IHC; catalog no. AF2944, R&D Systems), caspase-3 (1:250 for IF; catalog no. 559565, BD Biosciences — Pharmingen), DSred (detects tdTomato; 1:100 for IF; catalog no. 632496, Clontech), GCNA (1:200 for IHC; provided by G.C. Enders, University of Kansas, Kansas City, Kansas, USA; ref. 39), Ret (1:20 for IHC; catalog no. 18121, IBL America), Gfrα1 (1:100 for IF; catalog no. AF560, R&D Systems), LDB1 (1:10,000 IHC, 1:1000 IF, Epitomics, #S2318), ERG (1:100 IHC, 1:100 IF, Epitomics #2849-1), MATR3 (1:100 IHC, Abcam, ab53748). IGF2BP1 (1:100 IHC, 1:100 IF, MBL #RN001M), CRABP1 (IHC 1:100, Genetex #85869), CCND3 (1:800 IHC, 1:100 IF, Cell Signaling, #DCS22) NMT2 (1:10,000 IHC, 1:1000 IF Santa Cruz, H-45) VASA (1:10,000 IHC, Abcam, ab13840) PHOSPHO-H3 (Cell Signaling #9706S; 1:100 IF), CLEAVED CASPASE -3 (1:1000 IHC, 1:200 IF, Cell Signaling #9664), ID4 (1:100 IHC 3 hr RT, 1:50 IF, Santa Cruz, L-20). For an example of Pax7 staining, see **Figure 4.1**.

X-gal staining

Whole-mount X-gal staining was performed by manually dissociating tubules, fixing in 4% PFA and PBS for 30 minutes at RT, and staining as previously described (43) for 6 hours to overnight, followed by refixing in 4% PFA and PBS overnight.

Epitope mapping and phylogenetic analyses

An arrayed microchip was designed by LC Sciences as described previously (65). The chip included 12-mer tiling peptides sequences with 1-aa resolution corresponding to the entire chicken polypeptide immunogen (aa 300–523; Genbank NP_990396.1). The corresponding mouse aa sequence was also arrayed on the same microchip, also at 1-aa resolution. Peptide sequences were acetyl-capped at the N terminus. Pax7 antibody (1 μg/ml) was hybridized to the microarray in 1× PBS 7.4 for 2 hours at 4°C, then washed in 1× PBS with 0.05% Tween-20 and 0.05% TritonX-100, pH 7.0. Detection was performed with an anti-mouse IgG/Alexa Fluor 647 conjugate (10 ng/ml) in binding buffer for 1 hour at 4°C. The array was scanned at 635 nm on an Axon GenePix 4000B Microarray Scanner. Sequences were obtained from NCBI (HomoloGene 55665 and accession nos. XP_003989659.1, XP_003891265.1, and XP_003428482.1) and manually aligned. Gonadal samples were described previously (45).

Western blotting

For the blocking experiment, a 22-residue blocking peptide PSAVPPQPQADFSISPLHGGLD, spanning the 10-aa epitope, was synthesized. The peptide (0.1 μg/μl) and antibody (20 ng/μl) were incubated at 4°C for 24 hours in 500 μl PBS, then centrifuged at 4°C for 15 minutes (11,525 *g*). The supernatants with and without blocking peptide (500 μl) were added to 2.5 ml 5% milk 1× TBST and applied to the Western blots.

Spermatogonial stem cell cultures

SSC cultures from neonatal mouse testes were derived as previously described (79). Testes were dissected from DBA2 and mixed strain mice at PD7-14 and digested with dispase (BD Biosciences, 354235) at 37° C for 28min until visibly disassociated. After centrifugation, the tissue was washed with DMEM/F12 and resuspended in SF medium (recipe outlined in **Table 4.1**), and plated onto irradiated MEF feeder cells. Established SSC cultures were fed with SF medium every two days, and continually passaged onto fresh feeder cells.

To prepare gelatin-coated plates, a 0.2% gelatin solution was made with type A gelatin from porcine skin (Sigma, G-1890) and water, and then autoclaved and stored at 4°C. To coat tissue culture plates, solution was added and plates were incubated at 32°C for at least 30min. Solution was then removed and plates were washed with D-PBS before use.

Statistics

Statistics were calculated using GraphPad software. Error bars in all figures indicate SEM for at least 3 animals/replicates unless otherwise indicated. For Fisher exact tests, 2-tailed comparisons were performed to calculate *P* values. A *P* value less than 0.05 was considered significant.

Study approval

This study was approved by the UT Southwestern Institutional Animal Care and Use Committee.

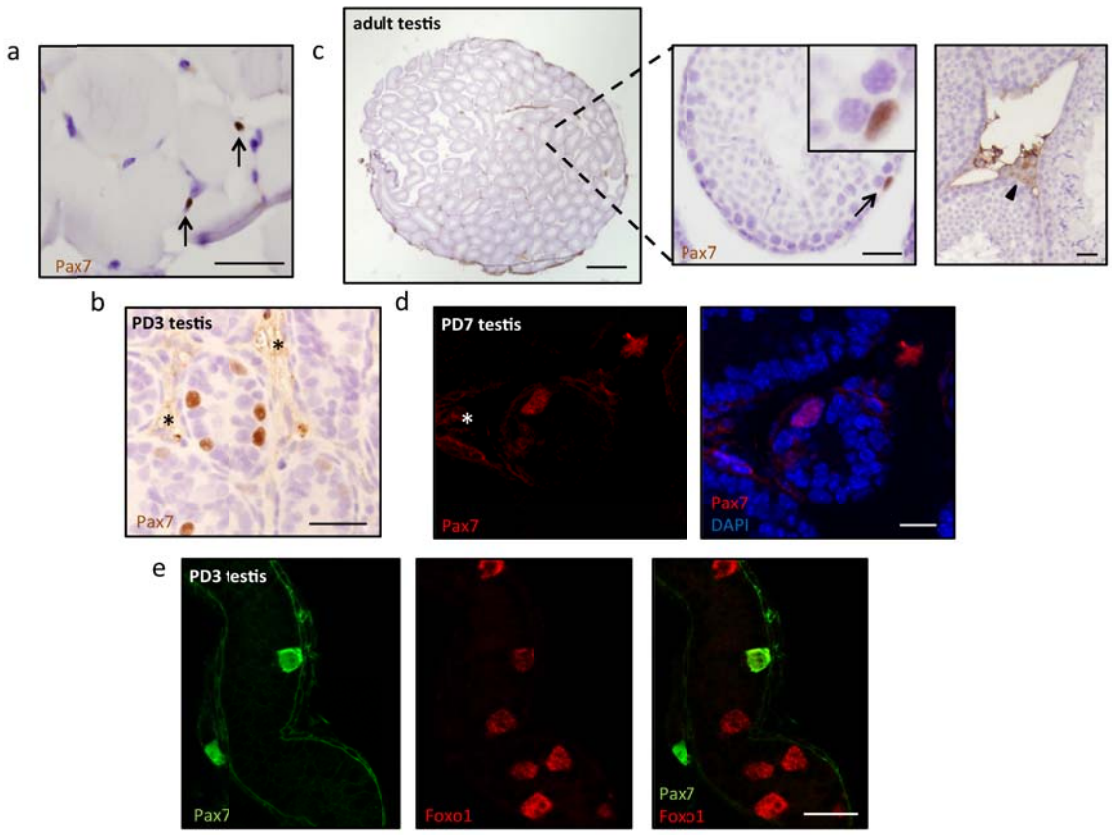

Figure 4.1: Methods of detecting Pax7 in the mouse testis. (A) Pax7 IHC of adult skeletal muscle. Pax7⁺ satellite cells are located beneath the basal lamina, and make up approximately 5% of adult skeletal muscle nuclei (37). (B) Pax7⁺ germ cells in the PD3 testis are relatively abundant. The staining is nuclear, and these cells make up approximately 25% of the germline at this timepoint (20). Note the non-specific staining of the interstitium, but lack of non-specific staining within tubules. Asterisk denotes non-specific staining of Leydig cells. (C) A complete cross-section of adult testis, stained for Pax7, and inset showing a single Pax7⁺ SSC within a tubule. Again, there is non-specific staining within the interstitium, but not within the seminiferous tubules. Inset shows specific nuclear staining of Pax7. In formalin-fixed testes, retraction artifact due to dehydration of tubules leads to separation of

tubules in the ensuing sections (asterisk); however, this does not affect interpretation of immunostaining. (D) Pax7 IF on formalin-fixed paraffin embedded tissues of PD7 testis. Some background staining is apparent with Pax7 IF. Again, the tubule interiors are free of background staining. (E) Wholemount immunofluorescence of Pax7 and Foxo1 in the PD3 testis. Pax7 stains only a fraction of germ cells at this timepoint. In wholemount immunofluorescence, the non-specific staining of the basement membrane is again apparent. A second cell stains positive for Pax7 in the adjacent tubule, slightly out of focus. Scale bars = 25μm for all figures except 100μm for (B) adult testis.

Table 4.1 Base media: StemPro34 SFM Base

Additional components	**Concentration**
Bovine Serum Albumin	5mg/mL
d- (+) glucose	6mg/mL
L-glutamine	2mM
100X Antibiotic-antimycotic	1X
100X MEM vitamins	1X
100X Non-essential amino acids	1X
d-Biotin	10µg/mL
Insulin	25µg/mL
Pyruvic acid, sodium salt	30µg/mL
dl-Lactic acid (60% solution)	0.06%
Ascorbic acid	100µM
Sodium selenite	30nM
Putrescine	60µM
Bovine Apo-transferin	100µg/mL
Progesterone	60ng/mL
β-estradiol 17-cypionate	30ng/mL
2-Mercaptoethanol	10µM
ESGRO	10^3 U/mL
Recombinant mouse EGF	20ng/mL
Recombinant human basic FGF	10ng/mL
Recombinant rat GDNF	15ng/mL
40x StemPro34 nutrient supplement	1X
Fetal bovine serum	1%

CHAPTER 5: DISCOVERING MARKERS OF SPERMATOGONIAL STEM CELLS

Introduction

To discover novel markers of spermatogonial stem cells, we employed an mRNA based screen that had been previous utilized to discover proteins specific to oogonia (80). This previous strategy compared the differential expression of proteins in oocyte populations separated by laser capture micro-dissection. In addition to these samples, we prepared adult testis, neonatal, and embryonic testis isolates. To examine proteins differentially expressed in distinct spermatogenic subsets, we utilized datasets available through the Gene Expression Omnibus (GEO). Several useful profiles consisted of distinct subtypes of cells were isolated using gravity sedimentation methods and have been previously validated by examining proteins expressed in these specific spermatogenic subtypes (81). In addition to these datasets, we isolated RNA from intact postnatal day 2 mouse testis, as well as cultured SSCs, and as a further control, RNA from a broad array of normal adult mouse tissue.

We reasoned that a marker of SSCs would be highly expressed in spermatogonial stem cell cultures, which are enriched in the stem cell fraction, and at low, perhaps undetectable levels in the adult testis. However, we did not want to exclude the possibility that spermatogonial stem cell cultures did not faithfully mimic the adult testis and therefore would not express similar protein markers. Therefore, we devised two schemes for identifying potential candidates for SSC markers. In one arm, probe sets were ranked on signal strength in SSCs as a

proportion of the adult testis. In the other, the sets were ranked by comparing the expression in Type A spermatogonia to the intact adult testis. One strength of this methodology was that there was no preset cutoff point at which a probe set would not be considered as a potential SSC candidate. Thus, all genes in the microarray were listed from the most differentially expressed to the least. Another advantage to only sorting based on these criteria was that high expression in other tissues did not exclude a probe set from being an SSC candidate.

I examined the expression profiles of 500 probe sets in each arm of the analysis. While ultimately comparing SSC cultures to the adult testis yielded the best results in terms of new candidates for SSC markers, both arms of the analysis yielded interesting results, and were validated both by examining known markers of distinct spermatogenic subtypes, as well as by pulling out known markers in our ranked lists.

Known markers of spermatogenic subtypes

One of the first germline markers I wanted to examine was Vasa, which is expressed in all spermatogenic subtypes, from early embryonic development (e12.5) to adulthood (61). While Vasa was not on our ranked list of SSCs vs. testis because of its high expression throughout the germline, it served as an important control. In our probe set, Vasa was expressed highly in the developing and adult testis, as well as in the developing ovary and oocytes. Expression of Vasa in spermatogenic subtypes was at near equivalent levels in Type A, B, pachytene, and round spermatids, akin to what is seen *in vivo* (**Figure 6.1**). This gave of confidence

both in the array as well as in datasets acquired from GEO and allowed us to move on to the ranked list of probe sets.

Plzf, expressed in A_{single}- A_{al16} spermatogonia (22), and Ret, expressed in mostly A_{single}- A_{pr} (82) were near the top of the SSC vs. testis list (**Figure 5.1**). Other known markers of spermatogonia that were highly ranked included Lin28, Gfrα1, and Foxo1. A common pattern to these known markers of spermatogonia included high expression in SSCs and type A spermatogonia, low expression in the more differentiated subtypes (Type B, pachytene, round spermatids). In the embryonic testis, expression was variable. However, there was a significant peak in the postnatal day 2 testis isolates. At this timepoint, the germline consists of prospermatogonia, which make up a significant part of the whole neonatal testis, and many known prospermatogonia markers are expressed in undifferentiated spermatogonia. Because of this commonality, I decided to use a peak at postnatal day two to prioritize my gene list.

Prioritizing 30 probe sets

In order to reduce the approximately 1000 gene list to a manageable number, I first started eliminating genes based on the overall strength of the probe set. If a probe set had an expression value of less than 200, it was assumed that the protein would be difficult to detect in sections and the probe set was eliminated from the gene list. I then looked at the RNA expression in other tissues. If a probe set was universally highly expressed across all adult tissues, I eliminated the probe from the list as well. The ranking of the probe set did not depend on whether the gene was

part of a common pathway in all tissues, such as homeostatic mechanisms. These criteria reduced the gene list to a more manageable number.

I then turned to the literature. Any gene that had been previously implicated in spermatogenesis was eliminated from the list, as we were trying to discover novel markers. Next, I began to look at patterns of expression in the known markers mentioned above. Genes of interest include those that have a peak in expression at postnatal day 2, high expression in the SSC cultures, as well as expression in Type A spermatogonia. At this point, the list had been reduced to approximately 200 genes. I then went back to the literature to see if any of the genes had been previously described to be involved in stem cell maintenance in other organ systems, as some of these mechanisms may be conserved in spermatogenesis. I also turned to the Mouse Geonome Informatics database to see which of these genes had previously been knocked out in mouse models. I eliminated any gene to which a knockout mouse was available but no phenotype was described. If a knockout mouse had been made and the phenotype described would preclude seeing any reproductive phenotype (i.e. neonatal lethality, mobility issues, tumors before puberty), the gene remained on the list. Finally, if floxed alleles were available, the gene was prioritized.

From these, I chose 20 genes with expression patterns similar to Plzf and Ret, and 5 genes with expression patterns dissimilar to these known markers, with or without high expression in the SSC cultures, the logic being that since a marker specific to the stem cell had not been discovered, the expression pattern could be vastly different from previously described markers of undifferentiated

spermatogonia. The list of 25 genes contained proteins known to be expressed in other stem cell populations, like Pax7 in muscle satellite cells, proteins whose function were still unknown but whose expression pattern had been described in other tissues, and proteins which had been completely uncharacterized.

Candidate genes and their expression in the adult testis

To examine the expression of these proteins *in vivo*, antibodies were purchased for the 30 candidate gene products. The gene list was screened by performing IHC on adult testis sections with 1:100, 1:1000, and 1:10,000 dilutions. Antibody detection was chosen over RNA in situ because the vast majority of the candidate genes already had antibodies available and furthermore the availability of antibodies would greatly increase the speed at which potential SSC markers could be pursued. Immunohistochemistry was chosen over other protein detection methods such as western blot because SSCs are a small subset of the testis, and identification of these stem cells is first based on their location on the basement membrane. IHC was chosen over IF as a preliminary screen due to the ease of scaling up experiments and to the stability of the signal.

Out of the 25 genes, 18 had antibodies available. Of these 18 genes, 9 had working antibodies that had a specific staining pattern in the testis. The other 9 genes failed to give a specific IHC signal in the testis. Of the 9 genes that had staining patterns in the testis, Pax7 was chosen as the final gene to pursue because of its restricted staining pattern in spermatogonia in the testis. Pax7 and the resulting data will be discussed in the following chapter. The remaining 8 genes from the list

of working IHC staining will be discussed below. It is important to note that the genes that were not pursued due to lack of specific staining patterns could merely reflect nonspecific antibodies (i.e. a gene could be expressed in SSCs but the purchased antibody could fail to detect the protein). Thus, the genes that were not detected in the testis should not necessarily be considered a failure of the methodology.

Ccnd3

As a cyclin, Ccnd3 associates with cyclin dependent kinases CDK4 and CDK6 to proceed through the G1/S transition of the cell cycle. Mutations in this gene have been described in a variety of cancer types, including breast cancer, myeloma, and bladder cancer (83-85). Ccnd3 had been reported previously to be expressed in the testis, but the precise localization of spermatogenic cell types had not been performed (86). Furthermore, some of these previous findings had found Ccnd3 in the cytoplasm instead of the nucleus as expected for a cyclin (87, 88). Performing IHC, I found that Ccnd3 was expressed in the nucleus of type A spermatogonia, as well as in the Leydig cells (**Figure 5.3**). Comparison to other subsets of known markers suggested that Ccnd3 would be expressed in undifferentiated spermatogonia, as cell counts were at similar levels as Plzf and Foxo1, which are also expressed in undifferentiated spermatogonia (**Figure 5.2**). A knockout of Ccnd3 has been described with no effects on reproduction. However, it was found that in many tissues, Ccnd2 can compensate for the loss of Ccnd3 (89). In fact, it has been reported that Ccnd2 is also expressed in the testis (86). Thus, the lack of phenotype

could be due to compensation of Ccnd2. Ccnd3 remains as a potential marker of undifferentiated spermatogonia and the precise function of Ccnd3 in spermatogonia is still unknown.

Crabp1

Cellular retinoic acid binding protein was high on the gene list for being expressed in SSC cultures relative to the adult testis. Crabp1 plays a role in proliferation and differentiation of cells, and is an interesting candidate for an SSC marker, as retinoic acid is essential for the differentiation of spermatogonia. However, knockout of Crabp1, its family member Crabp2, and double knockouts are essentially normal (90, 91). By IHC, I found that Crabp1 was expressed in spermatogonia on the basement membrane (**Figure 5.4**). Cell count per tubule suggested that Crabp1 was expressed in undifferentiated spermatogonia, as the number of cells per tubule was again akin to Foxo1 (**Figure 5.2**).

Erg

Erg is a member of the erythroblastosis transformation specific (ETS) family of transcription factors, which play diverse roles in embryonic development and cell proliferation, differentiation, and death. Erg has been implicated in many cancers, the most well-known of which being prostate and Ewing's sarcoma. In these cancers, Erg can form a fusion protein with another gene to make a transcription factor which causes unchecked growth. In prostate cancer, the fusion between Erg and TMPRSS2, a gene which is responsive to androgen, is present in more than 50%

of all prostate cancers (92). Current treatment options for prostate cancer work by eliminating androgen and thus reducing the unchecked growth due to the fusion protein (92). However, prostate cancers eventually develop resistance to androgen-related therapies, and there is much interest in developing treatments that specifically target Erg (93). Since Erg has been well-studied, it was an attractive candidate for an SSC marker.

In adult testis sections, Erg specifically stained only the nuclei of spermatogonia, as well as some Leydig cells (**Figure 5.4**). The number of Erg+ spermatogonia per tubule was similar to that of Foxo1 and Plzf counts, suggesting that Erg stained all undifferentiated spermatogonia (**Figure 5.2**).

Glis3

Glis3 is zinc finger Kruppel-like transcription factor that functions as both an activator and a repressor. Glis3 is involved on the development of the pancreas and thyroid, and mutations in Glis3 in mice and in humans cause neonatal lethality from diabetes, as well as hypothyroidism and polycystic kidneys (94-96). However, there were no reports of Glis3 being expressed in the developing or adult testis, but a reproductive phenotype could be masked by early neonatal death.

As Glis3 knockout mice were lethal, we pursued conditional knockout of Glis3, as mice were available as live animals from Jackson Labs. *Glis3$^{f/f}$* mice were crossed to *Vasa-Cre* and, in a separate arm of the experiment, to *Vasa-Cre ^{ERT2}* mice to generate *Glis3$^{f/t}$; Vasa-Cre^{+}* male mice. These mice were then backcrossed to *Glis3$^{f/f}$* female mice, since Vasa is expressed in the early embryo and thus using

female *Glis3*$^{f/t}$ *; Vasa-Cre*$^{+}$ mice would result in global recombination (61). Such care with the preliminary crosses is not needed for *Vasa-Cre* ^{ERT2}, as the Cre recombinase is only active with the addition of tamoxifen. *Glis3*$^{f/-}$ *; Vasa-Cre*$^{+}$ male mice were aged to 3mos before analysis. *Glis3*$^{f/-}$ *; Vasa-Cre*$^{ERT2+}$ male mice were injected with I.P. tamoxifen for three days at 6wks of age, and were analyzed at 3mos of age.

Conditional knockout of Glis3 in the testis resulted in paradoxical results. When Glis3 was deleted from early in embryonic development (*Vasa-Cre*), testes were highly abnormal, with many tubules showing a reduction in germ cell number. However, when Glis3 was deleted after puberty (*Vasa-Cre* ^{ERT2}), the testes appeared vastly normal, and no loss of germ cells was observed, suggesting that role of Glis3 was in establishment of the germline, and not in the maintenance of SSCs (**Figure 5.6**)**.** No phenotype was observed in female ovaries in either arm of the experiment. Furthermore, in *Glis3*$^{f/-}$ *; Vasa-Cre*$^{+}$ mice of both genders, occasional polycystic kidneys would be observed (**Figure 5.6**), suggesting that *Vasa-Cre* might be expressed at low levels in the kidney. This leakiness with *Vasa-Cre* has been noted previously in the cerebellum (unpublished results, Castrillon lab), but not in the kidney.

Overall, these results suggested a role for Glis3 in the establishment of the male germline, but not in the maintenance of the germline after puberty. This hypothesis was intriguing, but ultimately difficult to test as the purchased antibodies stained a few spermatogonia on the basement membrane, but also stained those same cells in the conditional knockout. Thus, the antibodies were thought to be cross-reacting with an unknown epitope, and were discarded. Later, it

was discovered independently that Glis3 is expressed in prospermatogonia in the early embryonic testis, but not during late embryonic development. Glis3 is thought to be involved in the extensive chromatin remodeling of the male germline. If these initial observations hold up, this data suggest some important differences in SSC culture vs. the adult testis. Glis3 was highly expressed in SSC cultures, even though these cultures were derived after Glis3 is thought to be down-regulated *in vivo.* Thus, SSC cultures may not faithfully recapitulate the behavior of SSCs in the adult testis. Further study of Glis3 past the pilot experiment stage was not performed, as another candidate gene, Pax7, was a higher priority as a marker of SSCs (see **Chapter 6**).

Igf2bp1

Igf2bp1, also called Imp1, is a member of the family of the insulin-like growth factor mRNA binding proteins. These proteins can control the mRNA transcription of Igf2 as well as c-myc and ß- actin (97). Global knockout using gene trapping led to mice that were grossly smaller, and had high rates of neonatal lethality (97). Although the mice which survived to adulthood were fertile and no abnormalities were observed in the testis, Igf2bp1 could still serves as a marker for SSCs, if not having a functional role. Furthermore, it is not known why the majority of mice die in the neonatal period, and some survive. Perhaps some of other Imps can compensate for the loss of Igf2bp1. Igf2bp1 made an attractive candidate for a marker of SSCs, as it had been described in both mouse and human spermatogonia, and also seemed to be associated with human testicular cancers (98). However, the

precise subsets of spermatogonia in which Igf2bp1 is expressed had not been described.

Using an antibody to Igf2bp1, I detected 3-4 positively staining spermatogonia on the basement membrane via IHC (**Figure 5.7**). This was in accordance with previously published data (98), once again confirming our methodology. Igf2bp1 was also found to be expressed in SSC cultures via IF.

Nmt2

Myristoltransferase genes add a myristol group to proteins either during synthesis or post-translationally, which can change or regulate the function of the protein. Nmt2 has not been very well-studied, but has been implicated in brain tumors as a cancer marker (99). Nmt2 was an attractive candidate for an SSC marker for various reasons. First, inhibitors of Nmt2 and its paralog Nmt1 had already been developed (100). Second, mutations in Nmt2 were associated with hypoplastic testes in humans, suggesting that if Nmt2 played an important role in maintenance of the germline in mice, this function would carry over to humans (101). However, the expression of Nmt2 had not been described in the testis previously. Finally, just recently and after the gene list was prioritized, methodology to visualize myristolation has become available (102).

By IHC, I found that Nmt2 was expressed in spermatogonia lying on the basement membrane (**Figure 5.8**)**.** Nmt2 seemed to be expressed in the cytoplasm of these cells, which could make it an attractive candidate for cell sorting. Still, Nmt2 was expressed in a large number of cells, and was therefore unlikely to be expressed

only in a restricted subset of spermatogonia. Foxo1, expressed in all undifferentiated spermatogonia, labels approximately 3 cells per tubule in adult testis cross sections. Kit, in all differentiating spermatogonia, is more abundant and labels approximately 11 cells per tubule. More abundant still are Nmt2$^+$ spermatogonia, at approximately 17 cells per tubule. This suggested that perhaps Nmt2 was expressed in both undifferentiated and differentiating spermatogonia. In fact, by wholemout IF, I found that Nmt2 was expressed similarly to Kit, in differentiating spermatogonia.

Lbd1

Ldb1 is a LIM binding domain protein, LIM domains being important in organogenesis as well as oncogenesis. Global knockout of Ldb1 is early embryonic lethal, with embryos displaying a wide range of abnormalities from lack of the heart precursor organ to truncation of the head (103). Ldb1 is also essential to normal erythroid differentiation (104). I found via IHC that Ldb1 is specifically expressed in the nuclei of a subset of spermatogonia on the basement membrane (**Figure 5.9**). There are approximately 5 Ldb1$^+$ spermatogonia per tubule, which is very similar to the number of Foxo1$^+$/Plzf$^+$ undifferentiated spermatogonia. In fact, via wholemout IF, I found that Ldb1 was expressed highly in undifferentiated spermatogonia, but was also expressed at low levels in other more differentiated cells.

Matr3

Matrin 3 is a nuclear membrane protein thought to stabilize mRNAs. Human mutations in Matr3 cause amyotrophic lateral sclerosis and myopathies (105-107). After the development of this gene list, a gene trap of Matrin 3 was described, causing early embryonic lethality prior to e8.5. In the adult testis, I detected Matr3 in more differentiated spermatocytes and round spermatids, with a distinct lack of staining in spermatogonia (**Figure 5.10**). Thus, Matr3 was abandoned as a potential marker of SSCs. Interestingly, the pattern of expression on the digital northern did not show expression of Matr3 in the SSC cultures. In fact, this gene was chosen for having a dissimilar pattern to Plzf and the other candidate genes (the 5 dissimilar patterns), to cover the possibility that a marker of SSCs, which had yet to be discovered, would have an expression pattern distinct from any of the previous markers of spermatogonia.

Conclusions

As a method for discovering new markers of spermatogonia, comparing the expression of markers in SSC cultures vs. whole testis seemed to be a viable method. Out of 18 genes to which antibodies were purchased, 9 showed specific staining patterns in the testis, and 8 of these specifically stained spermatogonia. Of the 9 genes which did not exhibit staining within the testis, none of these antibodies had been reported in the literature to give specific patterns in other tissues. Thus, the failure to detect a signal in the testis may be due to inability of these antibodies to detect their cognate antigens in paraffin-embedded, formalin-fixed tissues. Furthermore, one of these 9 genes was Tert, which once deleted, causes infertility

and loss of the male germline, and thus must be expressed in the testis (108). However, the protein is expressed at extremely low levels, making it difficult to detect.

On the other hand, of the 25 genes examined, only one, Pax7, was expressed in a more restricted subset of SSCs; of the genes that had antibodies that were useful for immunohistochemistry, the majority were expressed in all undifferentiated spermatogonia. Therefore, if the goal is to discover new and more restricted markers of stem cells and not merely markers of spermatogonia, some changes should be made to increase the probability of finding an SSC marker. This could be accomplished by a number of ways. First, $Pax7^{+}$ SSCs could be flow sorted and profiled, and this data could be used to discover novel genes expressed in the $Pax7^{+}$ subset of SSCs. Alternatively, genes could be selected that are not in the $Pax7^{+}$ subset, and new subsets of spermatogonia could be defined. Secondly, testes could be treated with genotoxic reagents, and profiling could be performed while the testis is recovering, as at this time there is an increase in the number of stem cells to repopulate the testis (see **Chapter 6**).

Finally, since no cut-off was applied to the sorting of the original gene list, more candidate genes could be ranked based on the availability of verified antibodies, thus eliminating the possibility that failure to detect a specific signal in the testis was due to failure of the antibody. This strategy was not chosen previously because we wanted to prioritize new and understudied genes. More genes could be screened than only the 25 that were chosen previously. In fact, it seems that brute force screening is the best predictor for success using the data sets available.

However, there are many unanswered questions to the nature of different subsets of A_{single} spermatogonia and stem cells that cannot be answered without new markers of these subsets. Thus, although the screening of different genes may be somewhat inefficient, the potential scientific payout is great. It is worth mentioning that without such screening, Pax7 would have not been found, and previously, the lack of SSC markers in the murine testis had been a hindrance to the field.

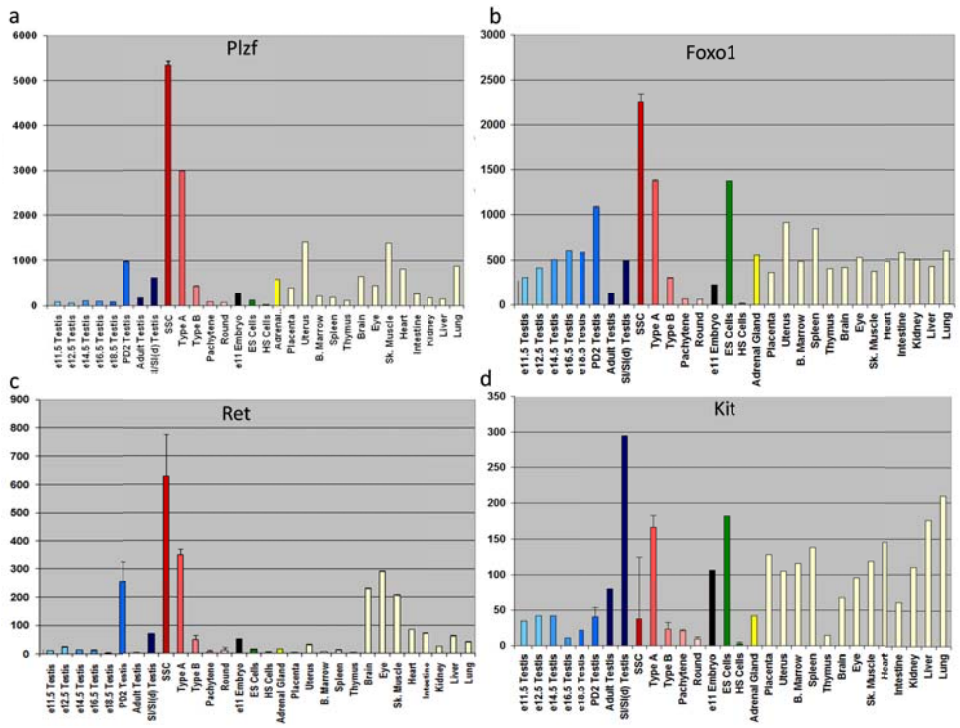

Figure 5.1: Expression levels of known markers of spermatogenic subtypes by microarray (A) mRNA profile for *Plzf*. *Plzf* is expressed at low levels in the embryonic testis, but had a small peak in expression at PD2. *Plzf* was not expressed highly in the adult testis and the highest expression was in SSCs and Type A spermatogonia. *Plzf* was not expressed in more differentiated cell types. Expression profiles which were similar to *Plzf* were prioritized as candidate genes. (B) mRNA profile for *Foxo1. Foxo1* is expressed in the embryonic testis, and at low levels in the adult. The highest expression of Foxo1 is in SSCs and Type A spermatogonia, as well as ES cells, where *Foxo1* is known to be expressed. (C) mRNA expression profile for Ret, which is very similar to *Plzf. Ret* was expressed at low levels in the embryonic testis, but high at PD2, SSCs, and Type A spermatogonia. (D) mRNA expression profile for *Kit.* Unlike the other markers, *Kit* is expressed in differentiating spermatogonia, and thus had a distinct expression profile. *Kit* was expressed at

higher levels in the adult testis than in the PD2 testis, and was not highly expressed in SSC cultures. Thus, expression profiles akin to *Kit*'s were generally avoided.

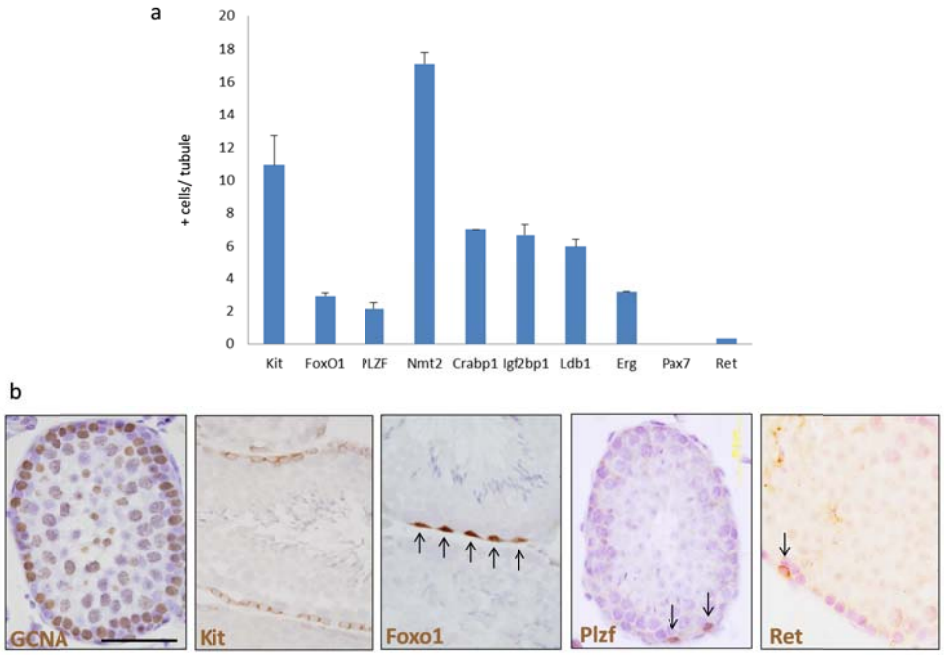

Figure 5.2: Expression levels of known markers of spermatogonia by IHC. (A) Number of cells per tubule of potential markers of SSCs. Kit is expressed in differentiating spermatogonia, while Foxo1 and Plzf are known to be expressed in undifferentiated spermatogonia. Nmt2 was expressed in more cells per tubule than Kit or Plzf, suggesting that Nmt2 may mark undifferentiated and differentiating spermatogonia. Crabp1, Igf2bp1, Lbd1, and Erg mark a similar number of cells per tubule as Plzf, suggesting they may be expressed in undifferentiated spermatogonia. Pax7 was the rarest marker observed. (B) Representative staining of antibodies used in this thesis. Scale = 50μm.

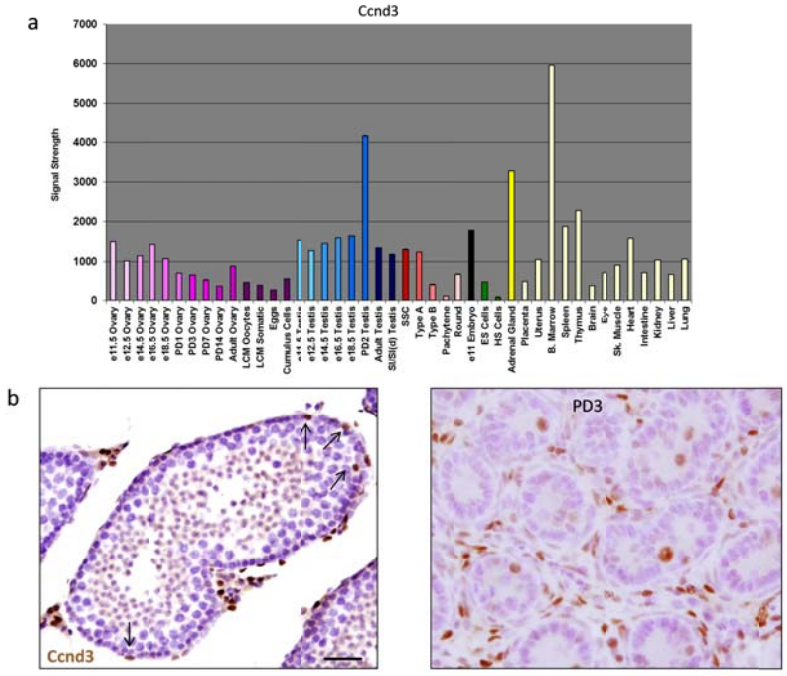

Figure 5.3: Ccnd3 is expressed in undifferentiated spermatogonia. (A) Expression of *Ccnd3* by microarray. (B) IHC of Ccnd3 in adult and PD3 testis. Scale =50µm.

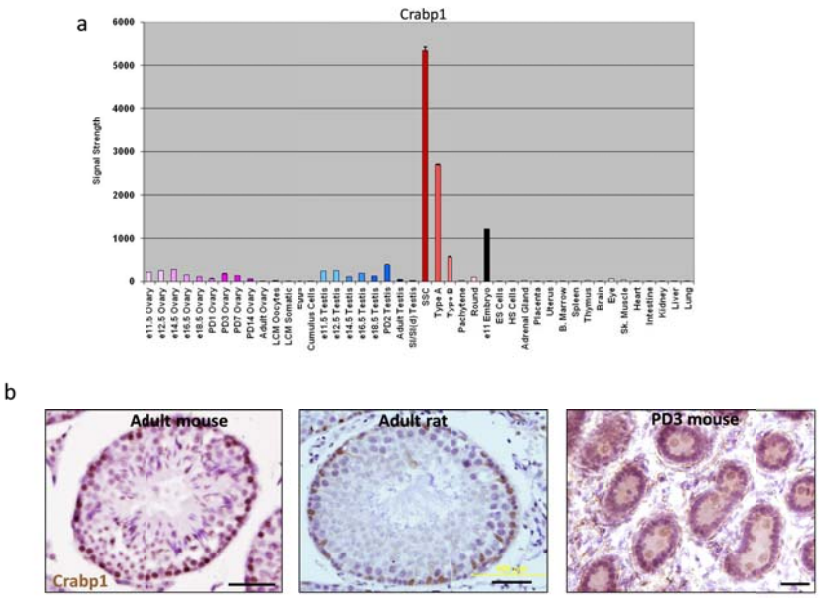

Figure 5.4: Crabp1 is expressed in spermatogonia on the basement membrane. (A) Expression profile of *Crabp1* via microarray. (B) Expression of Crabp1 in adult mouse and rat testes, and PD3 mouse testis. Scale = 50μm.

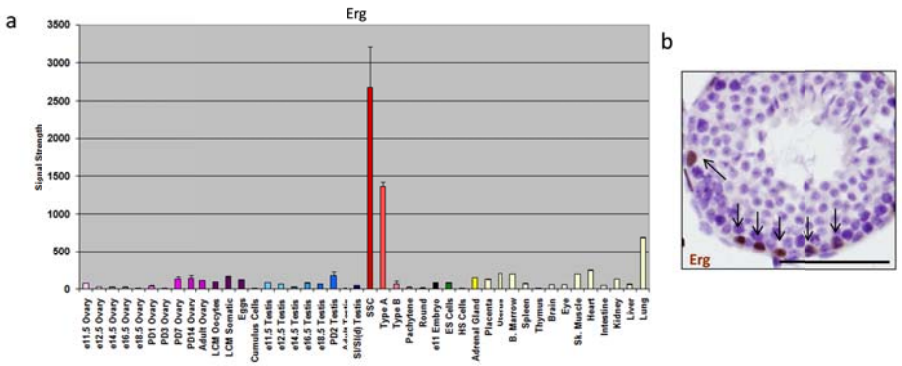

Figure 5. 5: Erg is expressed in undifferentiated spermatogonia. (A) Expression profile of *Erg*. (B) Erg is expressed in undifferentiated spermatogonia on the basement membrane. Scale = 50μm.

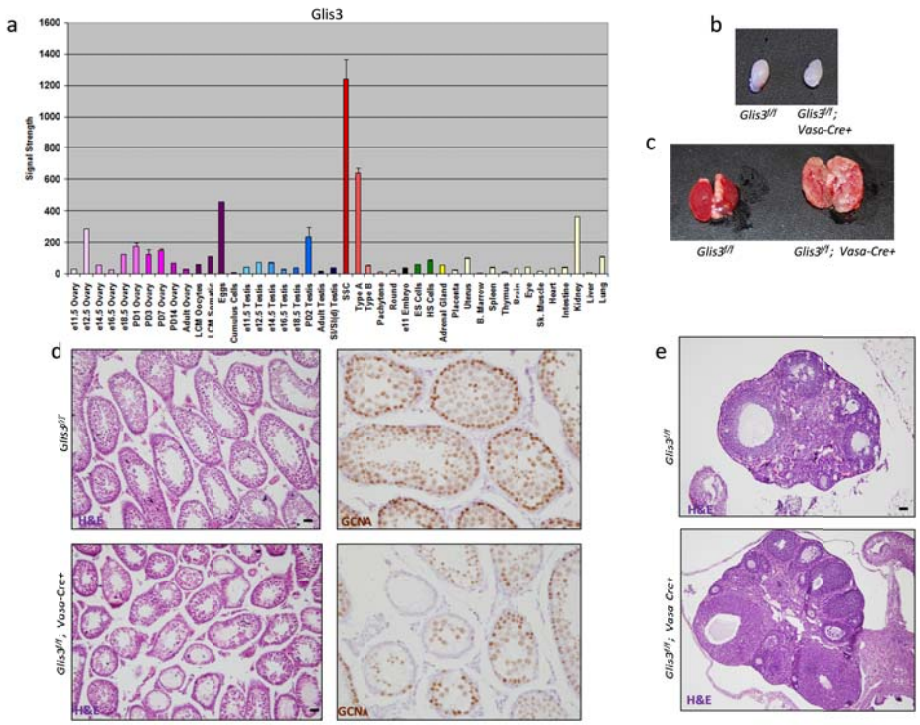

Figure 5.6 cKO of Glis3 causes defects in spermatogenesis. (A) Expression profile of *Glis3*. (B) cKO testes are slightly smaller than control testes. (C) cKO in the gonads causes ectopic recombination in the kidney, which causes polycystic kidney disease. (D) Histology of Glis3 cKO testes. H&E and GCNA show a reduction in germ cell number. (E) Histology of Glis3 cKO ovaries shows no defect in oogenesis. Scale = 50μm.

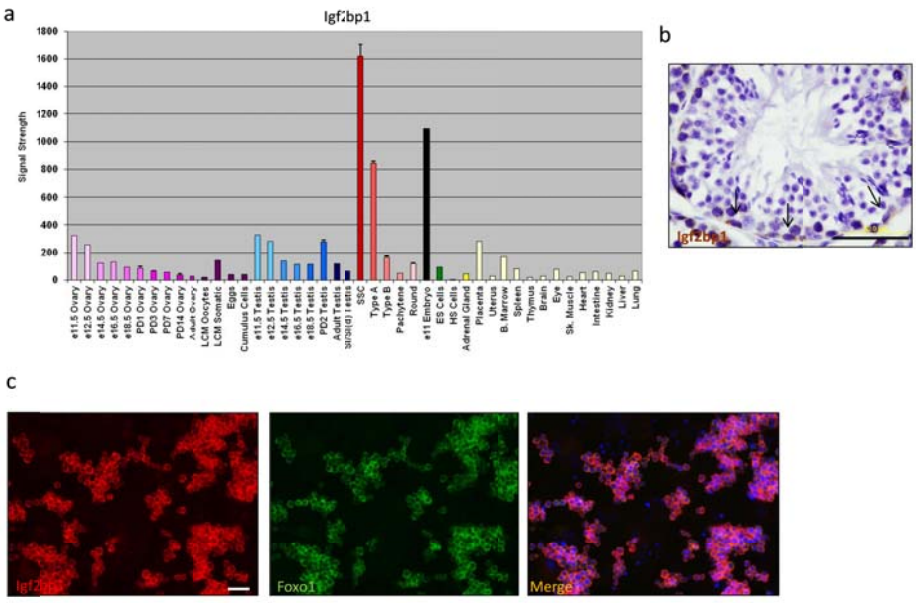

Figure 5.7: Igf2bp1 is expressed in undifferentiated spermatogonia. (A) Expression profile of *Igf2bp1*. (B) Igf2bp1 is expressed in the cytoplasm of spermatogonia on the basement membrane. The number of cells per tubule is similar to Foxo1 and Plzf, expressed in undifferentiated spermatogonia. (C) Igf2bp1 is expressed homogenously in SSC culture. Scale = 50μm.

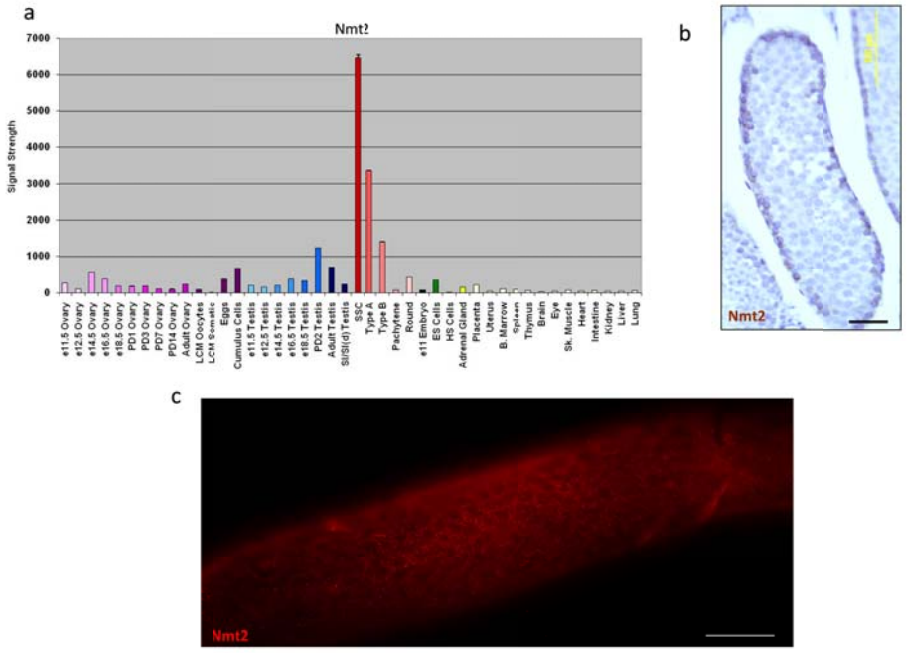

Figure 5.8: Nmt2 is expressed in both undifferentiated and differentiating spermatogonia. (A) Expression profile for *Nmt2*. (B) IHC for Nmt2 shows a large number of positive cells staining on the basement membrane. Cells per tubule is similar to the number of Kit and Foxo1 combined. (C) Wholemount of Nmt2 is similar to Kit, but stains far more spermatogonia. Scale = 50μm.

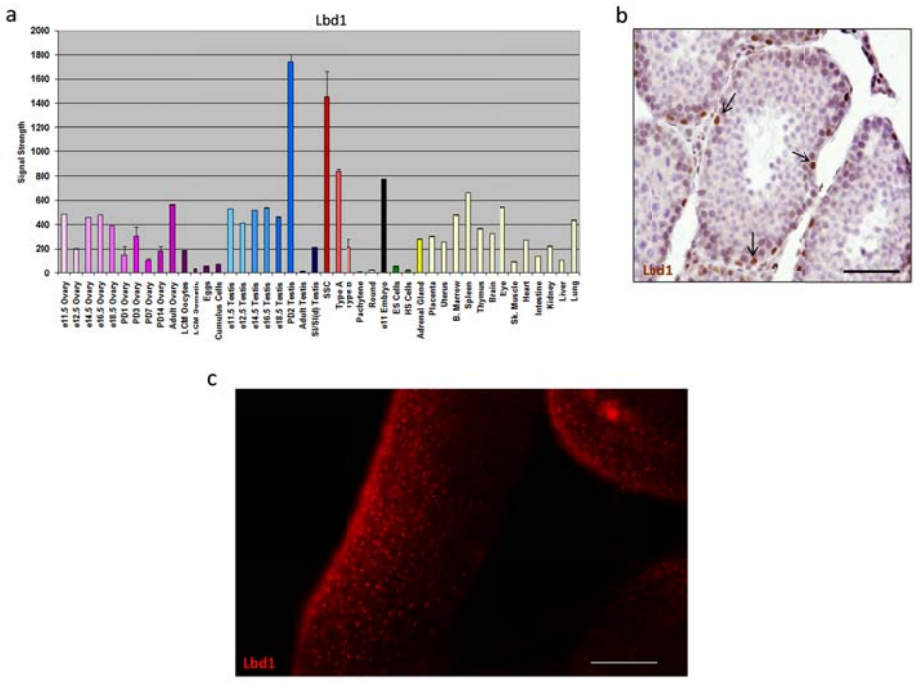

Figure 5.9: Lbd1 is expressed in undifferentiated spermatogonia. (A) Expression profile for *Lbd1*. (B) IHC for Lbd1 shows strongly staining spermatogonia along the basement membrane. (C) Wholemout of Lbd1. Lbd1 is expressed highly in undifferentiated spermatogonia, but is also expressed at low levels in more differentiated cell types. Scale = 50μm.

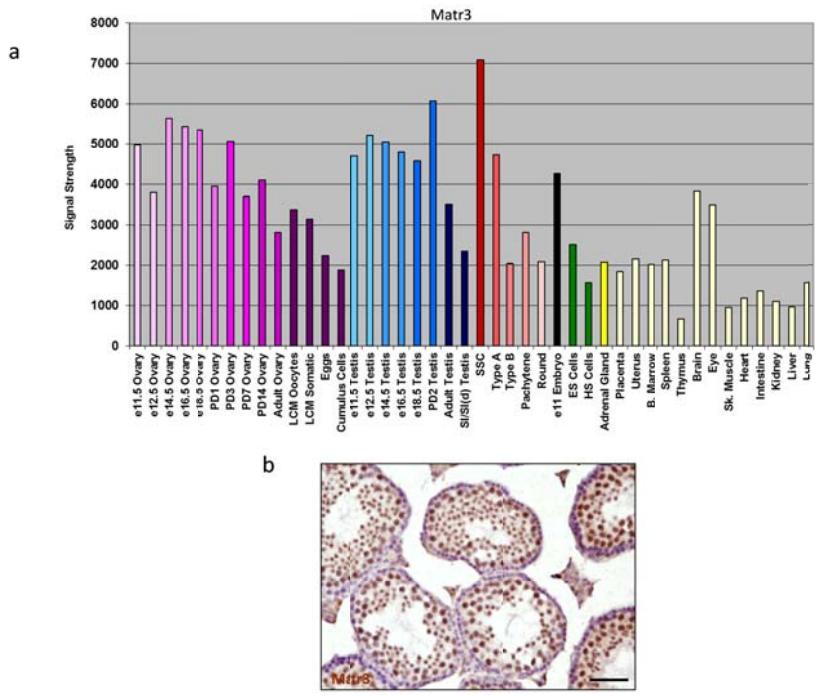

Figure 5.10: Matr3 is not expressed in spermatogonia. (A) Expression profile of *Matr3.* Note expression in Type A, B, pachytene, and round spermatids. (B) Matr3 is not expressed in spermatogonia, and was discarded as a potential stem cell marker.

CHAPTER 6: PAX7 EXPRESSION DEFINES GERMLINE STEM CELLS IN THE ADULT TESTIS

Pax7 specifically marks a small subset of A_{single} spermatogonia in vivo

We reasoned that a *bona fide* testis stem cell marker should be highly expressed in SSC cultures but at low (perhaps undetectable) levels in the adult testis, where true stem cells are a rare subpopulation. An RNA-based approach previously utilized for marker discovery in ovarian cell subpopulations (80) led us to the identification of *Pax7* (**Figure 6.1**, A). At the mRNA level, *Pax7* was highly expressed in SSC cultures but undetectable in adult testis (a relative difference >180x) (**Figure 6.1**, B). *In vivo*, *Pax7* transcripts were detectable in A (early) spermatogonia but not in differentiated B spermatogonia, spermatocytes, or round spermatids. *Pax7* transcripts were absent in embryonic testes (e11.5-e18.5) and first detected at postnatal day (PD) 2. Among adult tissues, *Pax7* was expressed only in skeletal muscle, consistent with Pax7's eminence as a marker of satellite cells, the dormant tissue stem cell population that regenerates skeletal muscle following injury (109, 110). In comparison, the pan-germ cell marker *Ddx4* (*Vasa*) was expressed in adult testis (111) and all germ cell subpopulations but not in any somatic tissues, and transcripts were markedly decreased in germ-cell deficient ($Kitl^{Sl}/Kitl^{Sl\text{-}d}$) testes, as expected (**Figure 6.1**, C). Thus, in contrast to *Pax7*, *Ddx4* did not exhibit a stem cell signature.

We sought to visualize $Pax7^{+}$ cells in sections of adult testis with an α-Pax7 monoclonal antibody. $Pax7^{+}$ cells were rare: a single $Pax7^{+}$ cell might be detected

within seminiferous tubules in one complete testis cross-section (**Figure 6.2**, A). Despite this rarity, several observations confirmed that the detection of $Pax7^+$ spermatogonia was specific, defining a novel population of spermatogonia. First, the $Pax7^+$ cells always rested on the basement membrane and were isolated, single cells (i.e., consistent with A_{single} spermatogonia; see also below). Secondly, Pax7 protein in spermatogonia was always nuclear, as expected based on its function and nuclear localization within satellite cells (109, 110).

To further define these $Pax7^+$ spermatogonia, we compared their abundance to other subsets of spermatogonia defined by well-characterized markers (see schematic in **Figure 1.2**). Kit^+ "differentiating" spermatogonia were the most abundant (10.9 Kit^+ cells/tubule) with $Foxo1^+$/$Plzf^+$ spermatogonia being more restricted as expected, given that Foxo1 and Plzf are both markers of "undifferentiated" (A_{single}→A_{al16}) spermatogonia, a less abundant population (14, 22). Ret^+ spermatogonia were rarer still, consistent with Ret's more restricted expression in A_{single} and A_{pair} spermatogonia (82). However, $Pax7^+$ spermatogonia were approximately two orders of magnitude rarer than Ret^+ spermatogonia (**Figure 6.2**, B). $Pax7^+$ spermatogonia were $Foxo1^+$ and Gfr□1^+, while most $Foxo1^+$ or Gfr□1^+ cells were $Pax7^-$, demonstrating that $Pax7^+$ spermatogonia are a subset of undifferentiated, Gfr□1^+ spermatogonia (**Figure 6.2**, C).

Confocal microscopy of intact seminiferous tubules further showed that $Pax7^+$ spermatogonia were a subset of A_{single} spermatogonia. $Pax7^+$ spermatogonia were singular, and larger chains of undifferentiated spermatogonia (i.e. A_{al4} to A_{al16}) never contained $Pax7^+$ spermatogonia (**Figure 6.2**, D, and Movie S1). Additional

confocal microscopy studies confirmed that Pax7$^+$ spermatogonia were always Kit$^-$; no Kit$^+$ Pax7$^+$ spermatogonia were ever observed (**Figure 6.2**, E). Thus, Pax7 defines a rare but specific subset of A_{single} spermatogonia, revealing striking heterogeneity within A_{single} spermatogonia *in vivo*.

Pax7$^+$ spermatogonia are rare in the adult testis, but constitute a much higher fraction of germ cells in the neonatal testis

Interestingly, a much higher percentage of germ cells (defined by the pan-germ cell marker GCNA) were Pax7$^+$ at birth (28% in neonates); however this fraction steadily decreased postnatally, stabilizing at 6 weeks of age (**Figure 6.3**, A). The much higher fraction of Pax7$^+$ germ cells at birth further underscores their rarity in adults, and also demonstrates that Pax7$^+$ spermatogonia can be reliably identified in tissue sections (analyses of conditional knockout testes described below confirmed antibody specificity).

This age-dependent decrease in the Pax7$^+$/GCNA$^+$ cell number could reflect decreased absolute numbers of Pax7$^+$ spermatogonia, *versus* their dilution due to the massive expansion of spermatogenic cells that normally occurs during postnatal life (e.g. testes weights increase from ~1 mg at birth to ~60 mg in adult males) (112). To distinguish between these possibilities, we serially-sectioned and immunostained entire PD1 and adult testes and documented similar numbers of Pax7$^+$ spermatogonia per testis (504 +/-29 and 402 +/- 33 S.E.M. respectively) (**Figure 6.3**, B). Thus, the dramatic age-dependent decrease in the fraction of Pax7$^+$ germ cells reflects mainly the rapid expansion of spermatogenesis, and not a large

decrease in absolute numbers of Pax7$^+$ cells. These results also strongly suggest that the postnatal Pax7$^+$ spermatogonia represent the initial founder population for Pax7$^+$ spermatogonia in adult testes.

Pax7$^+$ spermatogonia are rapidly cycling during normal spermatogenesis and function as robust stem cells that give rise to all stages of spermatogenesis

We considered the possibility that (by analogy with satellite cells) adult Pax7$^+$ spermatogonia might represent a quiescent subset of A_{single} spermatogonia. To our surprise, however, EdU labeling showed that Pax7$^+$ cells, like other subsets of spermatogonia, were rapidly cycling (**Figure 6.3**, C).

We then sought to explore the contribution of Pax7$^+$ spermatogonia and their descendants to normal, steady-state spermatogenesis in the undisturbed adult testis through lineage tracing. We employed a *Pax7$^{tm2.1(cre/ERT2)Fan}$*/J allele where the tamoxifen-inducible recombinase *Cre^{ERT2}* was knocked into the *Pax7* locus, driving *Cre^{ERT2}* expression in cells that express *Pax7*, such as satellite cells (**Figure 6.4,** A) (52, 113). We generated mice harboring *Pax7$^{tm2.1(cre/ERT2)Fan}$*/J and the *Rosa26* β-galactosidase *lox-stop-lox* reporter, *R26R* (66). Six week-old adult males were treated with tamoxifen to activate Cre in Pax7$^+$ cells. Untreated *Pax7$^{tm2.1(cre/ERT2)Fan}$*/J; *R26R* males exhibited no Cre-mediated recombination in testis or skeletal muscle, demonstrating tight control of Cre. Expression of Pax7 in labeled clones confirmed faithful *Pax7$^{tm2.1(cre/ERT2)Fan}$*/J expression in Pax7$^+$ spermatogonia (**Figure 6.4,** B-D). To characterize Pax7$^+$ descendants within the testis, labeled clones were analyzed after defined time intervals. By “clone” we refer not to individual spermatogonial

chains but rather to completely isolated groups of labeled cells that could comprise multiple chains but were clearly descendants of a common progenitor—despite their sometimes complex arrangements—because of their close proximity. Of note, clones were very distant to their nearest neighbors and were much more isolated than apparent in the figures shown, with no labeled clones evident in either direction along the tubule. Thus, there is no question that these clones were separate tracing events at every time point analyzed.

Four days after tamoxifen treatment, clones were very small, most consisting of single, isolated cells, similar to the Pax7 immunostaining pattern (**Figure 6.5**, A). The presence of slightly larger clones after 3 weeks and their subsequent rapid expansion is consistent with rapid cycling. There was striking clone expansion at successive timepoints, such that by 6 weeks of age, very large clones were readily visualized. Interestingly, larger clones were sometimes associated with distinctive "trails" of cells, some of which were clearly A_{single} spermatogonia based on their distance (multiple cell diameters) to other labeled descendants (**Figure 6.5**, A, #1-4, Movie S1). This implies complex patterns of migration of $Pax7^{+}$ cells and their descendants, but could also reflect chain fragmentation. Labeled elongate spermatid tails were first identified 6 weeks after induction (**Figure 6.5**, B-C). Average clone sizes (i.e. cells per clone) increased over time, but clone numbers remained stable over this prolonged interval. This argues that $Pax7^{+}$ spermatogonia are *bona fide* stem cells. If $Pax7^{+}$ spermatogonia were instead transit-amplifying intermediates, labeled cells would become diluted out with time and eventually disappear because

the total duration of spermatogenesis (i.e. from A_{single} spermatogonium to sperm release) is only 39 days in the mouse (114).

Lineage tracing experiments with *Pax7*$^{tm2.1(cre/ERT2)Fan}$/J and a double-fluorescent *mT/mG* reporter (68) gave nearly identical results. Clones began as single cells. One week after Cre induction, labeled A_{single}, A_{pair}, and $A_{al4\text{-}8}$ chains were identified. At six weeks, larger clones were visualized and elongate spermatid tails were first identified in tubular lumina. By 16 weeks, clones were even larger (**Figure 6.6**, A), and motile, labeled sperm were present in epididymides (Movie S2). Labeled A_{single} spermatogonia were observed at all timepoints (**Figure 6.6**, A, Movie S3 and S4). To more clearly delineate clonal architecture, we also analyzed frozen tissue sections of intact testes, which permitted better visualization of spermatogenic layers and cell types. In some clones, all of the germ cells in the entire tubular cross-section were clearly labeled (green), demonstrating that all the germ cells (spermatogonia, spermatids, and spermatocytes) were derived from a Pax7$^+$ progenitor (**Figure 6.6**, B). These results demonstrate that Pax7$^+$ spermatogonia give rise to full-lineage maturation (see also labeled sperm from epididymis, **Figure 6.6**, C), thereby fulfilling a key criterion of an adult testis stem cell. As with *R26R*-based lineage tracing, clone numbers did not decrease, even when the analyses were extended to 16 weeks after tamoxifen treatment (**Figure 6.6**, D-E). We conclude from these analyses with two distinct reporters that Pax7$^+$ spermatogonia are rare but robust tissue stem cells. They give rise to other A_{single} spermatogonia that persist even after very long intervals of 16 weeks, and also give rise to all stages of spermatogenesis—including motile sperm.

Lineage tracing studies of neonatal animals shows that neonatal Pax7⁺ spermatogonia have long term stem cell potential in vivo and also have stem cell activity in transplantation assays

Lineage tracing studies initiated with neonatal animals (PD1-3) confirmed that Pax7⁺ spermatogonia were rapidly expanding by PD3 and were progenitors of subsequent A_{single} spermatogonia and spermatogenesis; clones grew in size over time and persisted into adulthood (**Figure 6.7**, A, B). Concordantly, Pax7⁺ spermatogonia were rapidly proliferating by PD3 per EdU incorporation rates, without significant cell death (**Figure 6.7**, C). Finally, although flow sorting of live Pax7⁺ spermatogonia was not possible with available reagents, transplantations were conducted with unsorted cells from tamoxifen-treated *Pax7$^{tm2.1(cre/ERT2)Fan}$*/J; nuclear tdTomato reporter mice (67). Labeled, lineage-traced germ cells were observed in every host (n=3), demonstrating that Pax7⁺ spermatogonia and their descendants have stem cell activity in transplantation assays (**Figure 6.7**, D).

Pax7⁺ spermatogonia persist in mouse models of infertility while other germ cells are ablated

To first examine the behavior of Pax7⁺ spermatogonia during injury to the testis, I examined four mouse models of infertility, *Foxo1$^{f/f}$; Vasa-Cre, Foxo1/3/4 $^{f/f}$; Vasa-Cre,* and *Pten$^{f/f}$; Vasa-Cre.* All three of these mouse models begin with normal prospermatogonia, and eventually progress to seminiferous tubules which only contain Sertoli cells because all germ cells have undergone apoptosis (14). I found

that in all three models, Pax7$^+$ prospermatogonia seemed to increase in number when other germ cells were dying (**Figure 6.8**). One caveat to this finding was that in the Pten cKO, in which the reduction of germ cell number comes on more quickly than in the other two models, no Pax7+ spermatogonia were seen at late timepoints. In these models of infertility, Pax7$^+$ prospermatogonia seemed to be in clumps of cells, which had not been seen previously, suggesting that maybe these cells could divide to try and replace lost germ cells. By adulthood, these clumps of Pax7$^+$ spermatogonia were no longer observed, but a few Pax7$^+$cells still remained in the tubules, although at this point the germline was nearly completely ablated.

Pax7$^+$ spermatogonia persist after hypophysectomy, and increase in number

Removal of the pituitary eliminates the source of LH and FSH essential to maintain Leydig and Sertoli cells, and thus also to maintain the germline. Ablation of germ cells in these mice occurs gradually; while infertility occurs within 2wks after surgery (115), germ cells can persist even 12wks later, although the size of testis at this timepoint is greatly reduced.

To determine the behavior of Pax7$^+$ spermatogonia after loss of the pituitary, adult mice underwent hypophysectomy. As expected, germ cell number was greatly reduced, as determined by IHC of the pan-germ cell marker, GCNA (**Figure 6.9**). However, even 12wks after hypophysectomy, when the ablation of germ cells is nearly 90%, Pax7$^+$ spermatogonia could be seen via IHC. Furthermore, when counting the number of Pax7$^+$ spermatogonia per tubule and per germ cell, there was a modest increase in cell number. This argues that while other cell populations

undergo apoptosis, Pax7^{+} spermatogonia can persist, and perhaps divide to try and reestablish the germline. Furthermore, it seems that Pax7^{+} spermatogonia are insensitive to loss of LH and FSH. This is especially interesting in the light of the finding that suppression of testosterone after chemotherapy, which is highly damaging to the germline, can actually aid in spermatogenic recovery (116). The fact that Pax7+ spermatogonia do not necessarily depend on testosterone for cell survival suggests that, if these cells are indeed stem cells, they could be those cells which help to reestablish the germline after chemotherapy.

Pax7^{+} spermatogonia are 1) selectively resistant to anti-cancer therapies (radiotherapy and chemotherapy) that kill other germ cells in the adult testis and 2) contribute to spermatogenic recovery following ablation of most germ cells

Spermatogenesis is highly sensitive to systemic genotoxic stresses such as cytotoxic chemotherapy. Chemotherapy-induced ablation of germ cells has been studied in rodent models. Following treatment with the alkylating agent busulfan (a.k.a. Myleran, used to treat hematopoietic malignancies) germ cells undergo massive cell death in a dose-dependent manner—with higher doses leading to near total germ cell depletion. This results in an interval of azoospermia and infertility, followed by a gradual recovery of spermatogenesis, and in most animals, restoration of fertility even after high doses (34). Such spermatogenic recovery poses a paradox: the germline is almost entirely ablated, and yet the restoration of spermatogenesis implies the existence of rare stem cells that not only survive but replenish spermatogenesis during the recovery period (117).

To study the contribution of Pax7$^+$ spermatogonia to spermatogenic recovery, adult mice (6 weeks of age) were treated with busulfan. As expected, testes underwent massive germ cell death with dose- and time-dependent germ cell loss as visualized by immunohistochemistry with the pan-germ cell marker GCNA (118). In striking contrast, both relative and absolute numbers of Pax7$^+$ spermatogonia increased several-fold, also in a time- and dose-dependent manner (**Figure 6.10**, A). Absolute numbers of Pax7$^+$ cells peaked (>5x higher compared to untreated mice) 16 days after treatment with the highest dose of busulfan (40 mg/kg). Pax7$^+$ cell counts then decreased between 16 and 32 days, most likely a consequence of differentiation (see below). This association remained even when normalizing to Sertoli cells numbers (**Figure 6.11**), and therefore it is not merely the testis shrinking overall that leads to this increase in cell number. Thus, while germ cells as a whole were largely ablated by busulfan, Pax7$^+$ cells not only survived but expanded.

Histology and immunostaining confirmed massive loss of germ cells. Whereas in untreated animals virtually all Pax7$^+$ cells were single, isolated cells (with only extremely rare cells being present as pairs, and never in clusters ≥3), larger Pax7$^+$ clusters of 2-4 or more cells were observed following busulfan (**Figure 6.10**, B-C). This difference in cluster sizes (one versus ≥2) was highly statistically significant ($p=2x10^{-9}$) in untreated animals versus those treated with 40 mg/kg busulfan after 32 days. The Pax7$^+$ fraction undergoing DNA replication based on EdU incorporation was increased four days after busulfan treatment, demonstrating that busulfan treatment stimulated Pax7$^+$ cell division acutely, arguing that cell

division is one mechanism underlying the formation of Pax7$^+$ cell clusters (**Figure 6.10**, D). In contrast to Pax7$^+$ spermatogonia, Foxo1$^+$ undifferentiated spermatogonia counts fell by >15x eight days after 40 mg/kg busulfan administration, but then recovered coincident with the peak of Pax7$^+$ expansion (**Figure 6.12**, A). These data indicate that spermatogonia are sensitive to genotoxic stress as previously reported (119), emphasizing the unique properties and survival of Pax7$^+$ spermatogonia after treatments that ablate the vast majority of germline cells. That the increase in Foxo1$^+$ spermatogonia coincides with the decrease of Pax7$^+$ spermatogonia is further evidence that Pax7$^+$ spermatogonia eventually differentiate (**Figure 6.12**, B-C). In control experiments, neither tamoxifen nor the DMSO solvent had a significant impact on testis weights or morphology or Pax7$^+$ spermatogonia (**Figure 6.13**, A -D).

We then analyzed the response of Pax7$^+$ spermatogonia to ionizing radiation and a second chemotherapeutic agent commonly used in the clinic, cyclophosphamide. Cyclophosphamide is less toxic to the germline, necessitating a longer treatment protocol (150 mg/kg I.P. every 5 days for 25 days) than busulfan, which was administered as a single dose. Radiation was administered in a single (non-fractionated) dose of 5 Gray. Selective survival and clustering of Pax7$^+$ spermatogonia ($p<10^{-5}$) similar to that observed following busulfan were also observed after either external irradiation or cyclophosphamide (**Figure 6.14, 6.15**). Following the cessation of each treatment, the number of Pax7$^+$ spermatogonia increased, and subsequently declined, as was observed with busulfan. These results are significant in that they demonstrate that in the mouse, Pax7$^+$ spermatogonia

selectively survive first-line cancer therapies that often result in reversible or permanent sterility in men and boys (120). These findings make Pax7$^+$ spermatogonia strong candidates as the "spermatogenic recovery" cells postulated to be responsible for spermatogenic recovery following cytotoxic/genotoxic treatments in rodent models (121).

To further explore this possibility, lineage tracing studies were performed with adult mice treated with 20 mg/kg busulfan. In one experiment, lineage tracing was initiated by tamoxifen (usual three-day regimen) followed by busulfan (tam→bu). In a second experiment, the order of treatments was reversed, and tamoxifen was administered 15-17 days after busulfan administration (the timepoint coinciding with the peak of Pax7$^+$ cells) (bu→tam) (Fig. 9A). In each experiment, Pax7$^+$ spermatogonia contributed to spermatogenic recovery, as evidenced by the presence of labeled clones eight weeks after the last treatment. With the tam→bu protocol, the number of clones was fewer than in untreated control mice ($p=0.002$), whereas the number of clones was greater than controls in the bu→tam protocol ($p=0.021$). These results are consistent with the expansion of Pax7$^+$ cells observed at 16 days after busulfan (**Figure 6.10**, A, **6.16,** B-C). The somewhat smaller mean clone sizes in the bu→tam vs. tam→ bu experiments (161 vs. 378) could be explained by the administration of tamoxifen 15-17 days after busulfan (bu→tam), whereas in the tam→bu protocol busulfan was administered only 8 days after tamoxifen. This 7-9 day difference might permit one or more additional cell doublings to occur in the tam→bu protocol, thus accounting for the modestly (~2x difference) increased clone size. Clone morphology was similar to

that observed in the prior lineage tracing experiments; an example of a large clone is shown (**Figure 6.16**, D). In tissue sections of the larger clones, the labeled cells made up all of the germ cells in a tubular cross section, demonstrating that, as in normal spermatogenesis in untreated mice, Pax7^{+} spermatogonia contributed to full-lineage maturation following busulfan (**Figure 6.16**, E). Together, these data show that Pax7^{+} spermatogonia not only selectively survive but also contribute to the reestablishment of spermatogenesis following diverse genotoxic insults to the germline including radiotherapy and chemotherapy (117).

Elimination of Pax7^{+} spermatogonia is not feasible using a specific conditional allele of DT

I attempted to eliminate all Pax7^{+} SSCs with a well-known *lox-stop-lox diphtheria toxin (DT)* allele crossed with the *Pax7$^{tm2.1(cre/ERT2)Fan}$*/J line. Since mice do not have a receptor for diphtheria toxin, expression of the toxin under the influence of Cre recombinase should result in the immediate and specific death of Pax7^{+} cells. Unfortunately, these cell-deleting tools often suffer from significant technical limitations. Ideally, Cre-mediated recombination would lead to immediate death of all Cre-expressing cells; in practice, cell killing is often inefficient in particular cell types, and in the experience of many investigators working with diverse cell types, cell death is not achieved, or is inefficient. This is particularly a problem because then all of the descendants of the progenitor cells will express DT, which will continue to have a toxic, sublethal effect throughout the lineage (**Figure 6.17**). We believe this is what occurred in our *Pax7$^{tm2.1(cre/ERT2)Fan}$*/J; *DT* mice, because we

observed abnormal spermatogenesis including decreases in all stages of spermatogenesis with ensuing abnormal tubules - but spermatogenesis was not completely ablated. These results are consistent with the role of Pax7 spermatogonia as progenitor stem cells.

Preliminary observations demonstrate that Pax7 is dispensable for spermatogenesis

To study the genetic requirements for *Pax7* in spermatogenesis, we performed conditional genetic knockout (cKO) with the germline-specific *Vasa-Cre* (*VC*), which we had previously generated and characterized (61) and a conditional (floxed) $Pax7^{f}$ allele (52). *Pax7* germline cKO testes were morphologically normal, and harbored normal spermatogenesis as evidenced by normal weights and histological analyses. Furthermore, all males (n=3) were fertile, with normal litter sizes, demonstrating that *Pax7* is dispensable for male fertility in mice (**Figure 6.18**A-D). *VC*; $Pax7^{-/f}$ female ovaries were also histologically normal and contained all stages of follicles from primordial to secondary (**Figure 6.19**). *VC*; $Pax7^{-/f}$ males treated with busulfan (n=3) showed a significant lag in spermatogenic recovery 8 weeks after treatment (**Figure 6.20**), although this lag was somewhat variable. In *VC*; $Pax7^{-/f}$ males, testes showed a trend towards smaller size (p=0.25) but many tubules lacked complete spermatogenesis, while in control animals, practically all tubules had recovered (p=0.016).

The availability of *Pax7* germline cKO testes permitted us to confirm the specificity of Pax7 immunodetection. Whereas intratubular germ cells were readily

detectable by GCNA immunostaining of control and cKO testes, Pax7 expression was abolished in cKO testes (**Figure 6.18**E), confirming the specificity of Pax7 immunodetection. Thus, *Pax7* appears to be dispensable for spermatogenesis, at least in the laboratory setting, but may make a functional contribution to the recovery of spermatogenesis under conditions of germline stress (see discussion).

Pax7⁺ spermatogonia are present across mammalian species

We sought to determine if Pax7⁺ spermatogonia are phylogenetically conserved in spermatogenesis, as many aspects of spermatogenesis are shared by diverse species (122-125). The monoclonal antibody that we employed to detect Pax7⁺ spermatogonia was generated against chicken Pax7 (*Gallus gallus,* aa 300-523), suggesting that the epitope might be broadly conserved (126). However, there was no *a priori* guarantee that this would be the case. We epitope-mapped the □-Pax7 monoclonal antibody with a tiled peptide array of both the chicken and corresponding mouse amino acid sequences at single amino acid resolution. This identified a distinct 10 aa peak at identical positions in the chicken and mouse polypeptides (**Figure 6.21,** A). Western blotting with a 22 aa blocking peptide spanning this epitope effectively eliminated the Pax7 signals (but not non-specific background bands) confirming that this was the epitope detected by the Pax7 monoclonal antibody (**Figure 6.22,** B). Alignment of corresponding amino acid sequences from diverse species revealed that the 10 aa Pax7 epitope is conserved across all mammalian Pax7 homologs evaluated (n=11), but not the zebrafish (*Danio rerio*) or the fruit fly (*Drosophila melanogaster*) (**Table 6.1**). We then performed

immunolocalization of Pax7 in tissue sections of paraffin-embedded, formalin-fixed testes from diverse mammalian species. Rare basal Pax7$^+$ spermatogonia were present in mammalian species including companion and domestic animals, non-human primates, and humans (**Figure 6.21,** C). Interestingly, Pax7$^+$ cells were more abundant in juvenile testes (available for cat and baboon) with multiple cells in some tubules, similar to our observations in mice. These results suggest that Pax7$^+$ spermatogonia serve important roles as adult testis stem cells and contribute to spermatogenesis in a wide range of species.

Discussion

Our data reveal surprising heterogeneity in cells previously identified through morphologic criteria as A_{single} spermatogonia. This also suggests the existence of further A_{single} subtypes, which may be characterized by the expression of other distinct markers, such as Id4 or Erbb3 (18, 19, 26) Pax7 defines an unexpectedly small subset of A_{single} spermatogonia. Pax7$^+$ spermatogonia are highly proliferative in steady-state spermatogenesis and fulfill criteria of self-renewal and complete lineage differentiation in the adult testis. That Pax7 is a marker of germline stem cells in the testis is notable in light of extensive studies of Pax7 as a marker of satellite cells (109, 110). Our work shows some commonalities between Pax7$^+$ stem cells in the testis and skeletal muscle but also some important differences. Pax7$^+$ cells are rarer in the testis, making them difficult to detect. In skeletal muscle, a tissue characterized by little cellular proliferation, Pax7$^+$ cells are normally quiescent, only to become reactivated after injury. In contrast, in the testis,

Pax7^{+} spermatogonia are highly proliferative and continually replenish spermatogenesis.

Pax7 as a testis stem cell marker

Our data are consistent with a model where Pax7^{+} A_{single} spermatogonia function as stem cells in the adult testis. The fact that only a minority of A_{single} spermatogonia are Pax7^{+} demonstrates that the A_{single} population is more heterogeneous that some models propose, although elegant studies previously suggested that only a subset of A_{single} spermatogonia function as true stem cells (23, 127). Our studies indicate that the fraction of A_{single} spermatogonia that are Pax7^{+} is in the range of 1-10% (16). We speculate that Pax7^{+} spermatogonia sit at the top of the differentiation hierarchy, further suggesting that there are other subsets of A_{single} spermatogonia—perhaps defined by currently unknown markers—that function as transit-amplifying intermediates prior to differentiating to A_{pair} spermatogonia (**Figure 6.21**). However, other models are possible (128, 129), necessitating future investigations to gain a complete understanding of the cellular hierarchies underlying stem cell maintenance and differentiation in the mammalian testis.

Some have argued that spermatogonial stem cell transplantation represents a gold standard and is the only reliable assay for studying testis stem cell activity. Reconstitution of a self-maintaining cellular clone in a host organ is indisputable evidence that the cell of origin functioned as a stem cell in the assay. However, other investigators in the stem cell field have challenged the assumption that

transplantation assays recapitulate stem cell function in native, undisturbed organs, and have pointed out limitations inherent in transplantation assays (130). These concerns are valid for spermatogonial stem cell transplantations (127-129, 131) particularly since transplantation requires treatments (cell dissociation in the donor, nearly complete germ cell ablation in the host) that may strongly stimulate regenerative potential in ways that are not fully understood. There is an important distinction to be made between actual stemness and the potential for stemness. Transplantation assays are clearly useful for studying the latter, but do not necessarily accurately reflect the former (130). Future investigations are needed to define plasticity with respect to actual stemness versus stemness potential (132) in the adult testis.

Here, we took advantage of lineage tracing as a method to explore the stem behavior of a novel population of spermatogonia defined by Pax7$^+$ expression. We propose some criteria by which stem cell lineage tracing studies should be evaluated in the context of the adult testis, in the addition to the requirement for full-lineage maturation. First, we believe one important criterion is that the labeled germ cell clones begin as single cells. For example, lineage tracing initiated with a Cre driver expressed in broad subsets of spermatogonia (e.g. Foxo1$^+$ or Plzf$^+$ spermatogonia) would initiate labeling in $A_{single} \rightarrow A_{al16}$ spermatogonia including larger chains of spermatogonia, only a few of which represent actual stem cells. Extending this logic to our study, it is possible that only a subset of Pax7$^+$ spermatogonia function as stem cells, although the remarkable rarity of Pax7$^+$ spermatogonia is one argument against this possibility. Another criterion we believe

should be considered is the long-term perdurance of labeled clones. Such perdurance excludes the possibility that the labeled cells represent transit-amplifying intermediates, which would be diluted out and thus disappear with time. In the lineage tracing studies with the *mT/mG* reporter, we studied clones for up to 16 weeks (112 days), and observed no decrease in clone numbers, while the duration of spermatogenesis in mice is approximately 40 days (114).

Lack of genetic requirement for Pax7 in normal spermatogenesis in the mouse

In preliminary genetic studies, we did not find evidence for a functional requirement for *Pax7* in spermatogenesis. Germ-cell specific *Pax7* inactivation (confirmed by lack of Pax7 protein in germ cells) did not result in male infertility or have a discernable impact on spermatogenesis. It will be interesting to study the impact of *Pax7* inactivation in spermatogonial stem cell cultures, which may exhibit phenotypes not apparent *in vivo*. Challenging these conditional knockout mice with busulfan, however, demonstrated that lack of Pax7 caused a delayed spermatogenic recovery, a finding that should be further explored, particularly as the number of animals analyzed was relatively small and busulfan was tested at only one concentration.

The lack of a functional requirement for fertility in the undisturbed testis—at least under laboratory conditions—may be surprising given the phylogenetic conservation of $Pax7^+$ spermatogonia. On the other hand, several other conserved and canonical stem cell markers like Lgr5 (gut) and CD150 (hematopoiesis) are also dispensable for stem cell function in the respective organs where they serve as

useful markers (133-136). Although *Lgr5* conditional inactivation in intestinal epithelium yielded no apparent phenotype, simultaneous inactivation of *Lgr5* and *Lgr4* (which is expressed more broadly than *Lgr5*) enhanced an intestinal crypt loss phenotype observed with *Lgr4* (135). It is similarly possible that other factors—perhaps other *Pax* genes—are functionally redundant with *Pax7* and compensate for its loss, although we did not identify any *Pax* genes that were specifically expressed in SSCs in gene expression analyses. Furthermore, the floxed allele (*Pax7* $^{tm1.1Fan}$) used for this study was recently found to give rise to a hypomorphic mutation that expresses low levels of a truncated Pax7 protein from an alternative ATG start site, and thus does not appear to be a true biological or phenotypic null (52). In the more recently described floxed allele *Pax7* $^{tm1.1Thbr}$, the transcriptional start site and the first three exons are floxed, preventing the generation of any mRNA from the *Pax7* locus following Cre-mediated recombination (75). Thus, even though Pax7 protein is clearly greatly reduced in the conditional knockout analysis we performed with *Pax7* $^{tm1.1Fan}$ (**Figure 6.19,** E), it will be of interest to conduct future investigations with the *Pax7* $^{tm1.1Thbr}$ allele.

Implications for iatrogenic male infertility

Infertility is a common and well-known complication of cancer treatment that profoundly affects men and boys (120). Virtually all standard therapies (e.g. cytotoxic chemotherapies, as well as radiotherapy) are highly toxic to the male germline. The likelihood of infertility with chemotherapy is drug-specific and dose-related. Alkylating agents pose the highest risk of infertility, with platinum analogs,

anthracyclines, and nitrosoureas posing an intermediate level of risk (31). The germline is also very sensitive to radiation-induced damage. Doses of 1.2 Gray and higher are associated with an increased risk of infertility (31).

Remarkably, murine Pax7$^+$ spermatogonia proved resistant to both radiotherapy and chemotherapy. They not only survived the immediate aftermath of these genotoxic insults but rapidly expanded, forming clusters of Pax7$^+$ spermatogonia never observed in normal, untreated mice. Lineage tracing studies confirmed that Pax7$^+$ spermatogonia contribute to the restoration of spermatogenesis. Future studies will be needed to more fully define the extent of the role of Pax7$^+$ spermatogonia as spermatogenic recovery cells, and determine the relative contributions of Pax7$^+$ vs. other spermatogonial subtypes to spermatogenic recovery. It is also interesting to consider the possibility that Pax7$^+$ spermatogonia might contribute to the recovery of fertility in cancer patients, or that their failure to recover might account for permanent sterilization following chemotherapy or radiotherapy. If so, an improved understanding of the biological pathways regulating the behavior of Pax7$^+$ spermatogonia might someday lead to strategies to protect the male germline in cancer patients. It will also be interesting to explore the biological mechanisms that render Pax7$^+$ spermatogonia resistant to genotoxic stresses.

The resistance of Pax7$^+$ spermatogonia to both radiation and chemotherapy argues against models where resistance is mediated by active drug efflux (MDR1 or other transporters), as is the case with several types of stem cells (e.g. the “side population” effect due to the efflux of fluorescent dyes) (137, 138). In closing, Pax7$^+$

spermatogonia are a rare but functionally-important stem cell population in the healthy adult testis, and also serve an important role in spermatogenic recovery following injury to the germline, such as occurs following chemotherapy or radiotherapy. That $Pax7^{+}$ spermatogonia are rapidly cycling and yet resistant to such stress are notable aspect of their biology.

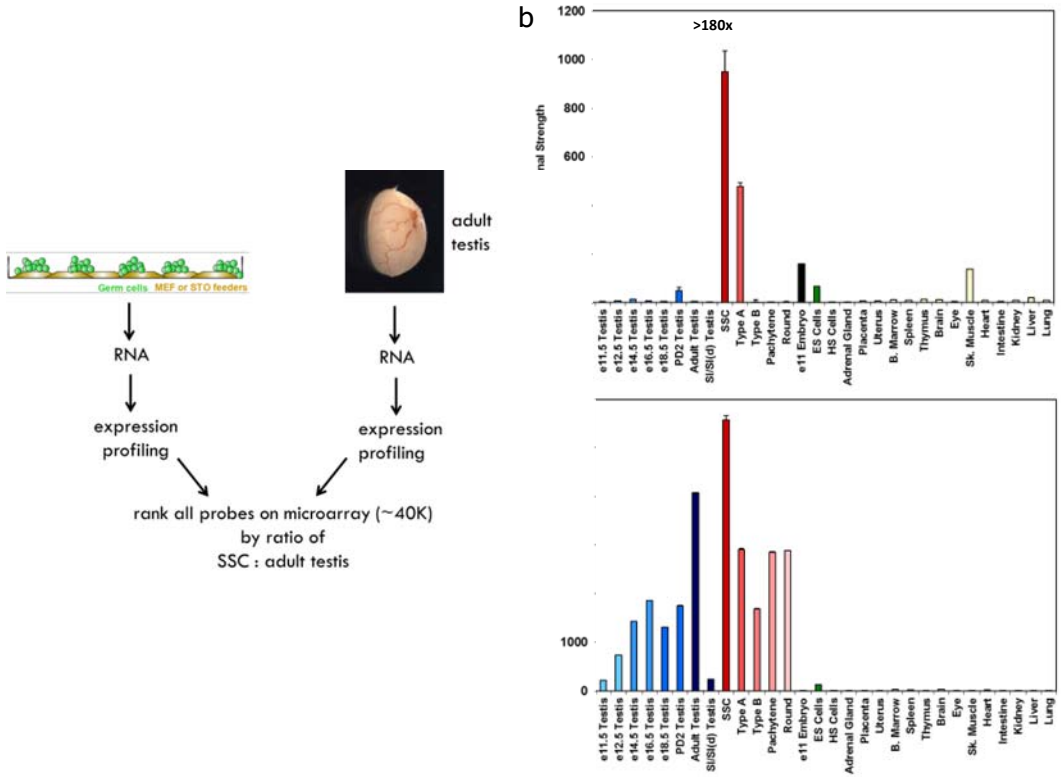

Figure 6.1: Digital Northern analysis identifying Pax7 as potential adult testis germline stem cell marker. (A) General RNA-based approach to identify markers that were highly expressed in cultured SSCs relative to adult testis. (B and C) Relative expression levels of (B) *Pax7* and (C) *Ddx4* across multiple samples. Error bars denote SEM. *Pax7* mRNA levels were >180-fold higher in established spermatogonial cultures relative to adult testis. SSC, cultured SSCs; Sl/Sl(d), $Kitl^{Sl}/Kitl^{Sl-d}$ germ cell–deficient adult testes; ES, embryonic stem; HS, hematopoietic stem.

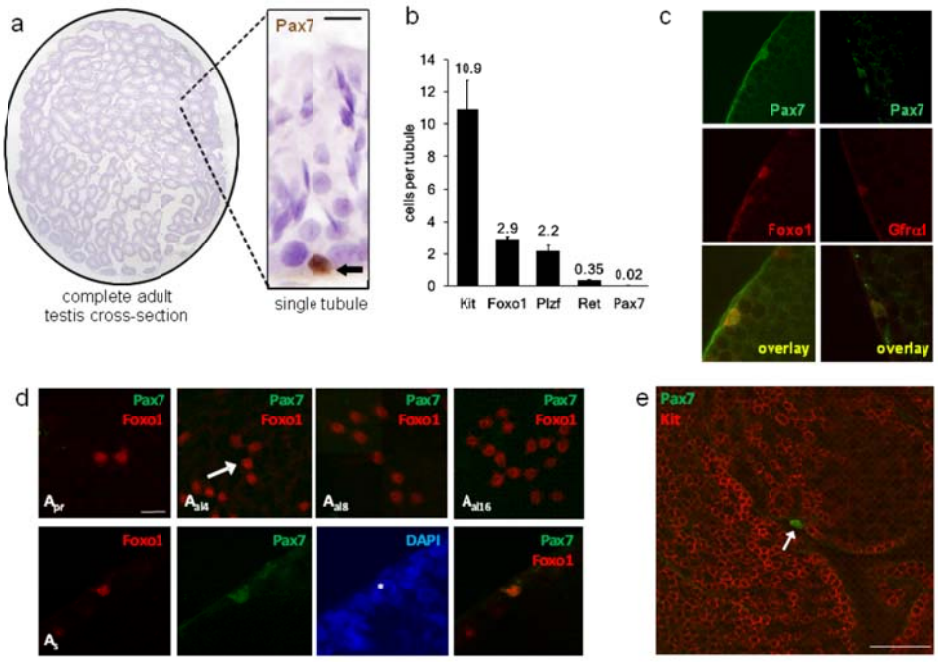

Figure 6.2: Pax7⁺ spermatogonia in normal testes. (A) Rarity of Pax7⁺ cells in adult (6-week-old) testis cross-section. Arrow denotes a Pax7⁺ cell within a single seminiferous tubule. (B) Relative number of spermatogonia positive for known markers compared with Pax7 in tissue sections, with >90 tubules counted per testis. Error bars denote SEM of averages derived from 3 6-week-old animals. (C) Double-labeling (confocal microscopy) showing that Pax7⁺ cells were Foxo1⁺ and Gfrα1⁺ (representative examples among ≥10 Pax7⁺ cells). Basement membrane staining is nonspecific. (D) Foxo1 and Pax7 double-labeling of A_{single}, A_{pair}, and A_{al4}–A_{al16} chains, visualized by confocal microscopy. Pax7⁺ spermatogonia were Asingle spermatogonia; larger chains did not contain Pax7⁺ spermatogonia. Arrow indicates an A_{al4} chain. Bottom panels show different channels for the same field of a single Pax7⁺Foxo1⁺ spermatogonium (asterisk in DAPI channel). (E) Kit and Pax7 double-labeling (confocal microscopy) showed that Pax7⁺ spermatogonia (arrow) were

isolated (i.e., A_{single}) and Kit^{-}. No $Kit^{+}Pax7^{+}$ spermatogonia were observed. Pax7 was nuclear, whereas Kit was membrane-associated, as expected. Image shows 3 tubules optically sectioned close to the level of the basement membrane to visualize large numbers of spermatogonia. Scale bars: 10 μm (A); 25 μm (C and D); 50 μm (E).

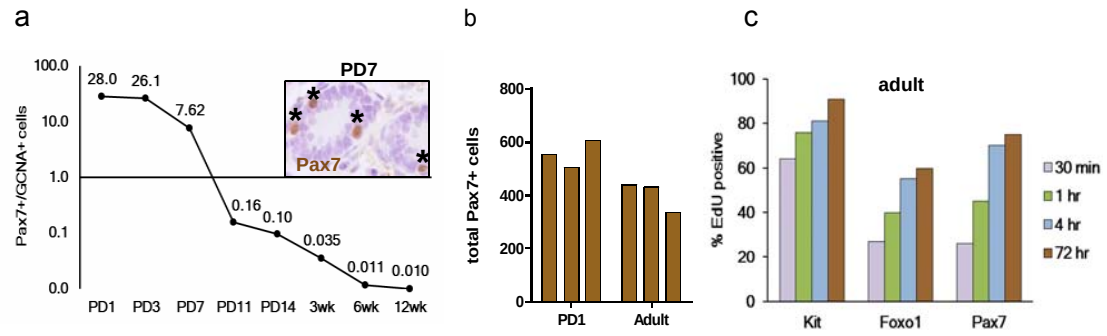

Figure 6.3: Pax7⁺ spermatogonia make up a higher percentage of germ cells in the neonatal versus adult testis. (A) Pax7⁺ cell frequency, expressed as a percentage of total GCNA⁺ cells. Inset: Pax7 IHC at PD7, showing several Pax7⁺ spermatogonia (asterisks). Magnification, ×250. (B) Counts of total Pax7⁺ cells by IHC of serially sectioned PD1 and adult testes (n = 3). Each bar represents a single testis. Total numbers were similar in neonatal and adult testes. (C) 6-week-old animals were injected with EdU, and testes were harvested after the indicated times. The experiment was repeated twice with similar results.

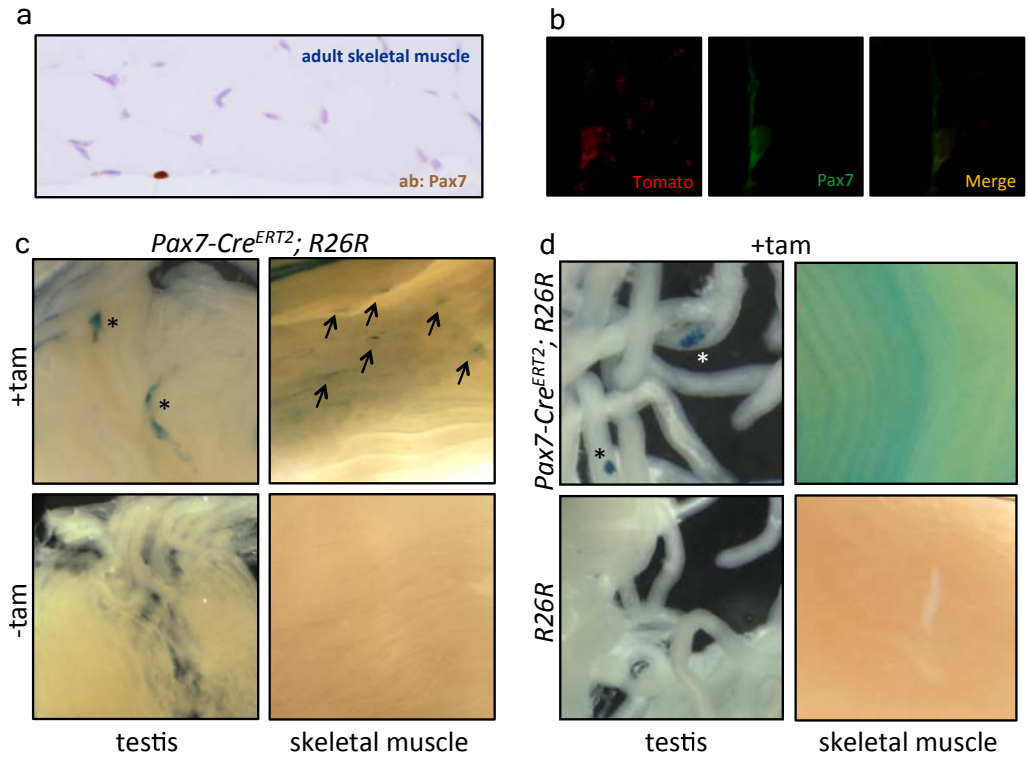

Figure 6.4: Validation of reagents employed in this study. (A) α-Pax7 antibody shows expected pattern in adult skeletal muscle, with single labeled cell consistent with satellite cell in field shown (note nuclear localization). Immunohistochemistry was conducted by identical protocol used for testis. For B-C, seminiferous tubules were separated from the capsule and gently disaggregated with forceps. (B) Co-localization of endogenous Pax7 and reporter by immunofluorescence in mice harboring *Pax7-Cre* ^{ERT2} and nuclear *tdTomato* reporter. Mice were treated with tamoxifen at PD14 and testes harvested at PD17. All (25/25) labeled clones analyzed by confocal microscopy showed Pax7 expression demonstrating faithful expression of *Pax7-Cre*^{ERT2} in Pax7^{+} spermatogonia. (C) Comparison of adult *Pax7-Cre* ^{ERT2}; *R26R* mice (6 weeks of age) treated with tamoxifen versus untreated

controls. Testes were harvested after 6 weeks. Note absence of labeled cells in untreated animals, confirming induction of Cre by tamoxifen. Asterisks denote labeled clones, while arrows point to muscle satellite cells. (D) Comparison of *Pax7-Cre^{ERT2}*; *R26R* mice vs. *R26R* controls treated with tamoxifen at PD2 and harvested at PD21. Asterisks denote labeled clones. Note absence of β-galactosidase activity in control samples. More diffuse pattern in skeletal muscle is consistent with early activation of the reporter.

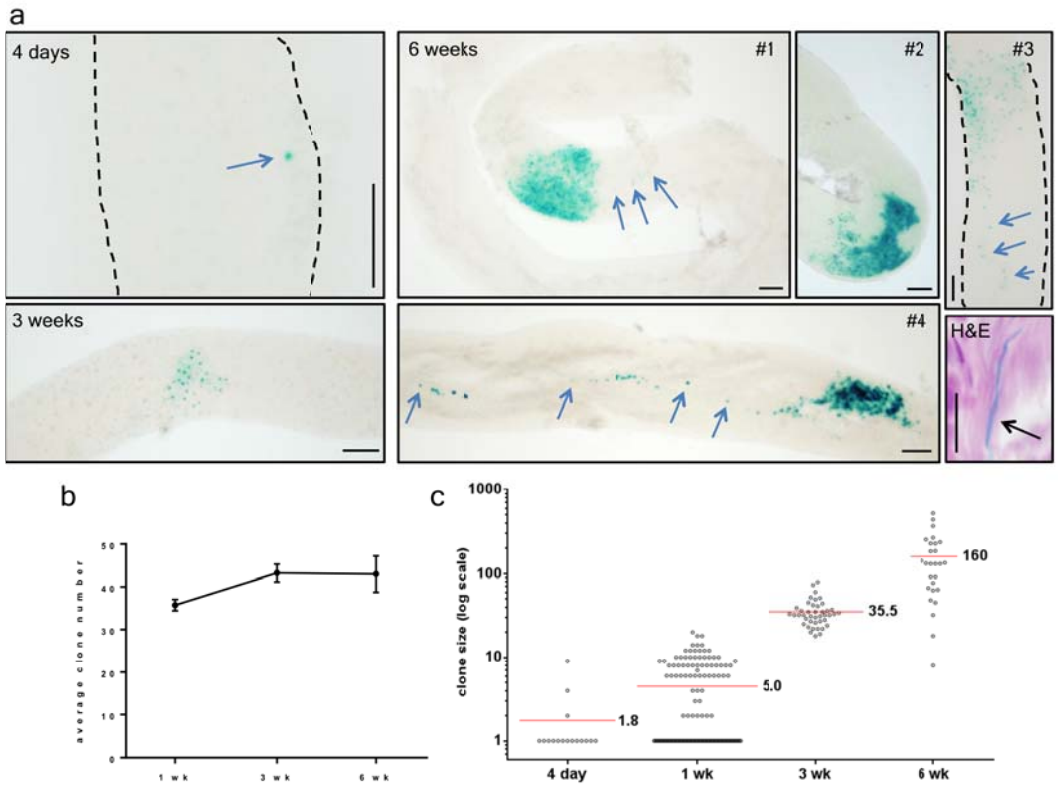

Figure 6.5: Lineage tracing of Pax7⁺ descendants in *Pax7-Cre^{ERT2}; R26R* testes. Mice were treated with tamoxifen at 6 weeks of age then aged for the indicated intervals. (A) Representative clones at 4 days, 3 weeks, and 6 weeks. Dashed lines demarcate tubule borders. Arrows denote a 1-cell clone at 4 days or isolated Asingle spermatogonia at the periphery of larger clones at 6 weeks. All marker-expressing cells in these fields are considered clonal because there were no additional marked cells in the tubule. The H&E-stained section of Xgal-treated testis at 6 weeks showed a single-labeled (blue) elongate spermatid tail among many unlabeled (pink) spermatid tails in the tubular lumen. Other labeled spermatid tails were outside the field of view. Scale bars: 100μm; 10μm (H&E). (B) Average clone numbers in n = 4 testes. The 1-week time point may represent undercount due to difficulty in

visualizing single-cell clones, or marker expression lag. Clone numbers were consistent with the presence of approximately 400 $Pax7^+$ cells per testis and 10% recombination efficiency for *Pax7-Cre^{ERT2}* after tamoxifen administration (31). (C) Clone size. Red bars denote means. Larger clones were composed of large labeled zones and peripheral smaller chains including A_{single} spermatogonia.

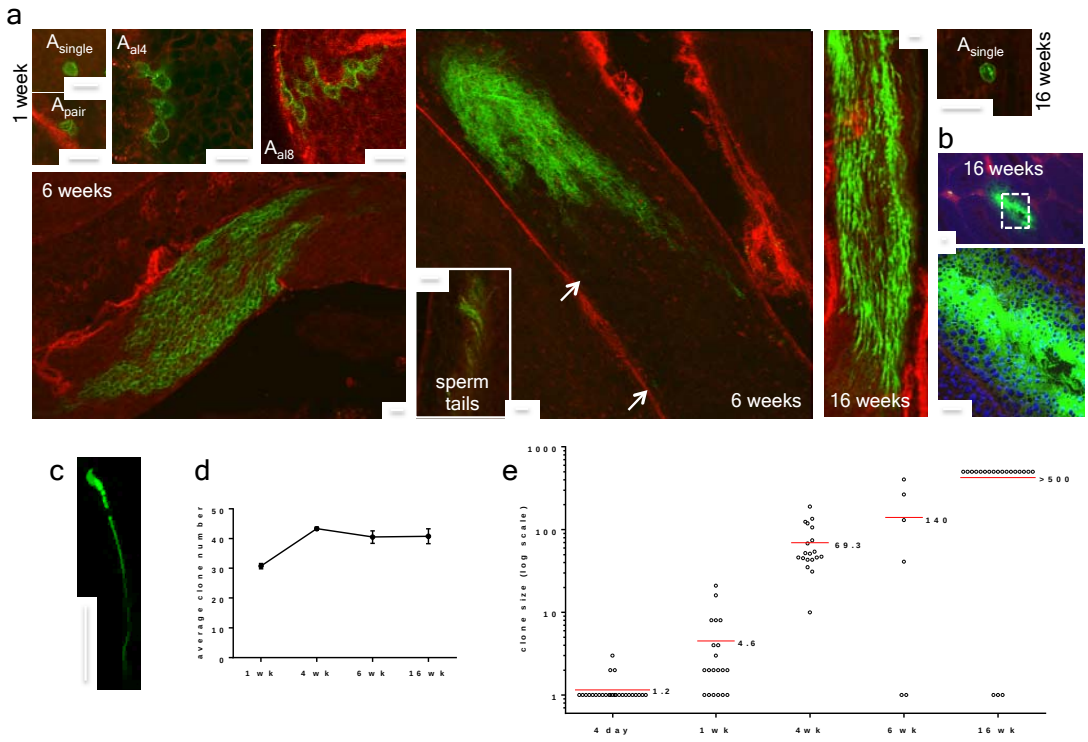

Figure 6.6: Lineage tracing of Pax7⁺ descendants in *Pax7-Cre^{ERT2};mT/mG* testes. Adult males were treated with tamoxifen at 6 weeks of age, then aged for the indicated intervals. (A) Clone morphology by confocal microscopy of isolated tubules. Representative A_{single}, A_{pair}, A_{al4}, and A_{al8} clones 1 week after tamoxifen administration are shown. Other panels show larger clones at 6 weeks; arrows indicate detached A_{single} spermatogonia that were part of larger clones. Inset: elongated spermatid tails in tubular lumen. Clones >500 cells could not be reliably counted. Larger clones were associated with smaller separate chains at their periphery, including A_{single} spermatogonia. The few 1-cell clones at 6–16 weeks represent A_{single} spermatogonia too distant from the nearest clone to be confidently identified as part of it, but may reflect long-distance migration. Green motile sperm were observed in the epididymis. (B) Clone morphology in tissue sections (16 weeks

after tamoxifen). Pax7^{+} descendants gave rise to all spermatogenic stages, as evidenced by circumferential full-thickness labeling of all spermatogenic stages throughout the tubule. Tissue sections were counterstained with DAPI. (C) Labeled sperm from epididymis showing bright green fluorescence and characteristic hook morphology. The majority of sperm did not exhibit fluorescence, and control epididymides did not contain spermatozoa with comparable fluorescence (i.e., the signal shown is not background autofluorescence of sperm). (D) Average clone number in n = 4 testes. Clone numbers did not decrease over time. (E) Clone size. Red bars denote means. Larger clones included detached smaller chains and A_{single} spermatogonia. Scale bars: 25μm.

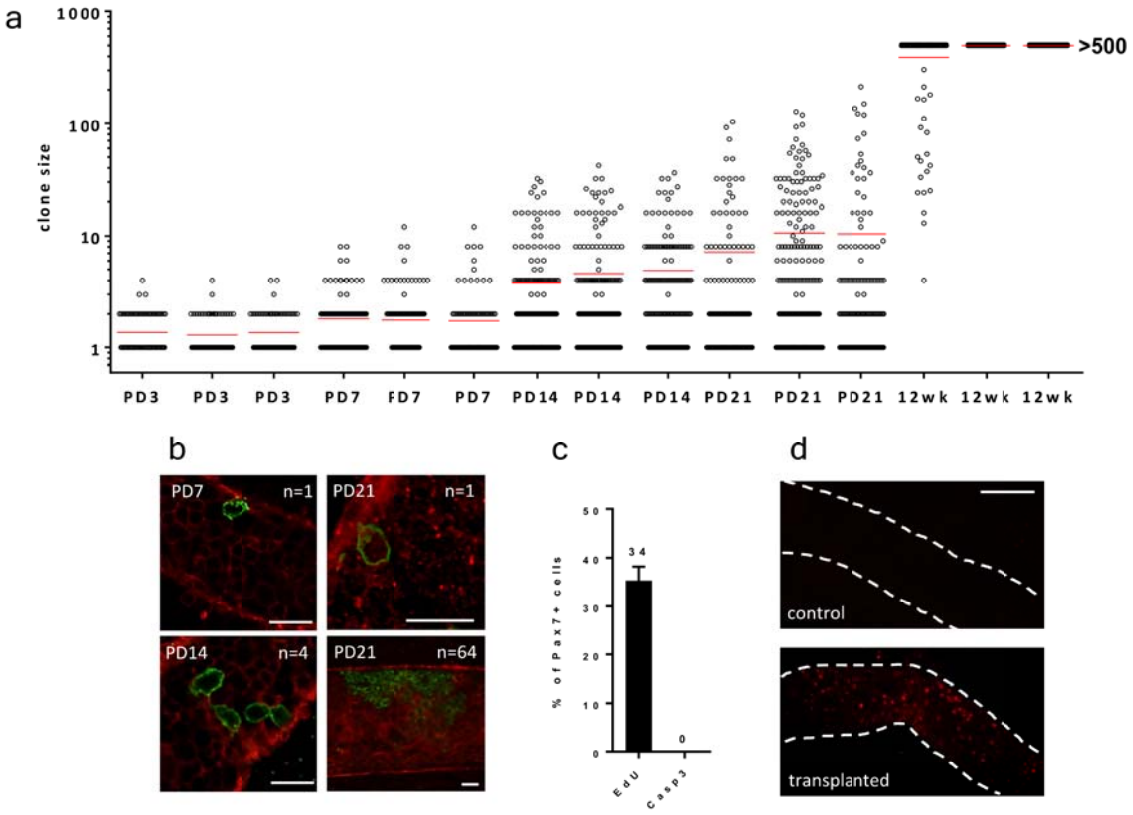

Figure 6.7: Pax7⁺ spermatogonia have long-term stem potential in vivo, and their descendants function as stem cells in transplantation assays. For PD3 time points, tamoxifen injections were performed at PD1 and PD2; for later time points, tamoxifen administration was performed for 3 consecutive days starting at PD3. (A) Clone size. Each column represents 1 testis from separate animals (total *n* = 15); red bars denote means. Note that many labeled Asingle spermatogonia were present at PD21, demonstrating that PD21 Pax7⁺ spermatogonia are derived from neonatal Pax7⁺ spermatogonia. Clones grew over time and persisted in aged animals (12 weeks). (B) Representative clone morphologies by confocal microscopy (*n* denotes number of cells in labeled chain shown); *z* stacks confirmed cell counts and

A_{single} status. (C) Mitotic and apoptotic indices of $Pax7^+$ cells at PD3 (*n* = 3 animals) demonstrated that early $Pax7^+$ cells were highly proliferative and not characterized by significant apoptosis. Error bars denote SEM. (D) Transplantation assay. A *Pax7-Cre^{ERT2};tdTomato* donor was treated with tamoxifen at PD3. Testes were disaggregated at PD14 and transplanted into germ cell–deficient *Kit^{W}/Kit^{W-v}* hosts, which were sacrificed after 4 weeks (*n* = 3). All hosts (but no controls) showed multiple labeled clones (i.e., 15–20); representative examples are shown. Scale bars: 25μm (B); 100μm (D).

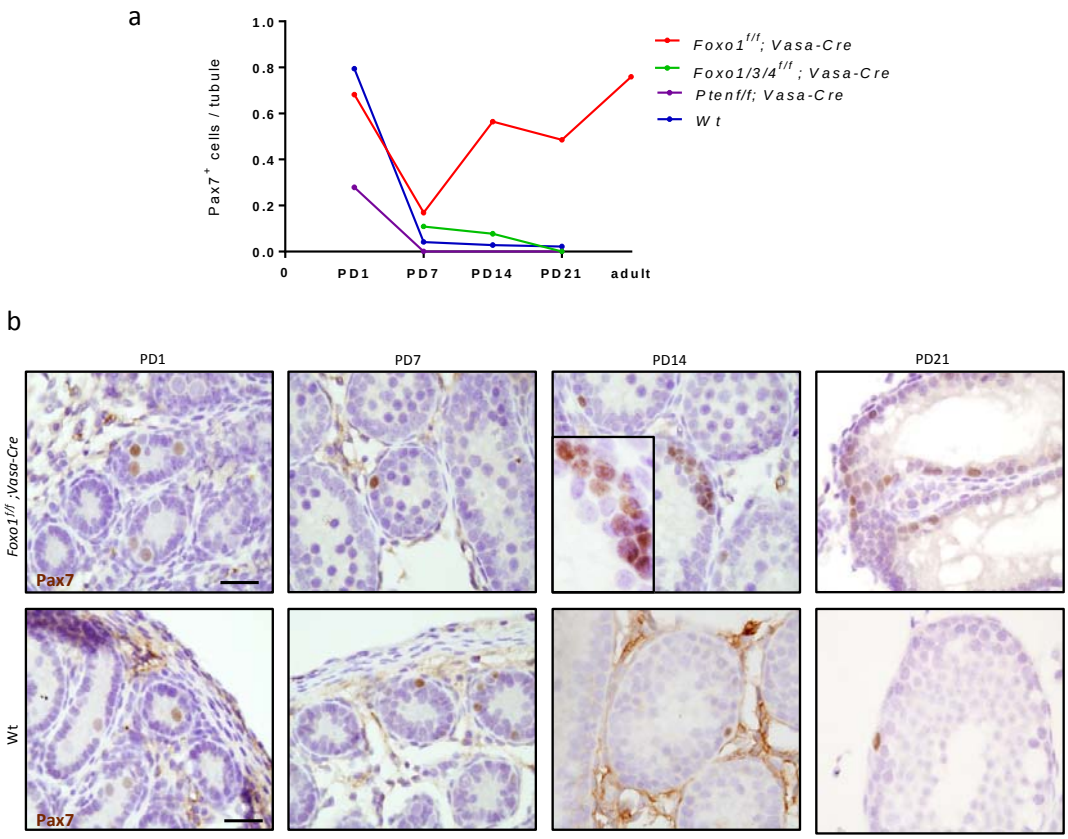

Figure 6.8: Pax7⁺ spermatogonia persist in genetic models of infertility. (A) In three distinct genetic mouse models of infertility, Pax7+ spermatogonia perdure even when the majority of germ cells are ablated. (B) Histology of Pax7+ spermatogonia. Large clumps of Pax7+ spermatogonia could be observed, that had never before been seen in WT testis. Scale = 25µm.

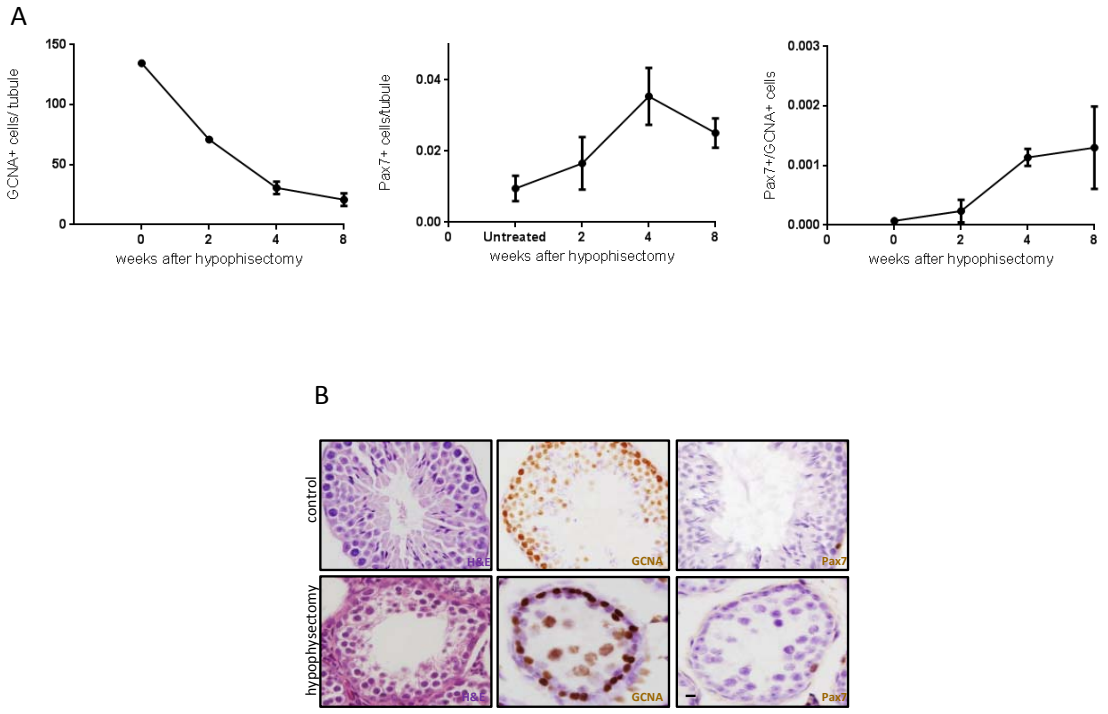

Figure 6.9: Pax7⁺ spermatogonia persist after hypophysectomy. (A) After surgical loss of the pituitary, nearly all germ cells are ablated. However, both the number of Pax7⁺ spermatogonia per tubule and the number of Pax7⁺ spermatogonia per remaining germ cell increases, suggesting that Pax7⁺ could be increasing to replenish the germline. (B) Histologic analyses showing that even while most germ cells are ablated after hypophysectomy, Pax7⁺ spermatogonia persist. Scale = 10μm.

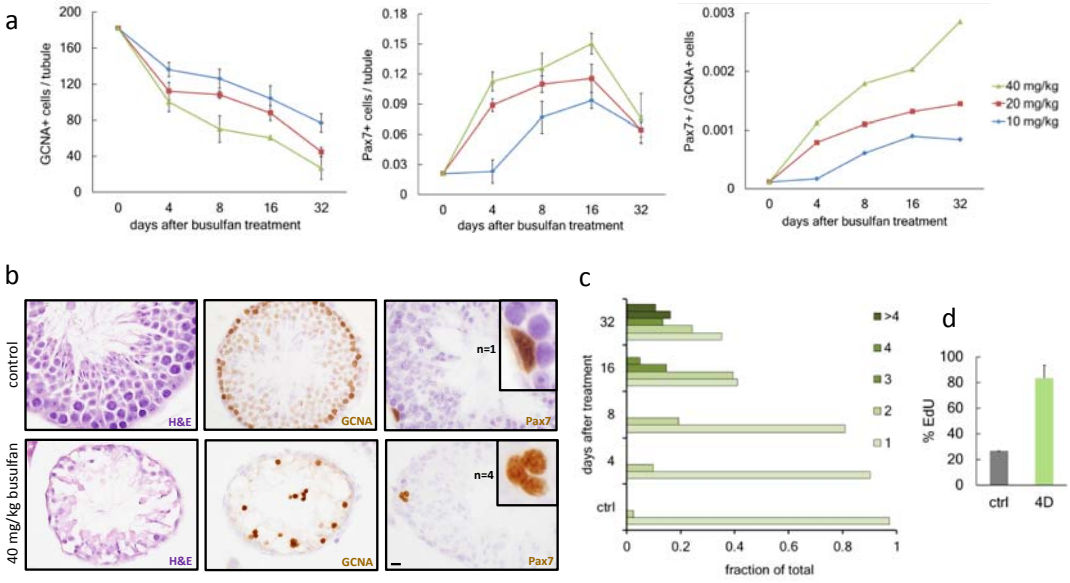

Figure 6.10: Germline ablation with busulfan has dose-dependent effects on Pax7⁺ spermatogonia. (A) Number of cells expressing GCNA (pan-germ cell marker) and Pax7. Error bars denote SEM for *n* = 3 animals at 6 weeks of age. (B) H&E and immunostained sections 16 days after a single dose of 40 mg/kg busulfan. GCNA stains all germ cells to the round spermatid stage. Busulfan resulted in expansion of Pax7⁺ clusters never observed in untreated testes; an example of a 4-cell group is shown (insets; enlarged ×4). (C) Fractions of Pax7⁺ clusters of different sizes. For each time point, fractions add up to 1. The difference in cluster sizes (1 versus ≥2) was highly statistically significant in untreated animals versus those treated with 40 mg/kg busulfan after 32 days (P = 2 × 10–9). (D) Percent EdU incorporation in Pax7⁺ spermatogonia 4 days after busulfan administration. Scale bar: 10μm.

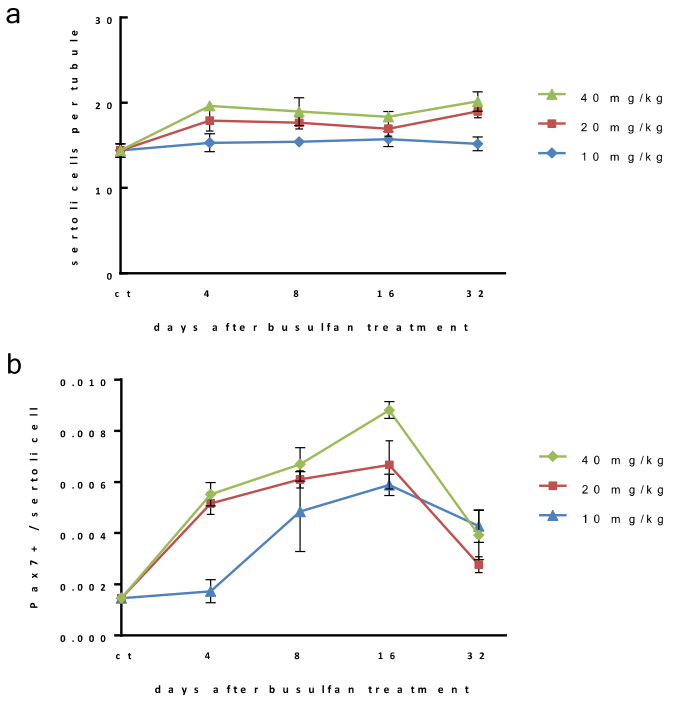

Figure 6.11: Number of Sertoli cells after busulfan treatment does not change. (A) Number of Sertoli cells per tubule after treatment with busulfan. Busulfan does not affect Sertoli cell number. (B) Pax7⁺ spermatogonia per Sertoli cell. The increase in the number of Pax7⁺ spermatogonia is not due to testis shrinking, as the increase is still observed when normalizing to Sertoli cell number.

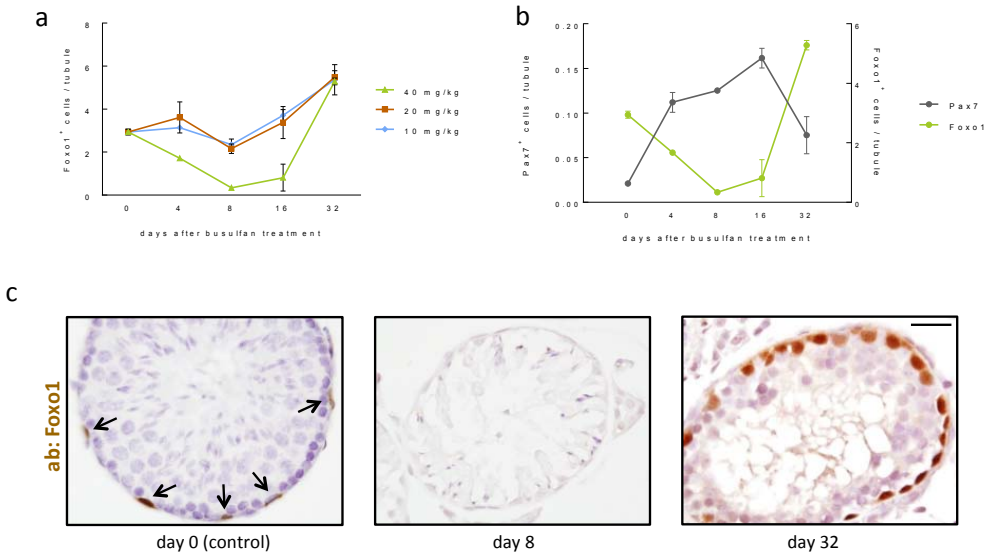

Figure 6.12: Counts of Foxo1⁺ spermatogonia after busulfan administration at 6 weeks of age. For each time point, *n* = 3 animals were analyzed; error bars denote SEM. (A) Foxo1⁺ spermatogonia per tubule. (B) Foxo1⁺ counts per tubule compared with Pax7⁺ counts. (C) IHC showing Foxo1⁺ spermatogonia (arrows). Unlike Pax7⁺ spermatogonia, Foxo1⁺ (undifferentiated) spermatogonia were not resistant to busulfan. Scale bar: 25μm.

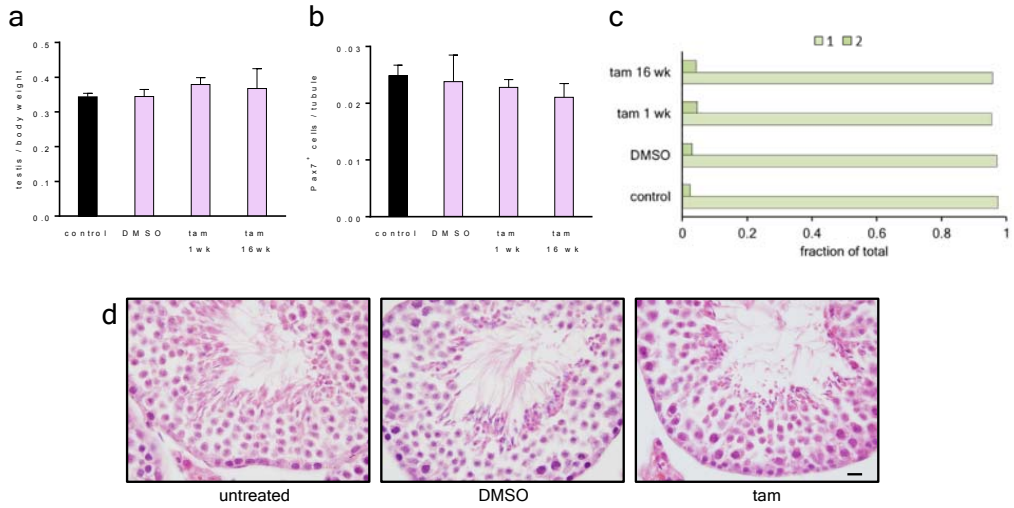

Figure 6.13: Neither tamoxifen nor DMSO have demonstrable impact on spermatogenesis or Pax7⁺ spermatogonia. Animals were treated at 6 weeks of age and euthanized 1 or 16 weeks later (n=3 animals per observation; error bars=SEM). (A) Testis weight expressed as percent of total body weight. (B) Pax7 counts in testes from control and treated mice. (C) Pax7 cluster sizes in control and treated animals.(D) Testis morphology and spermatogenesis are unaltered by DMSO or tamoxifen. Bar=10μm; all panels at same magnification.

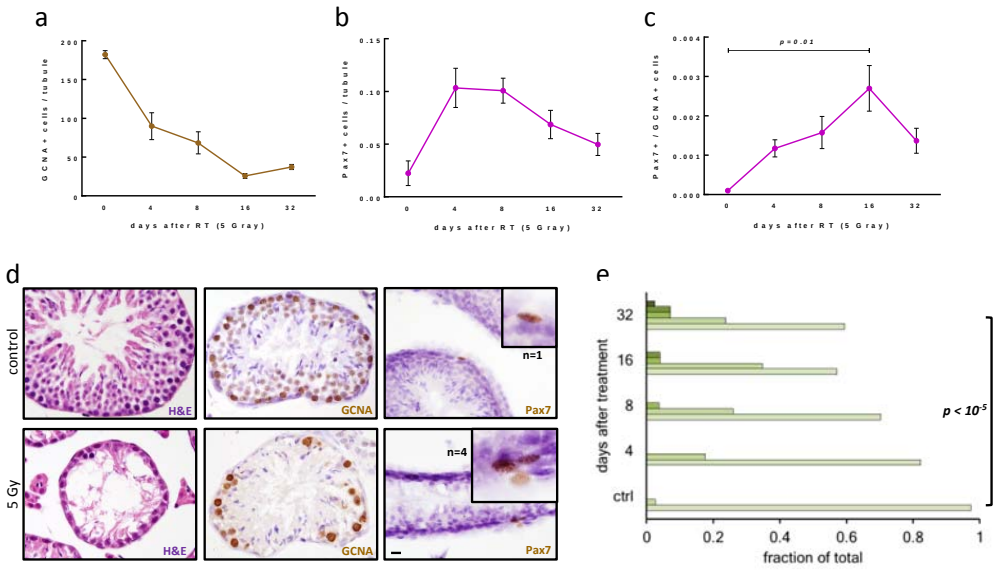

Figure 6.14: Pax7⁺ spermatogonia are selectively resistant to radiation treatment. Mice were subjected to a nonfractionated dose (5 Gray) of X-rays at 6 weeks of age. Testes were harvested at timepoints shown. For A-C, error bars=SEM for n=3 animals per timepoint. (A) GCNA⁺ cells per tubule. (B) Pax7⁺ spermatogonia per tubule. (C) Pax7 spermatogonia normalized to GCNA counts; P value calculated by unpaired t-test. (D) H&E or immunostained slides 16 days after irradiation. Bar=10μm; all panels at same magnification. (E) Fractions of Pax7+ clusters of different sizes (0 to 4); $p<10^{-5}$ by Fisher Exact Test for clusters of 1 vs. 2 or more at 16 days.

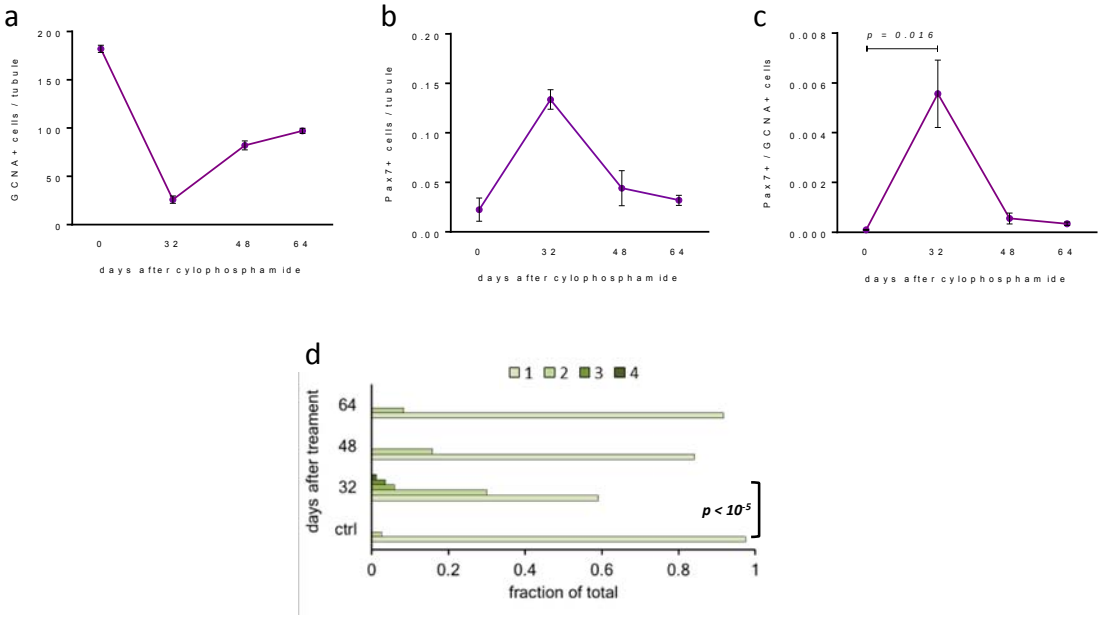

Figure 6.15: Pax7⁺ spermatogonia are selectively resistant to cyclophosphamide. Mice were treated with cyclophosphamide at 6 weeks of age. Cyclophosphamide is a relatively mild germ cell toxicant compared to busulfan, necessitating a multi-dose regimen (150 mg/kg every 5 days for 25 days). Animals were euthanized and testes harvested after the last dose. For A-C, error bars=SEM for n=3 animals per timepoint. (A) GCNA⁺ cells per tubule. (B) Pax7⁺ spermatogonia per tubule. (C) Pax7⁺ spermatogonia normalized to GCNA counts. P value calculated by unpaired t-test. (D) Fractions of Pax7⁺ clusters of different sizes (0 to 4); $p<10^{-5}$ by Fisher Exact Test for clusters of 1 vs. 2 or more at 32 days.

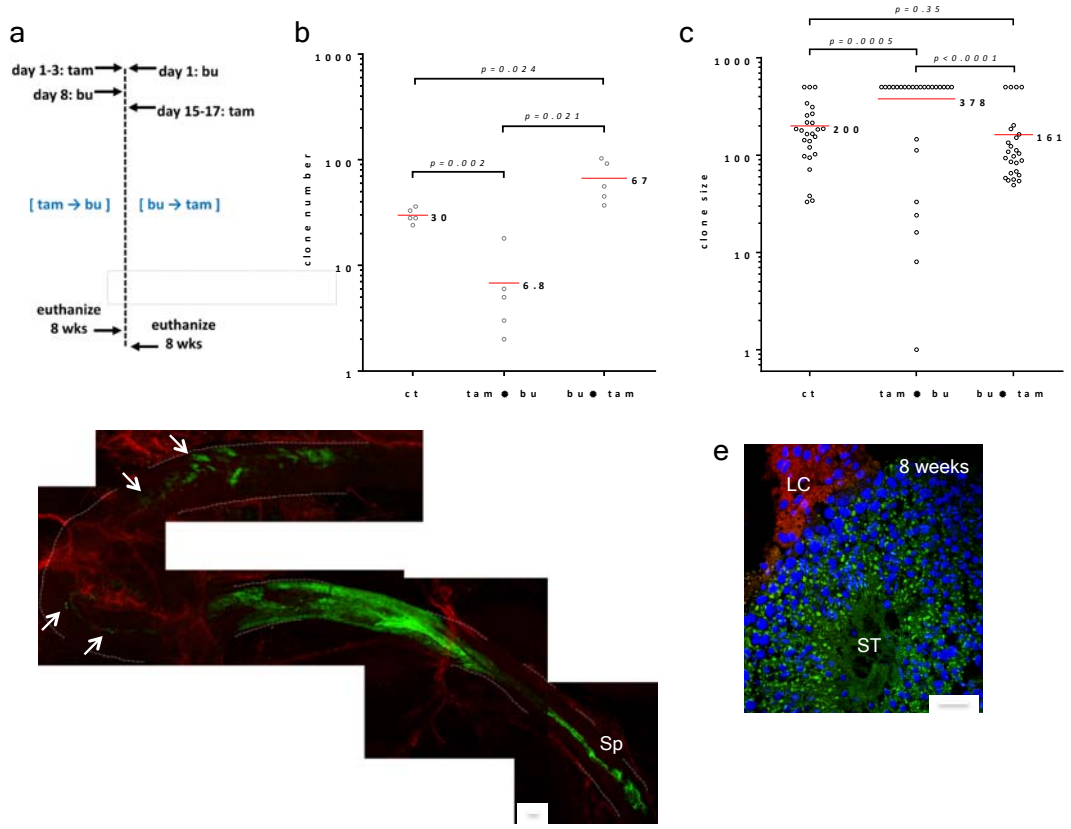

Figure 6.16: Lineage tracing of Pax7⁺ spermatogonia following busulfan (20 mg/kg) treatment of *Pax7-Cre^{ERT2} ;mT/mG* males at 6 weeks of age. (A) Schematic showing both busulfan lineage-tracing experiments. Testes were harvested 8 weeks after the last drug dose for each experiment. (B) Number of clones 8 weeks after busulfan administration. Each point represents 1 testis from 1 animal; red bars denote means; *P* values were determined by unpaired *t* test. (C) Clone size 8 weeks after tamoxifen administration. Red bars denote means; *P* values were determined by unpaired *t* test. (D) Composite image of representative large clone from tam→bu experiment. Tubule borders are highlighted with dashed lines. Sp, elongate spermatids (arrows denote individual cells or small groupings forming

a “trail” of cells). (E) Cryosection of testis from tam→bu experiment showing germ cell clone spanning the entire tubule. ST, seminiferous tubule; LC, Leydig cells. Scale bar: 200 μm (D); 25 μm (E).

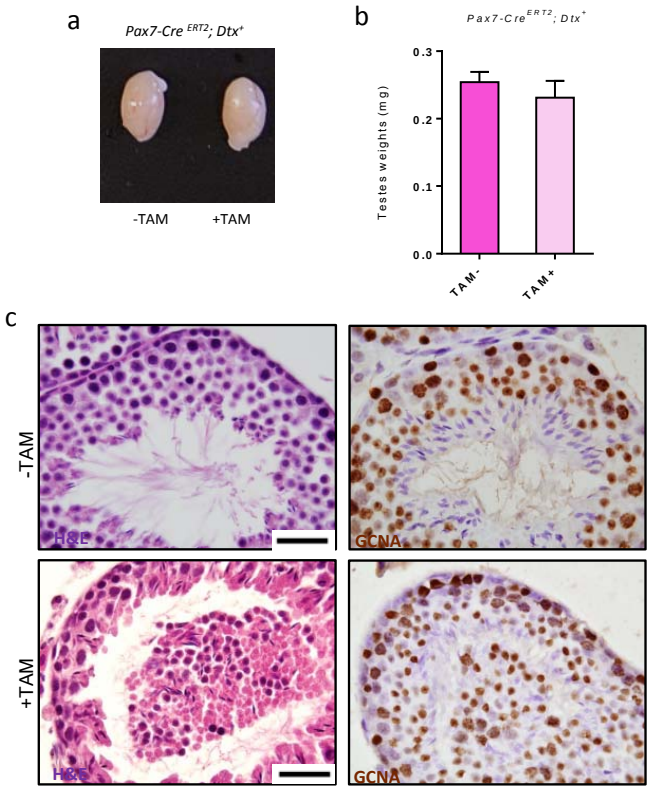

Figure 6.17: Pax7⁺ spermatogonia are not eliminated by DT. (A) *Pax7-Cre* ^{ERT2} *Dt⁺* testis are not any smaller when visually compared to controls, nor do they weigh less (B). (C) Histologic analysis of *Pax7-Cre* ^{ERT2} *Dt⁺* testis, demonstrating tubules where spermatogenesis has been disregulated, but not eliminated by loss of Pax7⁺ spermatogonia. Scale bar = 50µm.

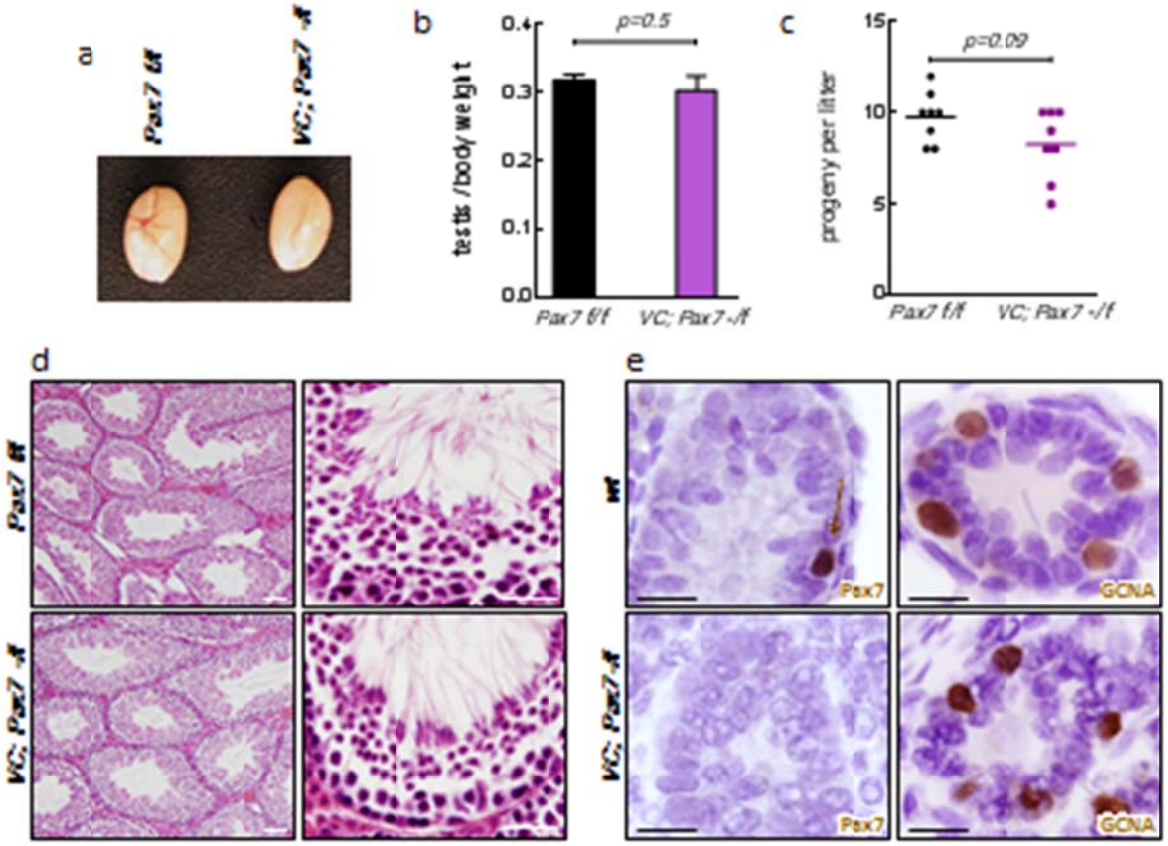

Figure 6.18: *Pax7* conditional knockout in the male germline. For each analysis, *n* = 3 animals were evaluated per genotype. (A) Testes from floxed *Pax7*$^{fl/fl}$ control and *Pax7* cKO (*VC;Pax7–/fl*) males at 6 months of age. No abnormalities or size differences were noted. (B) Testis weight expressed as percent of total body weight (6 months of age). (C) Fertility assays of 6 month-old males. Bars denote means. All floxed control and *Pax7* cKO males were fertile and sired litters of normal size. (D) Histological analyses at 6 months of age. No abnormalities in spermatogenesis or testis morphology were noted. (E) IHC analyses of *Pax7* cKO males at PD7. Pax7^{+}

spermatogonia were abundant and present in most tubules in wild-type controls (arrow), but absent in *Pax7* cKO tubules (multiple sections were stained and examined for each), confirming the specificity of the Pax7 antibody in testis sections. GCNA shows the presence of germ cells. Scale bars: 50μm.

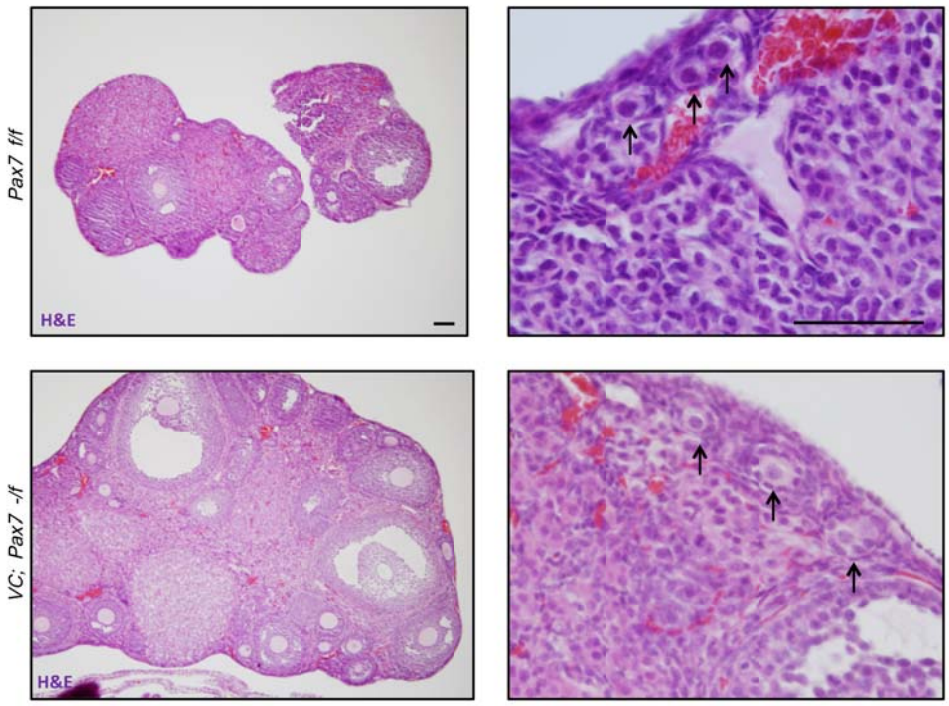

Figure 6.19: *Pax7* conditional knockout in the female germline. No difference in conditional knockout of Pax7 ovaries was observed. Follicles of all sizes were observed. Scale = 50μm.

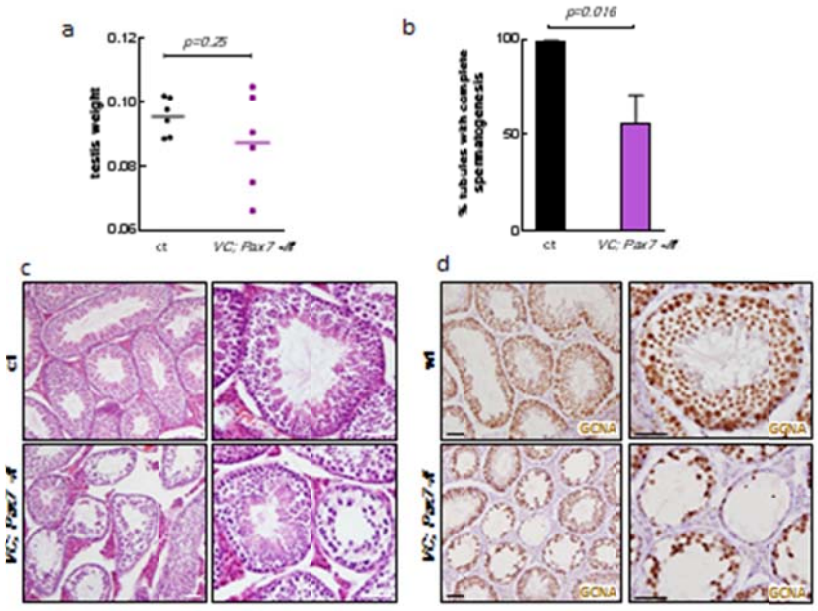

Figure 6.20: Loss of Pax7 is associated with delayed spermatogenic recovery after busulfan. (A) Testes from adult (>3 months of age) controls and *Vasa-Cre* (*VC*); *Pax7*$^{-/f}$ males were treated with a single dose of 20 mg/kg busulfan and allowed to recover for 8 weeks (testes from n=3 animals per genotype were analyzed). There was a trend towards lower testis weight in the conditional knockout animals and some of their testes were considerably smaller, but this did not achieve statistical significance. Bars=means. (B) Percent of tubules with complete spermatogenesis. *VC*; *Pax7*$^{-/f}$ males exhibited a significant lag in recovery of spermatogenesis, evidenced by higher numbers of tubules with decreased spermatogenesis, overall hypocellularity, and absence of full-lineage maturation (testes from n=3 animals per genotype). (C) Histological analyses 8 weeks after busulfan treatment. *VC*; *Pax7* testes contained tubules with grossly abnormal spermatogenesis, although some tubules were more affected than others. Bars=50μ.

(D) Immunohistochemical analyses 8 weeks after busulfan treatment. GCNA highlights complete or nearly complete recovery in control testes following busulfan. In contrast, in *VC*; *Pax7-/f* testes, germ cells were less abundant, with many tubules showing a much more limited recovery of spermatogenesis. Bars=50μm.

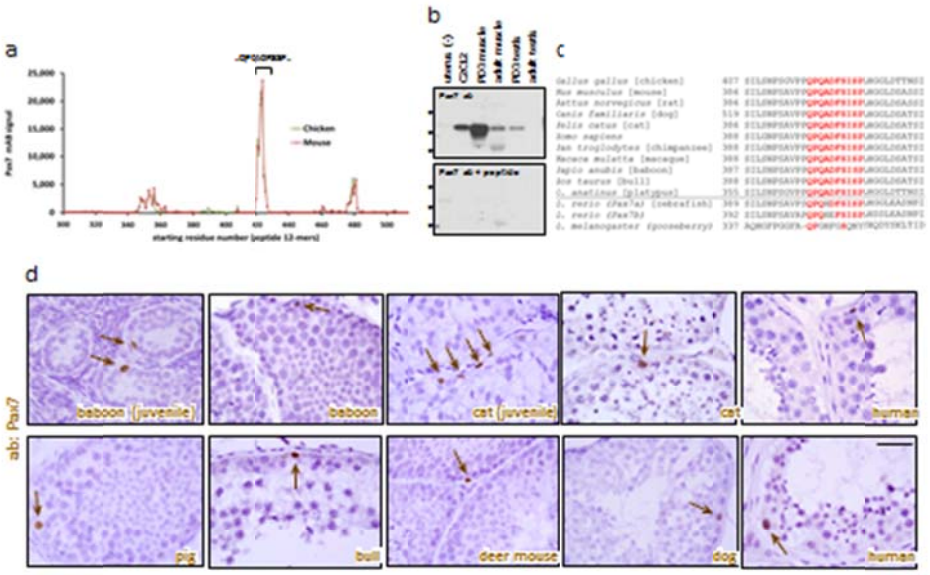

Figure 6.21 Pax7⁺ spermatogonia are conserved in mammals. (A) Epitope mapping of anti-Pax7 mouse monoclonal antibody (generated against chicken aa 320–523). Chicken and corresponding mouse polypeptide aa sequences were tiled as sequential 12-mers at 1-aa resolution. (B) Pax7 Western blot (uncropped to show all visible bands in lanes shown). Addition of blocking peptide (22 aa) confirmed that the anti-Pax7 monoclonal antibody bound to the QPQADFSISP epitope. C2C12, skeletal muscle myoblast cell line. Uterus was included as a negative control. Molecular weight markers denote 75, 50, and 37 kDa. (C) IHC of testes from 7 additional mammalian species, including juveniles for 2 species. Pax7⁺ spermatogonia (arrows) were rare and localized to the basement membrane. Scale bar: 25μm.

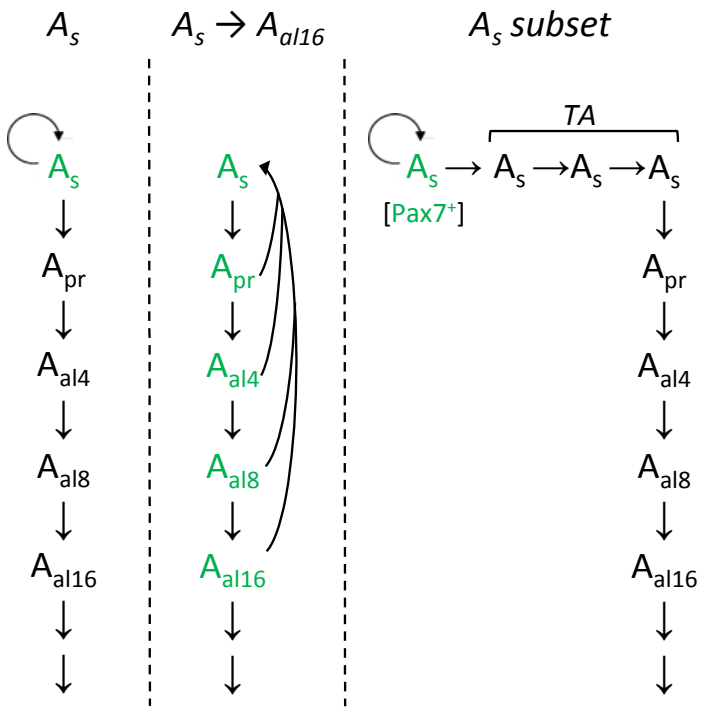

Figure 6.22: Models of stemness in mouse spermatogenesis. Spermatogonial subsets proposed as the bona fide stem cells are shown above each of the 3 models. In the classic A_{single} model (A_s), Asingle spermatogonia are homogeneous and share stem cell identity (green), having the capacity for self-maintenance (circular arrows; refs. 3, 4, 66). More recently, models have been proposed arguing for greater plasticity among undifferentiated ($A_{single} \rightarrow A_{al16}$) spermatogonia, with chain fragmentation representing one possible mechanism by which stemness is maintained or regenerated (5). Although fragmentation has been shown to occur in vivo, its contributions to stem cell maintenance under normal conditions or after chemotherapy/radiation have not been formally established. Our findings that only a subset of A_{single} spermatogonia expressed Pax7 and that these spermatogonia functioned as stem cells suggests a new A_{single} subset model, whereby Pax7+

spermatogonia are self-maintaining and may sit atop the hierarchy of spermatogenic differentiation. That A_{single} spermatogonia were heterogeneous and that only a subset functioned as stem cells was also suggested by previous studies (10, 67). If so, then this would suggest that some subset of A_{single} spermatogonia represent transit-amplifying (TA) intermediates. The number of such transit-amplifying steps between $Pax7^+$ A_{single} and A_{pair} spermatogonia is unknown. It will be interesting to determine whether ID4 and ERBB3, expressed in A_{single} spermatogonia, are expressed in overlapping or non-overlapping subsets of spermatogonia relative to Pax7 (9, 49, 50). Other models are possible, such as ones combining different aspects of these models (i.e., fragmentation with the presence of $Pax7^+$ spermatogonia, if fragmentation is confirmed as a functionally significant biological process).

Table 1. The QPQADFSISP *PAX7* epitope is perfectly conserved in mammals, but not zebrafish or *Drosophila*

Species	Sequence
Gallus gallus (chicken)	407 SILSNPSGVPP**QPQADFSISP**LHGGLDTTNSI
Mus musculus (mouse)	386 SILSNPSAVPP**QPQADFSISP**LHGGLDSASSI
Rattus norvegicus (rat)	386 SILSNPSAVPP**QPQADFSISP**LHGGLDSASSI
Canis familiaris (dog)	519 SILSNPSAVPP**QPQADFSISP**LHGGLDSATSI
Felis catus (cat)	386 SILSNPSAVPP**QPQADFSISP**LHGGLDSATSI
Homo sapiens (human)	388 SILGNPSAVPP**QPQADFSISP**LHGGLDSATSI
Pan troglodytes (chimpanzee)	388 SILGNPSAVPP**QPQADFSISP**LHGGLDSATSI
Macaca mulatta (macaque)	388 SILSNPSAVPP**QPQADFSISP**LHGGLDSATSI
Papio anubis (baboon)	387 SILSNPSAVPP**QPQADFSISP**LHGGLDSATSI
Bos taurus (bull)	388 SILSNPSAVPP**QPQADFSISP**LHGGLDSATSI
Ornithorhynchus anatinus (platypus)	355 SILSNPSGVPP**QPQADFSISP**LHGGLDTTNSI
Danio rerio (zebrafish), *Pax7a*	389 SILSNPSAVPS**QPQH**D**FSISP**LHGGLEASNPI
Danio rerio (zebrafish), *Pax7b*	392 SILSNPSAVAP**QPQ**HE**FSISP**LHSSLEASNPI
Drosophila melanogaster (fruit fly), *gsb-n*	337 AQHGFPGGFA**QP**GHFG**S**QNYYHQDYSKLTID

Table 6.1: The Pax7 epitope bound by the monoclonal antibody used in these studies is perfectly conserved in mammals, but not zebrafish or *Drosophila.*

CHAPTER 7: PAX7 IS EXPRESSED IN A RARE SUBSET OF PROSPERMATOGONIA

Pax7 is expressed in a small fraction of embryonic germ cells

The pre-spermatogonia residing in the embryonic testis are the cells which will eventually establish the SSC pool. However, it is currently unknown whether these precursor cells have predetermined cell fates, or if all cells have equal potential to become stem cells. Up until this point, all markers that are expressed in embryonic germ cells seemed to be expressed ubiquitously. For example, Foxo1, which marks only undifferentiated spermatogonia in the adult, is expressed in every prospermatogonia (**Figure 7.1**). In the neonatal period before PD3, Foxo1 is expressed in every or nearly every prospermatogonium, though there is difference between nuclear and cytoplasmic localization (14). However, even at this early timepoint, Pax7 is expressed in a fraction of germ cells, which led to the hypothesis that this heterogeneity in pre-spermatogonia could be observed even prior to birth, and that this heterogeneity could be related to their eventual cell fates, and that stemness could be determined earlier than previously thought.

To examine if this heterogeneity was evident even in the embryonic testis, I wanted to visualize Pax7 expression in testis cross-sections from e15.5-e19.5 Surprisingly, I found that even embryonically, Pax7 is expressed in rare subset of prospermatogonia (**Figure 7.2**). At e15.5, no expression of Pax7 was observed in at least three cross-sections of three mice each. By e16.5, Pax7 could be observed in approximately one cell per cross-section. Pax7 was predominantly nuclear, but some cytoplasmic staining of Pax7 could be observed. This could be due to the first

transcription of Pax7, where is it is located in the cytoplasm, before Pax7 can translocated to the nucleus to perform its function as a transcription factor. There was a moderate increase in the number of $Pax7^+$ pre-spermatogonia from e16.5 to e19.5. This increase in cell number cannot be due to divisions of $Pax7^+$ pre-spermatogonia, as at this point in development, the germline is quiescent (**Figure 7.2**). Thus, currently unknown factors may play a role in inducing Pax7 in pre-spermatogonia. Importantly, this demonstrates for the first time heterogeneity in marker expression in these germ cells. All other markers examined, including Foxo1, Sall4, Oct4, Ret, Stra8, and Kit appeared to be expressed in either all or no germ cells prenatally (**Figure 7.1-7.6**).

From historical data, the number of $Pax7^+$ prospermatogonia sharply increases in the neonatal period around PD1-PD3. However, it was unknown whether this spike occurred prior to this timepoint at birth, or if the spike was specific to these timepoints. I found that while there are more $Pax7^+$ pre-spermatogonia at PD0 than in embryonic timepoints, but are still not at the levels seen during PD1-PD3. This increase could be due to either induction of Pax7 or division of Pax7.

I sought to identify differences between $Pax7^+$ and $Pax7^-$ prospermatogonia from e18.5 to PD7. At e18.5, $Pax7^+$ prospermatogonia are easy to identify compared to earlier timepoints, and by PD7, prospermatogonia are thought to have become spermatogonia (3). I hypothesized that if $Pax7^+$ prospermatogonia are responsible for establishing the stem cell pool by PD7, they might be more proliferative than other germ cells. However, this was not the case, and the percentages of

Pax7$^+$/Ki67$^+$ and Vasa$^+$/Ki67$^+$ prospermatogonia are nearly identical (**Figure 7.2**). Furthermore, there is no difference in pHH3 positivity (data not shown). Thus, Pax7$^+$ prospermatogonia do not progress through the cell cycle more quickly than other types of spermatogonia.

Pax7+ prospermatogonia are more likely to be basal than other germ cells

While examining multiple embryonic sections containing Pax7$^+$ pre-spermatogonia, it seemed that these cells were more likely to be located basally than other germ cells, which are predominately located in the lumen of the seminiferous cords. I quantified this by counting the location of Pax7$^+$ and Vasa$^+$ pre-spermatogonia, and found that indeed, Pax7$^+$ pre-spermatogonia are much more likely to be basal from e16.5 to e19.5 (**Figure 7.7, p value**). However, there are clearly basal germ cells which do not express Pax7. At birth, the percentage of Pax7$^+$ pre-spermatogonia decreases at PD0 and PD1, but by PD3 nearly all Pax7$^+$ pre-spermatogonia are basal, as are all germ cells. This change in preference of location coincides with the spike of Pax7$^+$ pre-spermatogonia. One possible explanation to unify these two finding would be that Pax7 is induced in prospermatogonia, which causes these cells to dive to their position on the basement membrane.

In fact, Notch signaling has been implicated in the luminal to basal transition of germ cells. Constitutive activation of Notch in Sertoli cells causes embryonic germ cells to be located more basally (139, 140). This change in location was not accompanied by an immediate change in proliferation, suggesting that position on the basement membrane and exit from quiescence are linked, although we did not

see any difference in Ki67 staining between basal and luminal germ cells (139, 140). This study also detected Notch signaling in embryonic, fetal, and adult testis with the use of a Notch GFP reporter allele. However, the GFP used was a stabilized form of the protein and thus may persist in cells longer than the actual Notch signal (140). I sought to visualize Notch signaling components in sections of embryonic and neonatal testis via IHC. I found that Notch1, the Notch protein examined in the aforementioned study was not expressed in the neonatal testis, but was highly expressed in the epididymis (data not shown). It may be that the reporter allele detects lower levels of Notch activation than does the Notch1 antibody. Therefore, it would be interesting to repeat these experiments with the Notch-GFP allele, as well as to examine other members of the Notch family and pathway.

Pax3 is not expressed in the testis

Because of the co-expression of Pax3 and Pax7 in the developing muscle, I wanted to determine if Pax3 was expressed in the embryonic testis. By digital Northern, Pax3 was not expressed in the testis, nor in SSC cultures, but was highly expressed in the e11 embryo, and had a moderate expression in the brain and skeletal muscle (**Figure 7.8**, A). As Pax3 expression becomes more and more restricted as the muscle develops, the digital Northern was in accordance with the literature. I acquired a monoclonal antibody to Pax3 and found strong nuclear expression in the developing muscle and nasal cavity (**Figure 7.8**, B). Thus, the antibody was functional and specific. Under the same conditions and with a control slide, I examined expression of Pax3 in the testis. Interestingly, Pax3 was not

expressed in the testis at any timepoint (**Figure 7.8**, C). This is in agreement with a study using a Pax3-Cre line that found no contribution of Pax3 to male germline (45). This suggests that Pax7 functions by distinct mechanisms in the testis than it does in the skeletal muscle.

Pax7+ prospermatogonia are not differentiating

Although heterogeneity in the embryonic testis had not been previously described, heterogeneity in the neonatal pre-spermatogonia has been appreciated for many years. In fact, the expression of certain markers is indicative of cell fate. To begin to determine the ultimate fate of $Pax7^+$ prospermatogonia, colocalization with Kit and Stra8. In the adult mouse, Kit+ spermatogonia have a 90% reduction in the transplantation as compared to Kit- fractions of spermatogonia (141). Via studies from neonatal mice comparing the transplantation efficiency of undifferentiated spermatogonia with or without Kit expression, it has been demonstrated that Kit^+ prospermatogonia do not transplant as well as Kit^-, and are again thought to be committed to differentiation even at this early stage (15). Stimulated by retinoic acid 8 (Stra8), serves as a marker of the presence of retinoic acid, which is necessary for entry into meiosis. Thus, $Stra8^+$ pre-spermatogonia are thought to be committed to differentiation as well (142, 143).

First, I documented the appearance of Kit^+ and $Stra8^+$ cells from embryonic development to PD7. I found that Kit^+ cells are visible even at PD1 (**Figure 7.6**), which is earlier than what has been previously described (14, 143). Stra8 was

evident by PD3 (**Figure 7.5**), and the expression pattern was similar to that found in the literature (142, 143).

Upon colocalization of these markers, Kit and Stra8 were rarely expressed in Pax7$^+$ prospermatogonia (**Figure 7.9**, A). Thus, these cells are not differentiating. Pax7$^+$ prospermatogonia seemed to prefer tubules that did not have Kit or Stra8+ cells (**Figure 7.9,** D), which may indicate that differentiation during the neonatal period occurs in certain areas of tubules more so than others. On the other hand, it could indicate that specific niches protect pre-spermatogonia from differentiation.

Lineage tracing with Pax7-Cre demonstrates that a substantial fraction of the germline derives from Pax7$^+$ germ cells

Although lineage tracing with tamoxifen inducible Pax7-Cre alleles had previously shown that 1) adult Pax7$^+$ SSCs can perdure for long periods and give rise to full lineage maturation clones and 2) neonatal Pax7$^+$ prospermatogonia can perdure for 12wks, the contribution of these cells to the overall germline was unknown. To further examine this, I crossed *Pax7-Cre* mice to *mT/mG* reporter mice. Using this strategy, Pax7$^+$ prospermatogonia would be labeled during embryonic development, and this Cre allele seemed to be more efficient than the tamoxifen-inducible lines.

At the earliest timepoint, e15.5, no labeled cells were observed, in accordance with the IHC data. At e18.5, very rare, at most one per section, labeled cells could be observed (**Figure 7.10,** D). The mGFP signal was relatively weak in these cells, which could indicate that these cells have just begun to undergo Cre

mediated recombination. By PD3, labeled cells were easier to locate, and most often existed as single cells, but were sometimes seen in pairs or clusters. By PD7, labeled cells were abundant, existing as singles, pairs, and clusters, and seemed to be spaced throughout the tubule in a deliberate manner (**Figure 7.10,** C). From PD7 to PD14, there is a drop in the percentage of labeled germ cells, most likely due to an expansion of differentiating (Kit^+) spermatogonia, which dilutes overall cell numbers (**Figure 7.10**, A). By 6wks, approximately 30% of the germline was labeled, and green motile sperm could be observed in the epididymis. At 12 wks, the percentage of germ cells increased to 50%. At 6mos, the final timepoint, approximately 60% of the germline was labeled demonstrating that Pax7+ spermatogonia make a major contribution to the germline (**Figure 7.10**, A).

Pax7-Cre faithfully replicates Pax7 expression patterns in the muscle and testis

To ensure that Pax7-Cre was expressed in the appropriate cell types, I examined whole body fluorescence at PD7. Skeletal trunk muscles as well as the nasal cavity were clearly labeled with GFP, while the rest of the body was labeled with the TdTomato (**Figure 7.11**, A). While *Pax7-Cre mT/mG* testes contained large GFP^+ clones, *mT/mG*$^+$ testes without Cre showed no recombination and no GFP^+ labeled clones (**Figure 7.11**, B) In skeletal muscle, approximately 90% of myocytes were labeled by 6wks. (**Figure 7.11**, C) Labeled cells were not observed in either the gross ovary nor in sections through the ovary, which is in agreement with both the digital Northern and IHC, which did not show Pax7 expression in the ovary (**Figure 7.11**, E, see also **Chapter 6**). The spleen, kidney, and liver also were not

labeled by Pax7-Cre (**Figure 7.11**, E, G, and H). Thus, Pax7-Cre mirrors expression of Pax7 in the skeletal muscle and gonads.

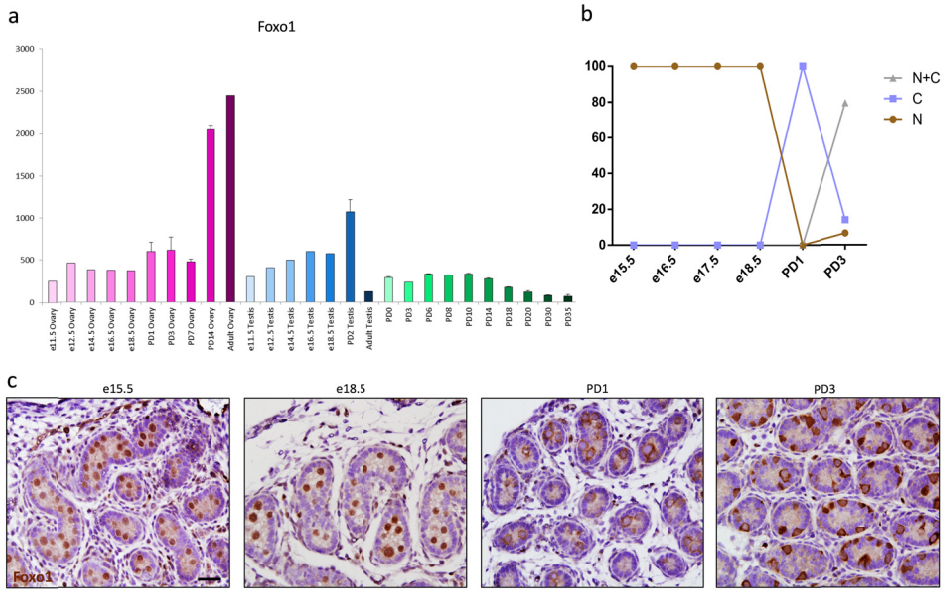

Figure 7.1: Foxo1 is located in the nucleus of pre-spermatogonia.

(A) Digital Northern of expression of Foxo1 in embryonic gonads and neonatal testis. (B) Localization of Foxo1 protein by age. In the embryonic gonad, Foxo1 is exclusively nuclear. At birth, localization shifts to exclusively cytoplasmic, and throughout neonatal development, the protein once again becomes predominately nuclear. In adulthood, Foxo1 is approximately 80% nuclear and 20% cytoplasmic. (C)Representative IHC staining on Foxo1 over embryonic and neonatal development. Scale = 25µm.

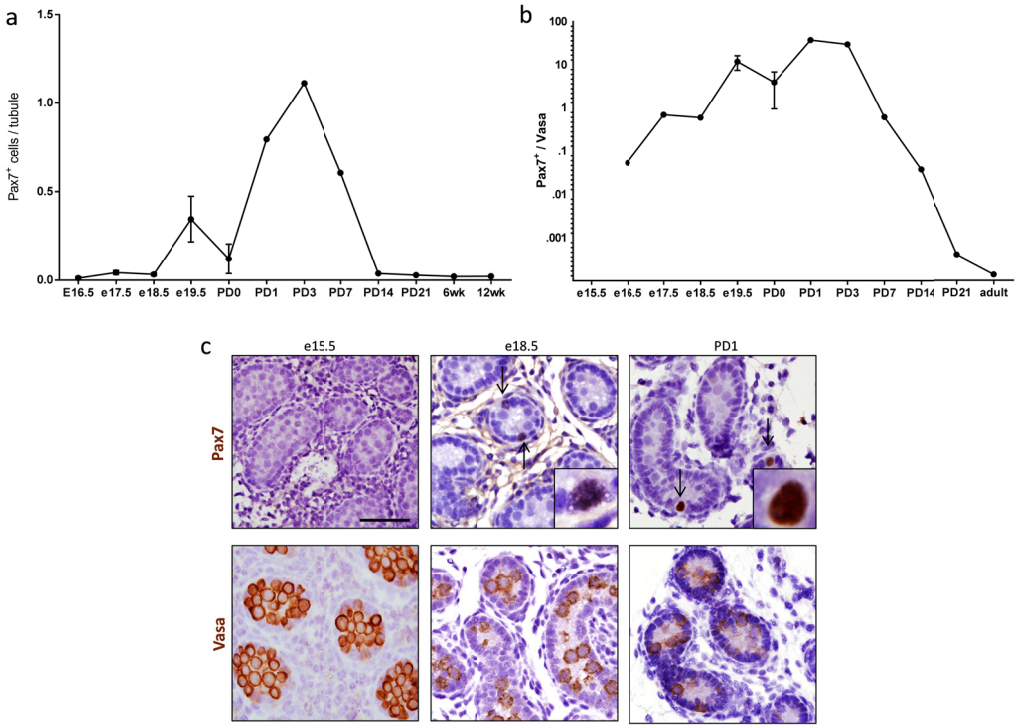

FIGURE 7.2: Pax7 is expressed in a subset of prospermatogonia. (A) Pax7+ spermatogonia per tubule. The number of Pax7+ spermatogonia per tubule is low during embryonic development, and peaks right around birth, and then falls to the low levels seen in adulthood. (B)Pax7+ spermatogonia per germ cell, demonstrating how exceedingly rare these cells are in adulthood. (C) Histology of embryonic testis. While many germ cells can be observed via Vasa IHC, only a subset of prospermatogonia express Pax7. At e15.5, no Pax7 staining is observed, and the number of Pax7+ prospermatogonia increases to peak around birth. Scale = 25µm.

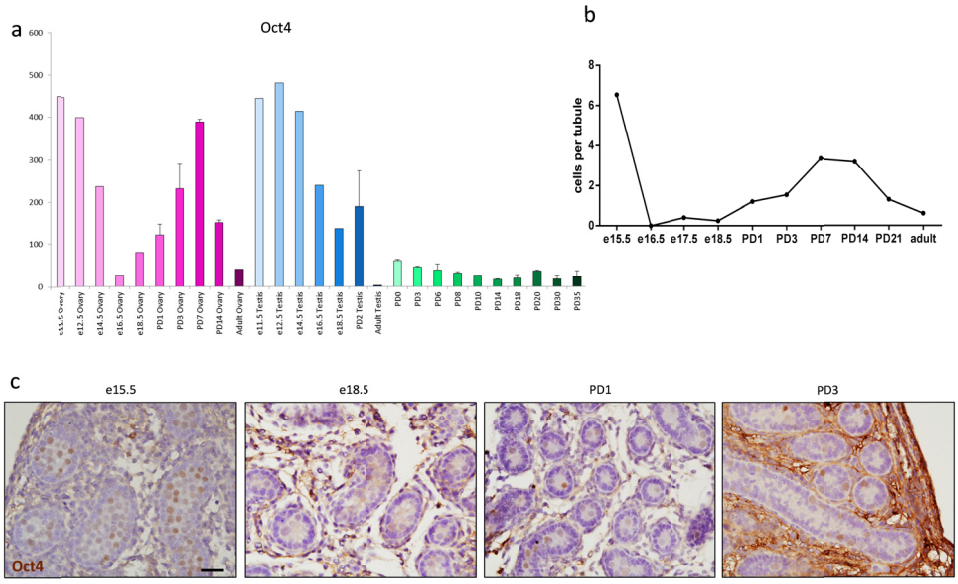

Figure 7.3: Expression of Oct4 in from e15.5-PD7. (A) Digital Northern of expression of Oct4 in embryonic gonads and neonatal testis. (B) Number of Oct4+ germ cells over embryonic and neonatal development. (C) Representative staining of Oct4 in embryonic and neonatal testis. Oct4 is expressed heterogeneously in the neonatal testis, but not in the embryonic testis. Scale = 25μm.

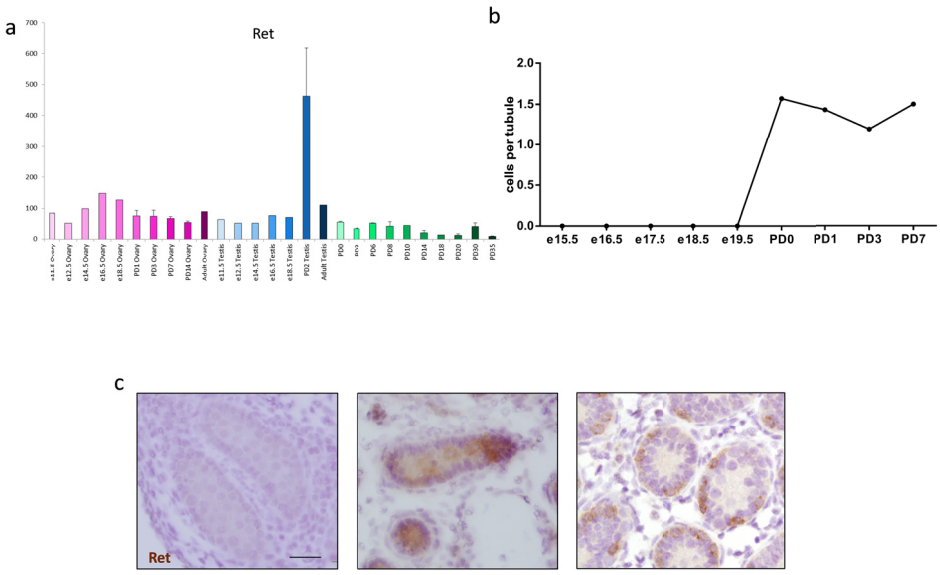

Figure 7.4: Expression of Ret in from e15.5-PD7. (A) Digital Northern of expression of Ret in embryonic gonads and neonatal testis. (B) Number of Ret+ germ cells over embryonic and neonatal development. (C) Representative staining of Ret in embryonic and neonatal testis. Oct4 is expressed heterogeneously in the neonatal testis, but not in the embryonic testis. Scale = 25μm.

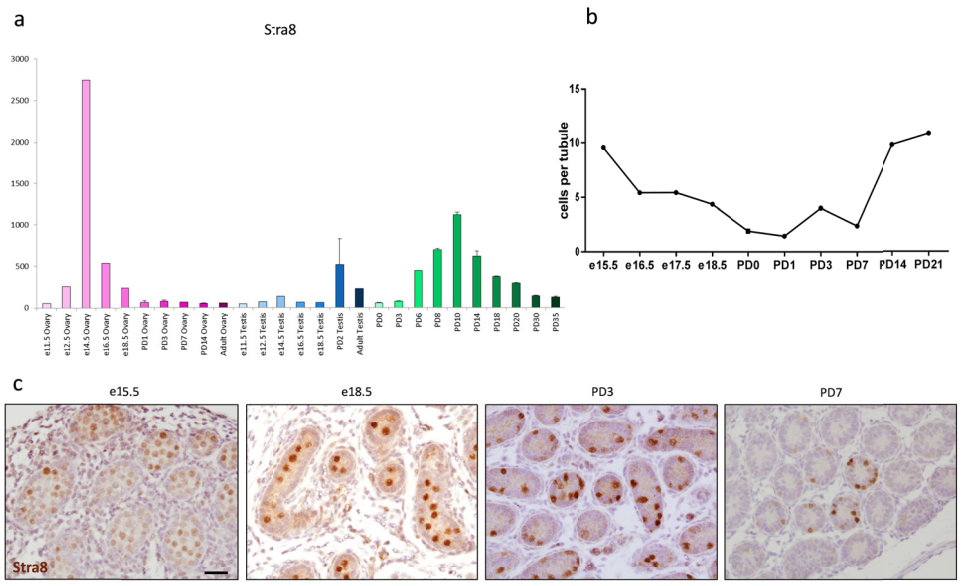

Figure 7.5: Expression of Stra8 in from e15.5-PD7. (A) Digital Northern of expression of Stra8 in embryonic gonads and neonatal testis. (B) Number of Stra8+ germ cells over embryonic and neonatal development. (C) Representative staining of Stra8 in embryonic and neonatal testis. Stra8 is expressed heterogeneously in the neonatal testis in cells which are thought to be differentiating, but it is expressed homogenously in the embryonic testis. Scale = 25μm.

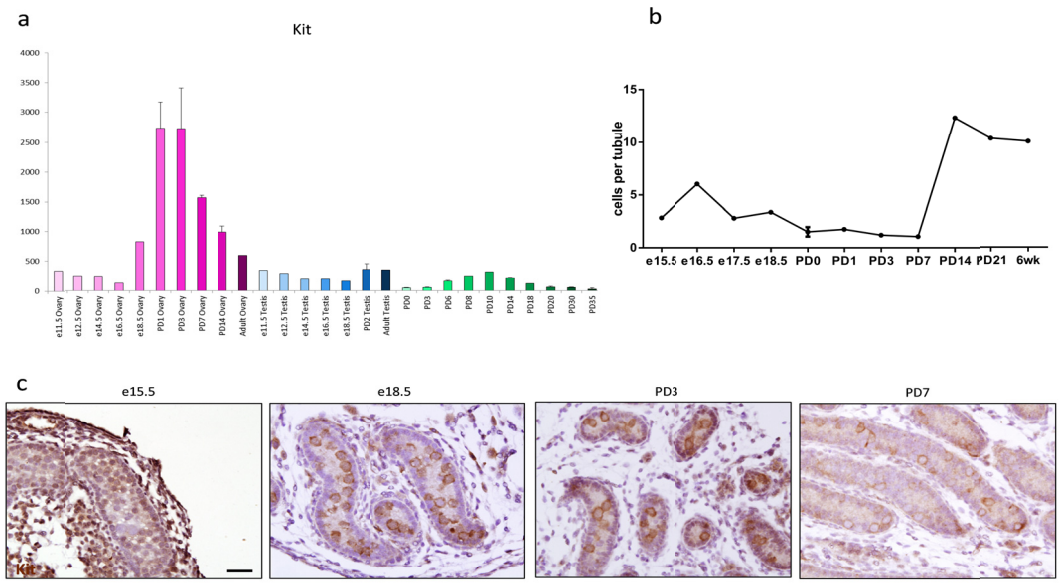

Figure 7.6: Expression of Kit in from e15.5-PD7. (A) Digital Northern of expression of Kit in embryonic gonads and neonatal testis. (B) Number of Kit+ germ cells over embryonic and neonatal development. (C) Representative staining of Kit in embryonic and neonatal testis. Kit is expressed heterogeneously in the neonatal testis in cells which are thought to be differentiating. Kit was detected earlier in neonatal development (PD1) than previously reported. Scale = 25μm.

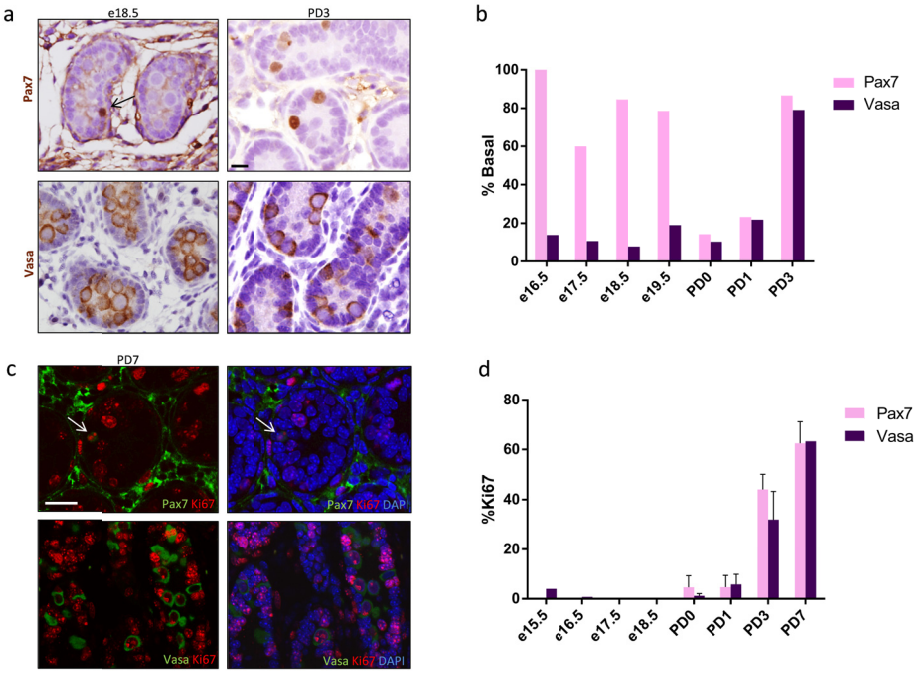

Figure 7.7: Pax7⁺ prospermatogonia are more likely to be located on the basement membrane during embryonic development.

(A) Histology of e18.5 and PD3 testis stained with Pax7 and Vasa. Pax7+ prospermatogonia are located on the basement membrane at e18.5, while only a small fraction of total germ cells are basally located. (B) Percentage of Pax7 and Vasa+ prospermatogonia located on the basement membrane. During embryonic development, Pax7+ prospermatogonia are predominately basal. At birth, the association is lost, and by PD3, nearly all germ cells are basal. (C) Representative colocalization of Ki67 and Pax7 and Ki76 and Vasa. (D) Even though the location on the basement membrane is associated with exit from quiescence, no difference in Ki67 positivity was observed between Pax7 and Vasa. Scale = 25μm.

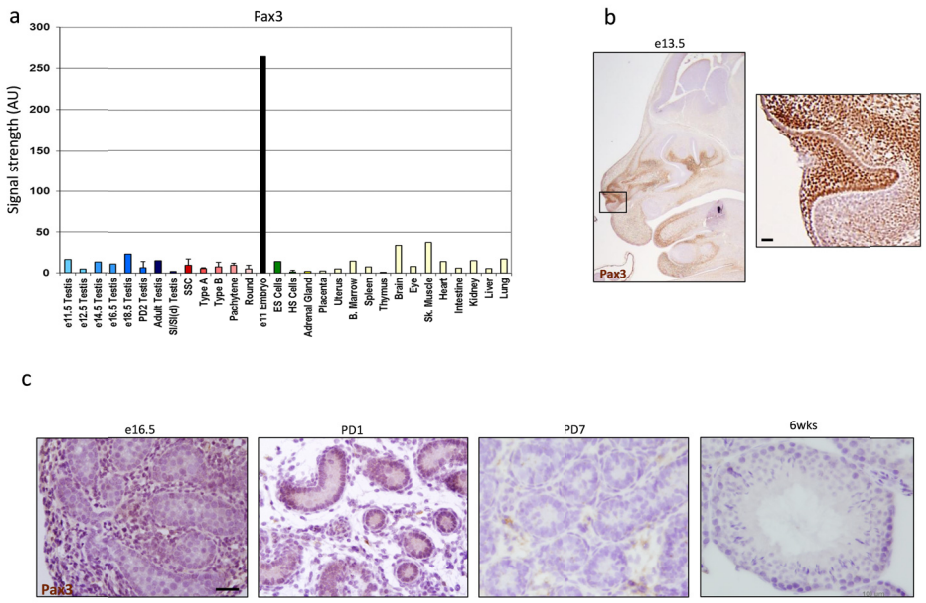

Figure 7.8: Pax3 is not expressed in the mouse testis. (A) Digital Northern showing a lack of Pax3 expression in the testis and in all stages of germ cells. (B) Monoclonal ANTI Pax3 antibody stains strongly in the embryonic nasopharynx. The staining is specific and nuclear, thus validating the antibody. (C) Pax3 is not expressed in the testis at any timepoint. Thus, Pax3 and Pax7 do not function in the testis as they do in the developing muscle. Scale = 25µm.

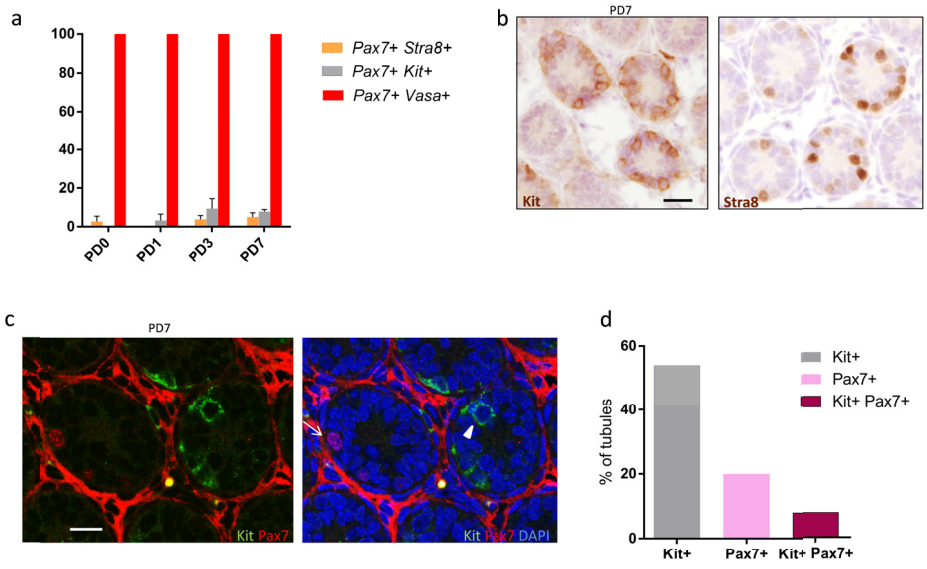

Figure 7.9: Pax7+ prospermatogonia are not differentiating (A) Colocalization of markers of differentiation, Kit and Stra8, with Pax7. The vast majority of Pax7+ prospermatogonia are not differentiating. All Pax7+ prospermatogonia are germ cells and colocalize with Vasa. (B) Representative staining of Stra8 and Kit. (C) Kit and Pax7 do not colocalize. (D) Pax7+ prospermatogonia seem to be located in tubules where Kit+ prospermatogonia are not located. Scale = 25μm.

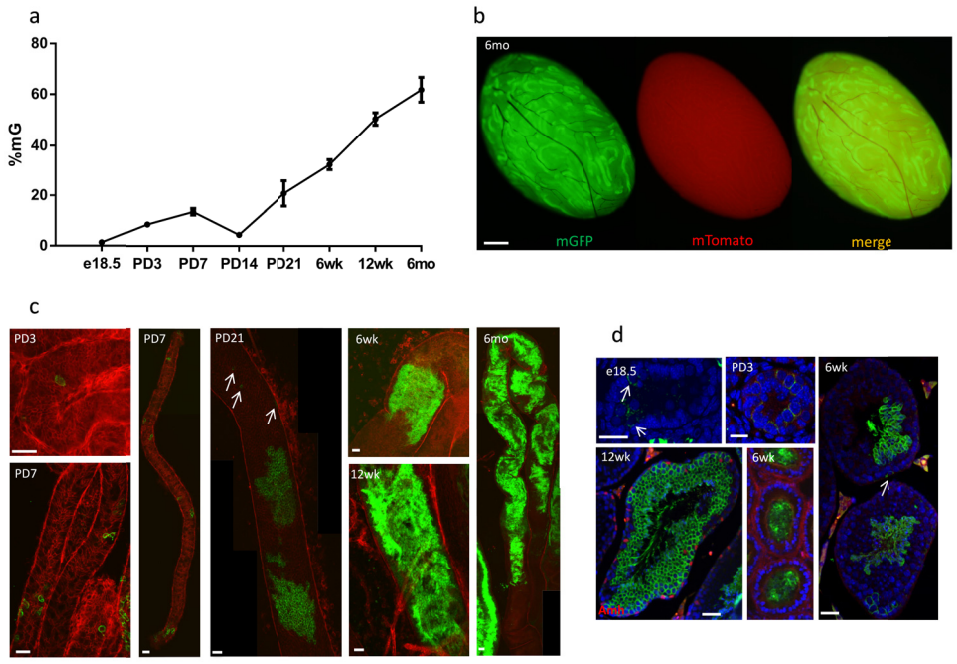

Figure 7.10: *Pax7-Cre; mT/mG* lineage tracing. (A) Percentage of the germline labeled by mG via Pax7-Cre mT/mG lineage tracing. The drop in labeling at PD14 could reflect an increase in other cells types, such as differentiating Kit+ spermatogonia, which are high in number at this timepoint. By 6mos, approximately 60% of germ cells derive from Pax7. (B) Whole Pax7-Cre mT/mG testis at 6mos showing large labeled clones. (C) Wholemount tubules of Pax7-Cre mT/mG testis. Clones begin usually as single cells and increase in number with age. At PD7, cells seem to take on a regular spacing pattern. At PD21, clones are larger, but single cells can be observed as well (arrow). By 6mos of age, clones are very large and extend throughout the tubules. (D) Immunofluorescence of GFP on sections of Pax7-Cre mT/mG testis. At e18.5, the GFP is very dim, which may reflect recent recombination. Cells are very rare, and reside on the basement membrane. By PD3 larger clones can be observed. At 6wks, labeled cells are very apparent, and

single cells can be seen, indicated by the arrow. Green labeled sperm were observed in the epididymis. By 12wks, all spermatogenic subtypes are labeled. Scale = 500 μm (B); 25μm (C) and (D).

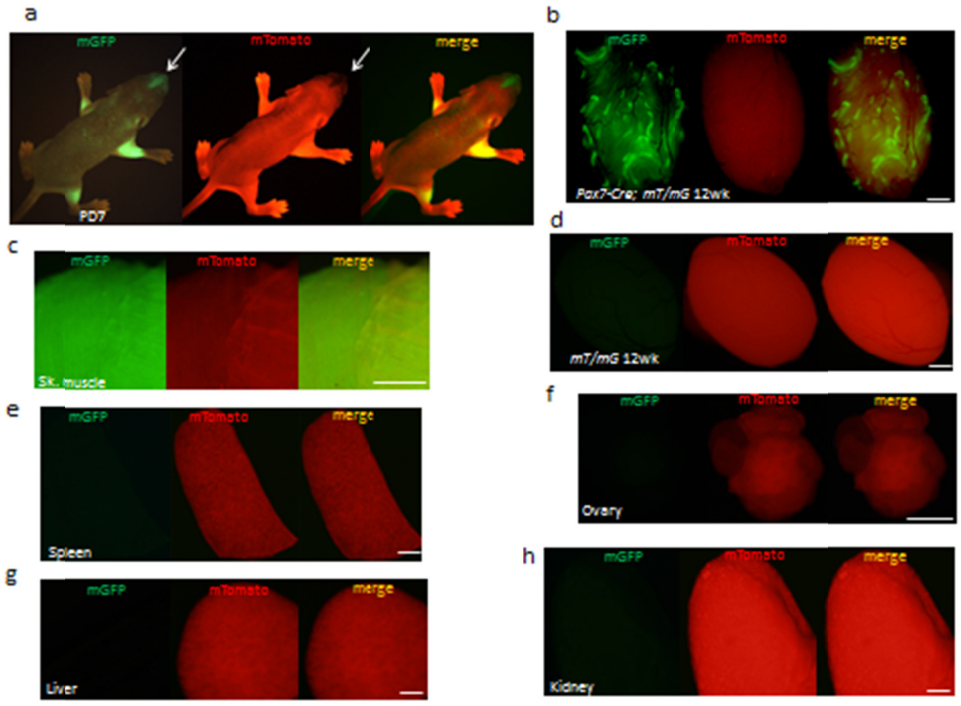

Figure 7.11: *Pax7-Cre* faithfully replicates expression of Pax7. (A) Whole PD7 Pax7-Cre mT/mG mouse. Trunk muscles are brightly labeled, as well as the nasopharynx. Arrow denotes exclusivity of mT and mG labeling, which is apparent due to the thin skin over the nose. (B) and (D) mG labeling is only observed with Pax7-Cre. (C) Skeletal muscle is nearly completely labeled by mG. (E)-(H) mGFP is not observed in spleen, ovary, liver or kidney. Scale = 500 μm

CHAPTER 8: BEHAVIOR OF PAX7^{+} SPERMATOGONIA IN SSC CULTURES

Pax7 is expressed heterogeneously in SSC cultures

Spermatogonial stem cell culture has been likened to culturing only undifferentiated spermatogonia. Cells are supported by a mix of growth factors, including GNDF, FGF, and EGF. Markers of undifferentiated spermatogonia such as Gfrα, Foxo1, and Plzf are expressed in SSC cultures, but uniformly in every cell. However, it is known that only a fraction of these cells can function as stem cells via transplantation studies. Furthermore, although expression of Kit in SSC cultures has not been visualized by IF, a variable percent of SSCs in culture express Kit by FACs (144). Thus, SSC cultures are a heterogeneous mix of stem cells and differentiating cells.

A very few number of markers are expressed in selected cells in the cultures, including Sohlh1, which is thought to be upstream of Kit (144), Oct4, which is important in maintaining stemness in a variety of cell types (144), and Id4, a recently described marker of SSCs (18). Sohlh1 and Oct4 are nearly mutually exclusive (144). Id4 is expressed in approximately 10% of unsorted SSC cultures (18), which is much higher than the estimate 1.33% of cultures SSCs which are capable of transplantation (145). On the other hand, taking into account that the homing efficiency of 12% (23), or how likely a stem cell is to find and colonize a niche, the 10% of SSC cultures which are positive for Id4 are very close to the estimated number of stem cells in the culture (1.33x 12 =15.96%)

I sought to visualize the expression pattern of Pax7 in SSC cultures. Do to the rarity of these cells *in vitro*, SSC cultures could serve as an easier means by which to understand the behavior of these cells. Expression of Pax7 was not seen in all cells, but only in a small number, approximately 10% (**Figure 8.1**). Pax7+ spermatogonia co-localized with Foxo1, but surprisingly did not co-localize with Oct4, and these cell markers seemed mutually exclusive (**Figure 8.1**). Since Id4 and Pax7 seem to be expressed in similar subsets of cells *in vivo*, I co-labeled SSC cultures with these two markers, and found that indeed, Id4 and Pax7 seemed to label the same subset of cells *in vitro*.

To begin to understand how $Pax7^{+}$ and $Pax7^{-}$ spermatogonia behave, I labeled cells with EdU and determined the incorporation rates of Foxo1+ (all spermatogonia in culture) and $Pax7^{+}$ and $Pax7^{-}$ spermatogonia (**Figure 8.1**). I found no difference in the EdU incorporation rate of any of these cell populations, similar to different subsets of spermatogonia *in vivo*.

Busulfan treatment of SSC cultures

To examine how SSCs respond to genotoxic stress, I treated SSC cultures with 0.01uM to 10mM busulfan to determine the LD50. SSCs were surprisingly resistant to busulfan, compared to their sensitivity *in vivo* (**Figure 8.2,** A). I then treated SSC cultures with these same doses of busulfan and counted $Pax7^{+}$ SSCs in the surviving fraction of spermatogonia to determine if $Pax7^{+}$ spermatogonia were more resistant to busulfan than other fractions. I found that only at the highest dose were Pax7

protein and Pax7+ SSC increased (**Figure 8.2,** B, C). Thus, SSCs appear to be more resistant to busulfan in vitro than in vivo.

Effect of Gdnf withdrawal on Pax7 expression

Gdnf is an essential growth factor for the survival of SSC cultures. It had been thought that SSCs have an absolute requirement for Gdnf. However, a recent study has demonstrated that a very small number of SSCs can be propagated even without Gdnf (146). Using a Ret mutant mouse incapable of responding to Gdnf signaling, Takashima et. al demonstrated that not only can SSC cultures be derived from these mice, but moreover these cells can form functional spermatogenic colonies via transplantation studies. Moreover, when Gdnf is withdrawn for 18hrs from SSC culture media, the number of colonies formed via transplantation actually increases (28), although the reason for this increase is not understood. Thus, while responsiveness to Gdnf has been historically viewed as a necessary characteristic of a spermatogonial stem cell, this criterion may have little to do with actual stemness.

I sought to determine how $Pax7^{+}$ SSCs in culture responded to Gdnf. I first turned the literature, where a microarray of genes affected by Gdnf withdrawal showed no change in expression of Pax7 (28). Therefore, I wanted to determine the effect of Gdnf withdrawal on the survival of Pax7+ SSCs. The normal media (SFM) contains 20μg/mL Gdnf. Therefore, I chose 1, 5, and 10 μg/mL, and counted the number of Pax7+ SSCs after 18 and 72hrs. As overnight withdrawal of Gdnf does not affect SSC numbers (28), I wanted to choose a longer timepoint that would challenge the SSCs to the extreme. I found that overnight withdrawal of Gdnf did not have any

impact of expression of Pax7 at any dose (data not shown). Furthermore, even at 72 hours of extremely reduced levels of Gdnf (10% of normal SFM conditions), Pax7^{+} SSCs persisted at normal numbers. At the lowest dose of Gdnf (1mg/mL) SSC cultures begin to die after 72hrs.

Live cell imaging of descendants of Pax7^{+} SSCs

I derived SSC cell lines from *Pax7$^{tm1(cre/ERT2)Gaka}$/J; mT/mG* PD7 male mice. Once the lines were established, I treated cells with 2 mg/mL tamoxifen to induce Cre recombinase. Approximately 1% of cells in culture were labeled after 4 days of tamoxifen treatment, giving an efficiency of approximately 10% (**Figure 8.3,** A). These labeled cells were stable in culture up to 3mos after three days tamoxifen treatment (**Figure 8.3,** A).

To observe the behavior of Pax7 descendants in real time, I employed live cell imaging on a LSM510 confocal microscope for up to 72h. While cell divisions of Pax7 derived cells were not observed, SSC cultures were quite motile. Furthermore, I observed the splitting and joining of cells from different clusters, meaning that each cluster is not necessarily clonal, and fragmentation does occur *in vitro*. However, the length of time and area observed (one section per imaging session) was not sufficient to draw conclusions as to how Pax7^{+} SSCs divide. On the other hand, live cell imaging is very feasible with *Pax7$^{tm1(cre/ERT2)Gaka}$/J; mT/mG* lines; the endogenous fluorescence is easily visible and SSC cultures can be maintained at the microscope. With a confocal capable of imaging multiple areas per time frame and a

live reporter of Pax7 expression, this methodology could serve as an attractive means to understand symmetric vs. asymmetric divisions of Pax7^{+} SSCs.

I then derived cell lines from 3 *Pax7$^{tm1cre\ Mrc}$/J; mT/mG* PD7 mouse testis, where labeled cells only represent approximately 10% of germ cells (see Chapter 7), and counted the percentage of green labeled cells over time. After 70 days in culture, nearly 70% of the germ cells were labeled with GFP, suggesting that Pax7+ SSCs function as the stem cells in SSC culture (**Figure 8.3,** B). However, longer experiments were not possible as both the mG and mT signal failed to be detected in cultures, which could be due to modification of the Rosa locus.

Overexpression of Pax7

Pax7 was cloned into a Plvx lenti expression plasmid, and SSCs were infected. As a control, cells were also infected with Plvx mCherry. Overexpression was confirmed via western blot, and also by IF (data not shown). Whereas 11% of cells in mCherry cultures expressed Pax7 via IF (equivalent to wild type), 70% of Pax7-overexpressing SSC cultures expressed Pax7. To determine how Pax7 overexpression effects cell growth, I examined EdU incorporation at 30min, 1h, 4h, and 24h. I found a trend in Pax7 overexpressing cell lines to have a higher incorporation rate than mCherry cell lines at all timepoints, and this was statistically significant at 1 and 4h (**Figure 8.4,** B). Furthermore, I found that Pax7 overexpressing cell lines have a higher cleaved caspase 3 positivity, indicated apoptosis. In accordance with this, short term growth analysis of mCherry vs. Pax7 overexpression revealed no difference (**Figure 8.4,** E). Long-term growth analysis of

5 wks demonstrated no significant difference between the overexpressing cells and the mCherry controls (**Figure 8.4,** C).

Knockout of Pax7

To determine how loss of Pax7 impacts SSC culture, *Pax7 $^{f/f}$ Vasa-Cre ^{ERT2}* SSC cultures were derived and then treated with tamoxifen to induce Cre. Loss of Pax7 was confirmed via western blot and also by IF. Whereas 11% of cells in cultures not treated with tamoxifen expressed Pax7 via IF (equivalent to wild type), 0.01% of Pax7-overexpressing SSC cultures expressed Pax7 (data not shown). I found that Pax7 cKO cell lines have a higher cleaved caspase 3 positivity, indicated apoptosis (**Figure 8.5,** D). Short term growth analysis of tamoxifen vs. non treated cell lines revealed no significant difference between these two conditions. In fact, tamoxifen treated lines seemed to grow slightly more than the non-treated, arguing against tamoxifen itself having any harmful effect on the cultures (**Figure 8.5,** A). Long-term growth analysis of 5 wks demonstrated no significant growth differences (**Figure 8.5**, B).

Pax7 and Id4

During the course of this project, Id4 was found to mark a small subset of A_{single} spermatogonia, akin to Pax7. To investigate the hypothesis that Pax7 and Id4 marked the same subset of cells, I first counted the number of Pax7 and Id4+ spermatogonia in SSC cultures. Localization of Id4 has been reportedly difficult, as antibodies to Id4 have deteriorated in specificity as new lots were produced. Using a

polyclonal antibody to Id4specify antibody, I , found that both markers were expressed in approximately 10% of cells. Co-localization of Pax7 and Id4 was observed within the same cells (**Figure 8.6,** A).

In vivo studies of these markers was aided by the development of an Id4-GFP mouse, developed by the Oatley lab (26). In this system, it was reported that only the brightest GFP+ spermatogonia truly replicate Id4 transcription, as the GFP is a stabilized protein and may last longer that Id4 itself (Jon Oatley, personal correspondence, (143)). Neonatal testis blocks were obtained from PD0 and PD6 mice and generously provided by the Oatley lab. Id4-GFP was found to be expressed in a subset of germ cells (**Figure 8.6,** C). Colocalization of GFP and Pax7 found that Pax7 is expressed in a subset of $Id4^{+}$ SSCs at both timepoints (**Figure 8.6,** D). Furthermore, colocalization of Id4 and GFP demonstrated that all GFP^{+} spermatogonia were also dually positive for Id4. Thus, it may be that the GFP faithfully replicates expression of Id4, or that the antibody used to detect Id4 is not specific to these pre-spermatogonia.

Conclusion

Here we demonstrate that Pax7 marks a subset of spermatogonia that function as stem cells in both normal spermatogenesis as well as during genotoxic injury. $Pax7^{+}$ spermatogonia are selectively resistant to chemotherapeutics, and directly contribute to the recovery of spermatogenesis after such treatments. While these cells make a significant contribution to the germline, it is possible that not all germ cells pass through Pax7 lineage, suggesting the existence of other populations

of germline stem cells in the testis. these stressors. Pax7 delineates a subset of germ cells even late in embryonic development, calling into question whether stemness can be determined prior to birth. Finally, Pax7 marks a subset of $Id4^{+}$ spermatogonia, which could suggest a hierarchy of differentiation even in the A_{single} population. This research may lead to new approaches to preserve the germline in male cancer patients or perhaps even pave the way for future research that could reverse male infertility.

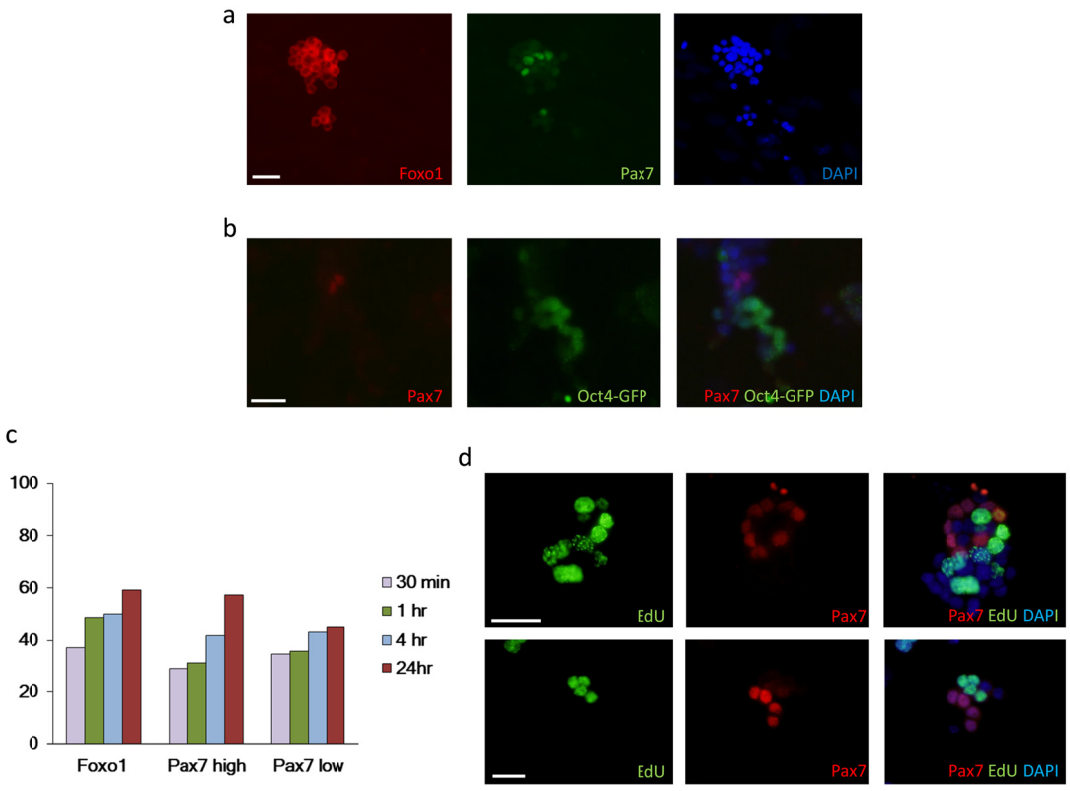

Figure 8.1: Pax7 is expressed in a subset of SSCs in culture. (A) Pax7 is expressed heterogeneously in SSC cultures. IF showing Foxo1 is expressed in every SSC, while Pax7 is only expressed in a small subset (approximately 11%). (B) Pax7 and Oct4 do not co-localize in SSC cultures. Out of 100 Pax7+ SSCs, none expressed Oct4, which is also expressed heterogeneously in culture. (C) EdU incorporation rates in Foxo1 (all SSCs), Pax7 high, and Pax7 low SSCs. No significant differences in EdU incorporation were noted. (D) Representative images of EdU incorporation of Pax7+ SSCs at 1hr. Complex patterns were observed at every timepoint. Cell division is asynchronous in clumps of SSCs. Scale = 50μm.

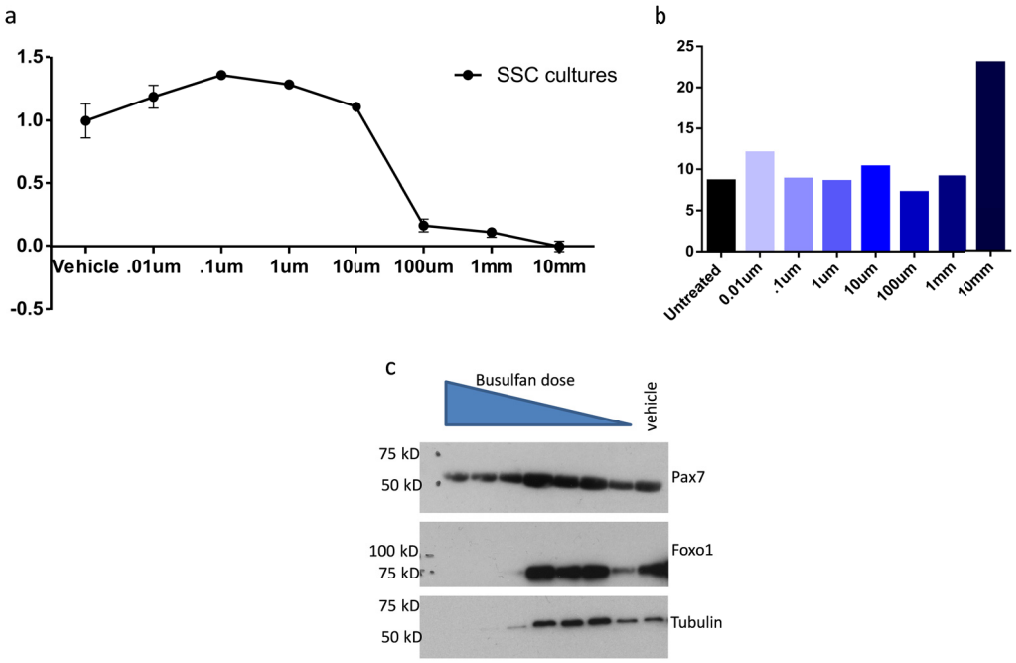

Figure 8.2: Busulfan treatment of SSC cultures. Kill curve for SSCs treated 24hr with busulfan. LD50 is between 10μM and 100μM. (B) Number of Pax7⁺ SSCs after 24hr treatment with busulfan. Only at the highest dose is an increase in the number of Pax7⁺ SSCs observed, suggesting that SSC culture may not faithfully replicate in vitro conditions. However, while the overall number of Pax7+ SSCs may not change, the amount of Pax7 staining that was determined to be "background". (C) Western blot of Pax7 protein levels after with the above doses. At the highest doses of busulfan, there is an increase in the amount of Pax7 protein relative to tubulin or to Foxo1, which could not be detected at high doses of busulfan.

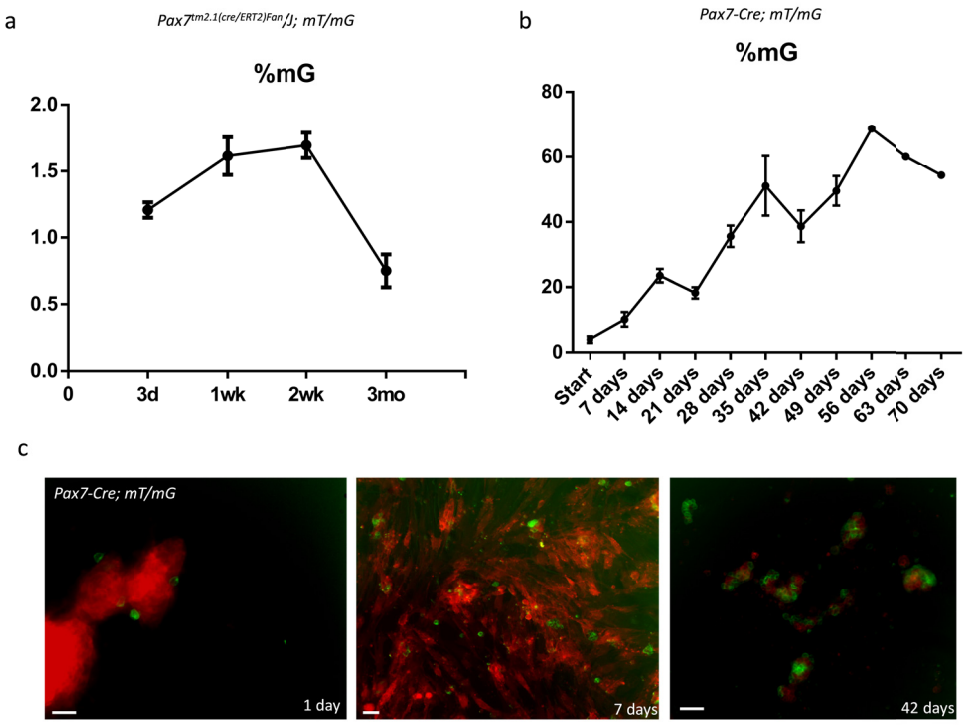

Figure 8.3: Lineage tracing of PAX7⁺ descendants in *Pax7-Cre^{ERT2};mT/mG* and *Pax7-Cre; mT/mG* SSC cultures. (A) SSC cultures derived from *Pax7-Cre^{ERT2};mT/mG* testis, treated 3 days with tamoxifen. The percentage of labeled cells was very low, but could be observed even 3 mos after tamoxifen administration. (B) SSC cultures derived from PD7 and *Pax7-Cre; mT/mG* testis. The percentage of labeled cells continues to increase with time, arguing that Pax7+ SSCs function as stem cells in vitro. However, lineage tracing at longer timepoints is not feasible as cells begin to lose both mT and mG signal around 70 days in culture. (C) Representative images of and *Pax7-Cre; mT/mG* SSC cultures. At 1 day, large clumps of cells are observed, where mG cells represent a small fraction. Scale = 50μm.

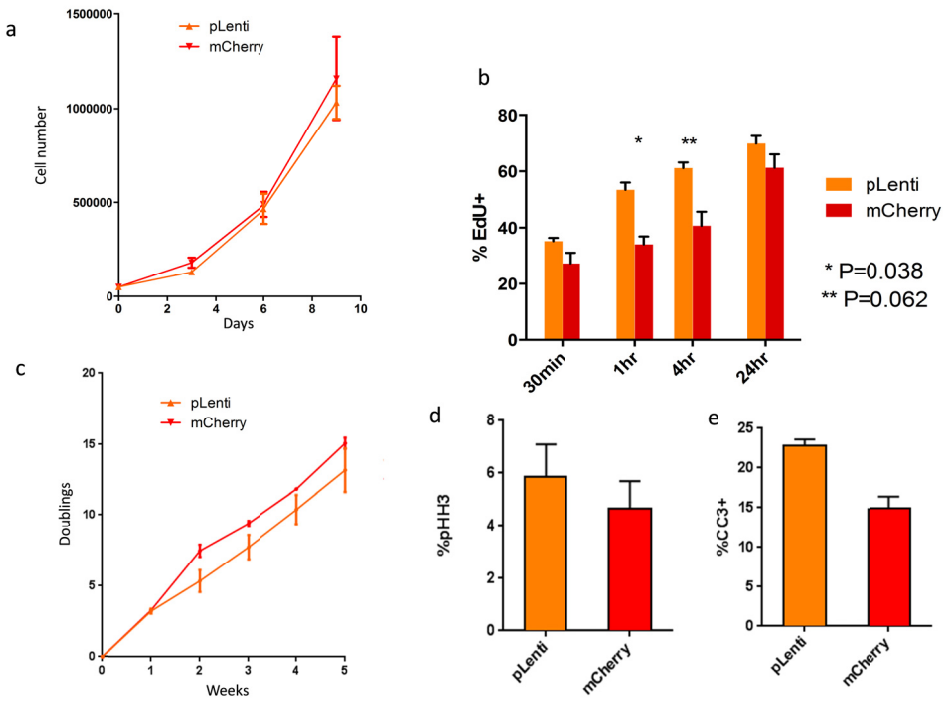

Figure 8.4: Overexpression of Pax7 in SSC cultures. (A) Short term growth curve of Pax7 overexpressing (pLenti) and control (mCherry) cell lines. No difference was observed in growth to 9 days. (B) EdU incorporation rates between Pax7 overexpression and mCherry cell lines. Pax7 overexpressing cells lines had a trend for higher incorporation rates that was significant at 4hrs. (C) Long term growth rates of 5wks showed no difference between the two cell lines. (D) The number of mitotic cells was slightly higher in Pax7 overexpressing SSCs. (E) Pax7 overexpressing SSCs had a higher rate of apoptosis, explaining why overall growth rates did not reflect the increased EdU incorporation rates.

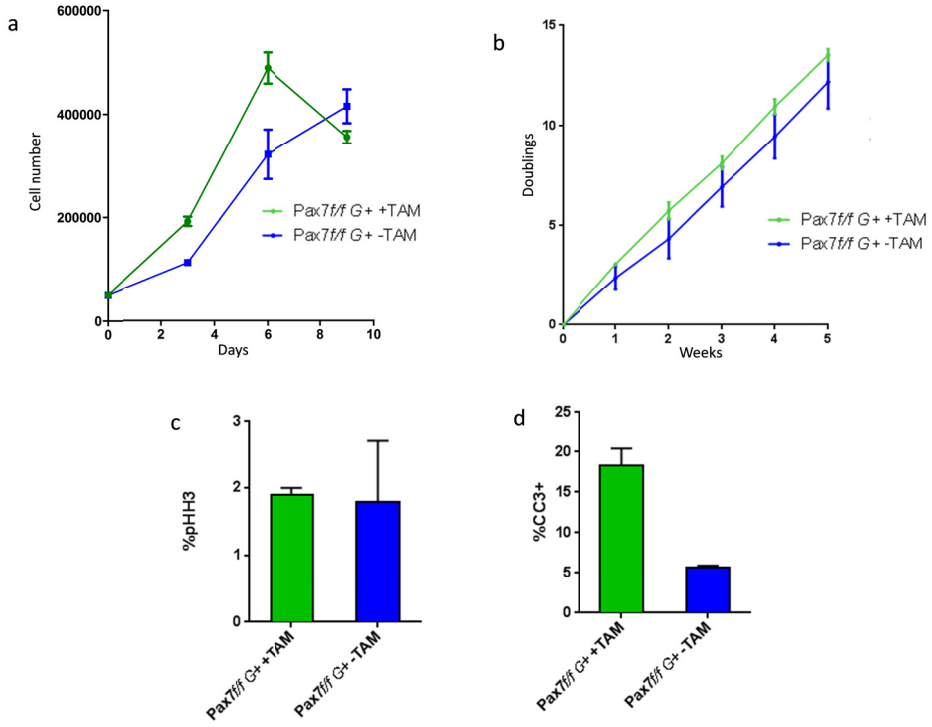

Figure 8.5: Conditional knockout of Pax7 in SSC cultures. (A) Short term growth curve of *Pax7 f/f Vasa-Cre ERT2* SSCs with and without tamoxifen. No difference was observed in growth rates. Thus, there is no impact on SSC growth from constant tamoxifen administration. (B) Long term growth curve of 5 wks showed no differences between with and without tamoxifen. (C) No difference was observed in mitotic index. (D) Conditional knockout of Pax7 leads to a higher rate of apoptosis.

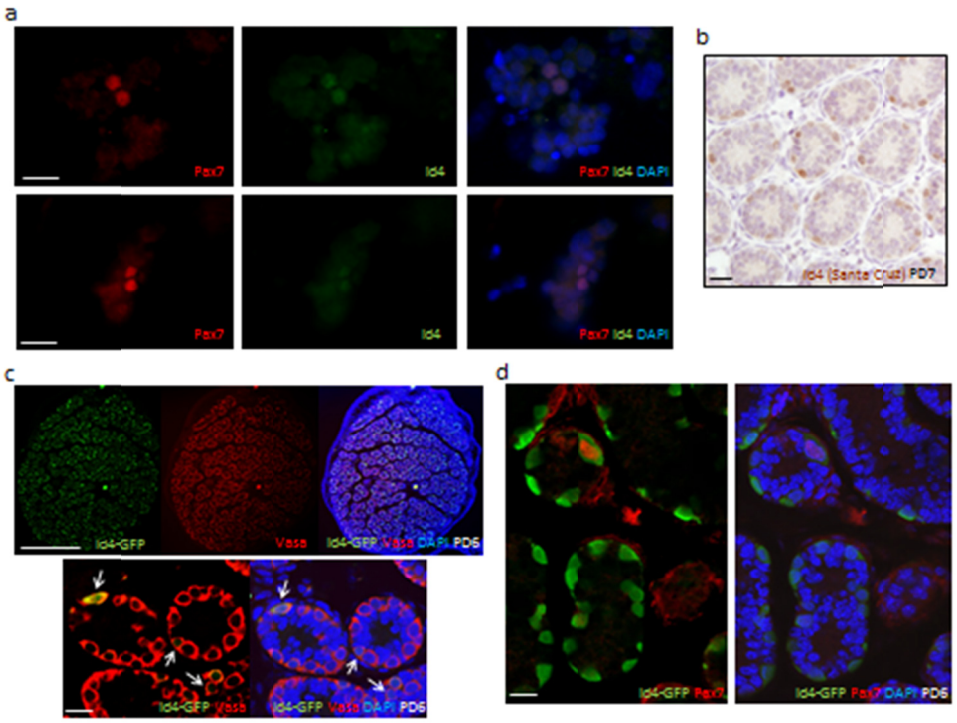

Figure 8.6: Pax7 marks a subset of Id4⁺ spermatogonia. (A) Colocalization of Pax7 and Id4 in SSC cultures. Pax7 and Id4 completely colocalized. Every Id4+ SSC also stained positive for Pax7. (B) Representative staining of Id4 on PD7 testis. (C) Id4-GFP is expressed in a subset of germ cells. (D) Pax7 is expressed in a subset of Id4-GFP+ prospermatogonia. Scale = 25μm, except (C) which is 500μm.

REFERENCES:

1. Kumar V, Abbas AK, Fausto N, and Mitchell R. Robbins Basic Pathology, 8th Edition. 2007.
2. Huber GC, and Curtis GM. The morphology of the seminiferous tubules of mammalia. *The Anatomical record.* 1913;7(6):207-19.
3. Culty M. Gonocytes, the forgotten cells of the germ cell lineage. *Birth defects research Part C, Embryo today : reviews.* 2009;87(1):1-26.
4. Lawson KA, Dunn NR, Roelen BA, Zeinstra LM, Davis AM, Wright CV, Korving JP, and Hogan BL. Bmp4 is required for the generation of primordial germ cells in the mouse embryo. *Genes Dev.* 1999;13(4):424-36.
5. Tres LL, Rosselot C, and Kierszenbaum AL. Primordial germ cells: what does it take to be alive? *Molecular reproduction and development.* 2004;68(1):1-4.
6. Ginsburg M, Snow MH, and McLaren A. Primordial germ cells in the mouse embryo during gastrulation. *Development.* 1990;110(2):521-8.
7. Richardson BE, and Lehmann R. Mechanisms guiding primordial germ cell migration: strategies from different organisms. *Nature reviews Molecular cell biology.* 2010;11(1):37-49.
8. Kobayashi H, Sakurai T, Miura F, Imai M, Mochiduki K, Yanagisawa E, Sakashita A, Wakai T, Suzuki Y, Ito T, et al. High-resolution DNA methylome analysis of primordial germ cells identifies gender-specific reprogramming in mice. *Genome research.* 2013;23(4):616-27.

9. Culty M. Gonocytes, from the fifties to the present: is there a reason to change the name? *Biol Reprod.* 2013;89(2):46.

10. McCarrey JR. Toward a more precise and informative nomenclature describing fetal and neonatal male germ cells in rodents. *Biol Reprod.* 2013;89(2):47.

11. Hilscher B, Hilscher W, Bulthoff-Ohnolz B, Kramer U, Birke A, Pelzer H, and Gauss G. Kinetics of gametogenesis. I. Comparative histological and autoradiographic studies of oocytes and transitional prospermatogonia during oogenesis and prespermatogenesis. *Cell and tissue research.* 1974;154(4):443-70.

12. McLaren A. Primordial germ cells in the mouse. *Dev Biol.* 2003;262(1):1-15.

13. Phillips BT, Gassei K, and Orwig KE. Spermatogonial stem cell regulation and spermatogenesis. *Philosophical transactions of the Royal Society of London Series B, Biological sciences.* 2010;365(1546):1663-78.

14. Goertz MJ, Wu Z, Gallardo TD, Hamra FK, and Castrillon DH. Foxo1 is required in mouse spermatogonial stem cells for their maintenance and the initiation of spermatogenesis. *J Clin Invest.* 2011;121(9):3456-66.

15. Ohbo K, Yoshida S, Ohmura M, Ohneda O, Ogawa T, Tsuchiya H, Kuwana T, Kehler J, Abe K, Scholer HR, et al. Identification and characterization of stem cells in prepubertal spermatogenesis in mice. *Developmental biology.* 2003;258(1):209-25.

16. de Rooij DG, and Russell LD. All you wanted to know about spermatogonia but were afraid to ask. *J Androl.* 2000;21(6):776-98.

17. de Rooij DG. Proliferation and differentiation of spermatogonial stem cells. *Reproduction.* 2001;121(3):347-54.

18. Oatley MJ, Kaucher AV, Racicot KE, and Oatley JM. Inhibitor of DNA binding 4 is expressed selectively by single spermatogonia in the male germline and regulates the self-renewal of spermatogonial stem cells in mice. *Biol Reprod.* 2011;85(2):347-56.

19. Abid SN, Richardson TE, Powell HM, Jaichander P, Chaudhary J, Chapman KM, and Hamra FK. A-single spermatogonia heterogeneity and cell cycles synchronize with rat seminiferous epithelium stages VIII-IX. *Biol Reprod.* 2014;90(2):32.

20. Aloisio GM, Nakada Y, Saatcioglu HD, Pena CG, Baker MD, Tarnawa ED, Mukherjee J, Manjunath H, Bugde A, Sengupta AL, et al. PAX7 expression defines germline stem cells in the adult testis. *J Clin Invest.* 2014.

21. Viglietto G, Dolci S, Bruni P, Baldassarre G, Chiariotti L, Melillo RM, Salvatore G, Chiappetta G, Sferratore F, Fusco A, et al. Glial cell line-derived neutrotrophic factor and neurturin can act as paracrine growth factors stimulating DNA synthesis of Ret-expressing spermatogonia. *International journal of oncology.* 2000;16(4):689-94.

22. Buaas FW, Kirsh AL, Sharma M, McLean DJ, Morris JL, Griswold MD, de Rooij DG, and Braun RE. Plzf is required in adult male germ cells for stem cell self-renewal. *Nat Genet.* 2004;36(6):647-52.

23. Nagano MC. Homing efficiency and proliferation kinetics of male germ line stem cells following transplantation in mice. *Biol Reprod.* 2003;69(2):701-7.

24. Ebata KT, Zhang X, and Nagano MC. Expression patterns of cell-surface molecules on male germ line stem cells during postnatal mouse development. *Molecular reproduction and development.* 2005;72(2):171-81.

25. Hirayanagi Y, Qu N, Hirai S, Naito M, Terayama H, Hayashi S, Hatayama N, Kuramasu M, Ogawa Y, and Itoh M. Busulfan pretreatment for transplantation of rat spermatogonia differentially affects immune and reproductive systems in male recipient mice. *Anatomical science international.* 2014.

26. Chan F, Oatley MJ, Kaucher AV, Yang QE, Bieberich CJ, Shashikant CS, and Oatley JM. Functional and molecular features of the Id4+ germline stem cell population in mouse testes. *Genes Dev.* 2014;28(12):1351-62.

27. Kubota H, Avarbock MR, and Brinster RL. Growth factors essential for self-renewal and expansion of mouse spermatogonial stem cells. *Proceedings of the National Academy of Sciences of the United States of America.* 2004;101(47):16489-94.

28. Oatley JM, Avarbock MR, Telaranta AI, Fearon DT, and Brinster RL. Identifying genes important for spermatogonial stem cell self-renewal and survival. *Proc Natl Acad Sci U S A.* 2006;103(25):9524-9.

29. Chapman KM, Medrano GA, Jaichander P, Chaudhary J, Waits AE, Nobrega MA, Hotaling JM, Ober C, and Hamra FK. Targeted Germline Modifications in Rats Using CRISPR/Cas9 and Spermatogonial Stem Cells. *Cell reports.* 2015;10(11):1828-35.

30. Dohle GR. Male infertility in cancer patients: Review of the literature. *Int J Urol.* 2010;17(4):327-31.

31. Howell SJ, and Shalet SM. Spermatogenesis after cancer treatment: damage and recovery. *Journal of the National Cancer Institute Monographs.* 200534):12-7.

32. Drumond AL, Weng CC, Wang G, Chiarini-Garcia H, Eras-Garcia L, and Meistrich ML. Effects of multiple doses of cyclophosphamide on mouse testes: accessing the germ cells lost, and the functional damage of stem cells. *Reproductive toxicology.* 2011;32(4):395-406.

33. Lu CC, Meistrich ML, and Thames HD, Jr. Survival of mouse testicular stem cells after gamma of neutron irradiation. *Radiation research.* 1980;81(3):402-15.

34. Bucci LR, and Meistrich ML. Effects of busulfan on murine spermatogenesis: cytotoxicity, sterility, sperm abnormalities, and dominant lethal mutations. *Mutation research.* 1987;176(2):259-68.

35. Brinster RL, and Zimmermann JW. Spermatogenesis following male germ-cell transplantation. *Proc Natl Acad Sci U S A.* 1994;91(24):11298-302.

36. Zohni K, Zhang X, Tan SL, Chan P, and Nagano MC. The efficiency of male fertility restoration is dependent on the recovery kinetics of spermatogonial stem cells after cytotoxic treatment with busulfan in mice. *Human reproduction.* 2012;27(1):44-53.

37. Seale P, Sabourin LA, Girgis-Gabardo A, Mansouri A, Gruss P, and Rudnicki MA. Pax7 is required for the specification of myogenic satellite cells. *Cell.* 2000;102(6):777-86.

38. Chang NC, and Rudnicki MA. Satellite cells: the architects of skeletal muscle. *Current topics in developmental biology.* 2014;107(161-81.

39. Mauro A. Satellite cell of skeletal muscle fibers. *The Journal of biophysical and biochemical cytology.* 1961;9(493-5.

40. Lagha M, Sato T, Bajard L, Daubas P, Esner M, Montarras D, Relaix F, and Buckingham M. Regulation of skeletal muscle stem cell behavior by Pax3 and Pax7. *Cold Spring Harbor symposia on quantitative biology.* 2008;73(307-15.

41. Relaix F, Rocancourt D, Mansouri A, and Buckingham M. A Pax3/Pax7-dependent population of skeletal muscle progenitor cells. *Nature.* 2005;435(7044):948-53.

42. Relaix F, Montarras D, Zaffran S, Gayraud-Morel B, Rocancourt D, Tajbakhsh S, Mansouri A, Cumano A, and Buckingham M. Pax3 and Pax7 have distinct and overlapping functions in adult muscle progenitor cells. *J Cell Biol.* 2006;172(1):91-102.

43. Relaix F, Rocancourt D, Mansouri A, and Buckingham M. Divergent functions of murine Pax3 and Pax7 in limb muscle development. *Genes Dev.* 2004;18(9):1088-105.

44. Buckingham M, and Relaix F. The role of Pax genes in the development of tissues and organs: Pax3 and Pax7 regulate muscle progenitor cell functions. *Annual review of cell and developmental biology.* 2007;23(645-73.

45. Engleka KA, Gitler AD, Zhang M, Zhou DD, High FA, and Epstein JA. Insertion of Cre into the Pax3 locus creates a new allele of Splotch and identifies unexpected Pax3 derivatives. *Dev Biol.* 2005;280(2):396-406.

46. Mansouri A. The role of Pax3 and Pax7 in development and cancer. *Crit Rev Oncog.* 1998;9(2):141-9.

47. Oustanina S, Hause G, and Braun T. Pax7 directs postnatal renewal and propagation of myogenic satellite cells but not their specification. *The EMBO journal.* 2004;23(16):3430-9.

48. Murdoch B, DelConte C, and Garcia-Castro MI. Pax7 lineage contributions to the mammalian neural crest. *PLoS One.* 2012;7(7):e41089.

49. Murdoch B, DelConte C, and Garcia-Castro MI. Embryonic Pax7-expressing progenitors contribute multiple cell types to the postnatal olfactory epithelium. *The Journal of neuroscience : the official journal of the Society for Neuroscience.* 2010;30(28):9523-32.

50. Lepper C, Partridge TA, and Fan CM. An absolute requirement for Pax7-positive satellite cells in acute injury-induced skeletal muscle regeneration. *Development.* 2011;138(17):3639-46.

51. Sambasivan R, Yao R, Kissenpfennig A, Van Wittenberghe L, Paldi A, Gayraud-Morel B, Guenou H, Malissen B, Tajbakhsh S, and Galy A. Pax7-expressing satellite cells are indispensable for adult skeletal muscle regeneration. *Development.* 2011;138(17):3647-56.

52. Lepper C, Conway SJ, and Fan CM. Adult satellite cells and embryonic muscle progenitors have distinct genetic requirements. *Nature.* 2009;460(7255):627-31.

53. Von Maltzahn J, Jones AE, Parks RJ, and Rudnicki MA. Pax7 is critical for the normal function of satellite cells in adult skeletal muscle. *Proc Natl Acad Sci U S A.* 2013;110(41):16474-9.

54. Hajar R. Animal testing and medicine. *Heart views : the official journal of the Gulf Heart Association.* 2011;12(1):42.

55. Rosenthal N, and Brown S. The mouse ascending: perspectives for human-disease models. *Nat Cell Biol.* 2007;9(9):993-9.

56. Nguyen D, and Xu T. The expanding role of mouse genetics for understanding human biology and disease. *Dis Model Mech.* 2008;1(1):56-66.

57. Hanahan D, Wagner EF, and Palmiter RD. The origins of oncomice: a history of the first transgenic mice genetically engineered to develop cancer. *Genes Dev.* 2007;21(18):2258-70.

58. Sauer B, and Henderson N. Site-specific DNA recombination in mammalian cells by the Cre recombinase of bacteriophage P1. *Proc Natl Acad Sci U S A.* 1988;85(14):5166-70.

59. Leone DP, Genoud S, Atanasoski S, Grausenburger R, Berger P, Metzger D, Macklin WB, Chambon P, and Suter U. Tamoxifen-inducible glia-specific Cre mice for somatic mutagenesis in oligodendrocytes and Schwann cells. *Molecular and cellular neurosciences.* 2003;22(4):430-40.

60. Friedrich G, and Soriano P. Promoter traps in embryonic stem cells: a genetic screen to identify and mutate developmental genes in mice. *Genes Dev.* 1991;5(9):1513-23.

61. Gallardo T, Shirley L, John GB, and Castrillon DH. Generation of a germ cell-specific mouse transgenic Cre line, Vasa-Cre. *Genesis.* 2007;45(6):413-7.

62. John GB, Gallardo TD, Shirley LJ, and Castrillon DH. Foxo3 is a PI3K-dependent molecular switch controlling the initiation of oocyte growth. *Dev Biol.* 2008;321(1):197-204.

63. Lecureuil C, Fontaine I, Crepieux P, and Guillou F. Sertoli and granulosa cell-specific Cre recombinase activity in transgenic mice. *Genesis.* 2002;33(3):114-8.

64. Keller C, Hansen MS, Coffin CM, and Capecchi MR. Pax3:Fkhr interferes with embryonic Pax3 and Pax7 function: implications for alveolar rhabdomyosarcoma cell of origin. *Genes Dev.* 2004;18(21):2608-13.

65. Murphy M, and Kardon G. Origin of vertebrate limb muscle: the role of progenitor and myoblast populations. *Current topics in developmental biology.* 2011;96(1-32.

66. Soriano P. Generalized lacZ expression with the ROSA26 Cre reporter strain. *Nat Genet.* 1999;21(1):70-1.

67. Madisen L, Zwingman TA, Sunkin SM, Oh SW, Zariwala HA, Gu H, Ng LL, Palmiter RD, Hawrylycz MJ, Jones AR, et al. A robust and high-throughput Cre reporting and characterization system for the whole mouse brain. *Nature neuroscience.* 2010;13(1):133-40.

68. Muzumdar MD, Tasic B, Miyamichi K, Li L, and Luo L. A global double-fluorescent Cre reporter mouse. *Genesis.* 2007;45(9):593-605.

69. Jockusch H, Voigt S, and Eberhard D. Localization of GFP in frozen sections from unfixed mouse tissues: immobilization of a highly soluble marker protein by formaldehyde vapor. *The journal of histochemistry and cytochemistry : official journal of the Histochemistry Society.* 2003;51(3):401-4.

70. Kusser KL, and Randall TD. Simultaneous detection of EGFP and cell surface markers by fluorescence microscopy in lymphoid tissues. *The journal of histochemistry and cytochemistry : official journal of the Histochemistry Society.* 2003;51(1):5-14.

71. van den Pol AN, and Ghosh PK. Selective neuronal expression of green fluorescent protein with cytomegalovirus promoter reveals entire neuronal arbor in transgenic mice. *The Journal of neuroscience : the official journal of the Society for Neuroscience.* 1998;18(24):10640-51.

72. Sullivan KF, Kay SA, and American Society for Cell Biology. *Green fluorescent proteins.* San Diego ; London: Academic Press; 1999.

73. Joosen L, Hink MA, Gadella TW, Jr., and Goedhart J. Effect of fixation procedures on the fluorescence lifetimes of Aequorea victoria derived fluorescent proteins. *Journal of microscopy.* 2014;256(3):166-76.

74. Chapman SC, Lawson A, Macarthur WC, Wiese RJ, Loechel RH, Burgos-Trinidad M, Wakefield JK, Ramabhadran R, Mauch TJ, and Schoenwolf GC.

Ubiquitous GFP expression in transgenic chickens using a lentiviral vector. *Development.* 2005;132(5):935-40.

75. Gunther S, Kim J, Kostin S, Lepper C, Fan CM, and Braun T. Myf5-positive satellite cells contribute to Pax7-dependent long-term maintenance of adult muscle stem cells. *Cell Stem Cell.* 2013;13(5):590-601.

76. Yang Y, Chang BH, Yechoor V, Chen W, Li L, Tsai MJ, and Chan L. The Kruppel-like zinc finger protein GLIS3 transactivates neurogenin 3 for proper fetal pancreatic islet differentiation in mice. *Diabetologia.* 2011;54(10):2595-605.

77. Li G, Robinson GW, Lesche R, Martinez-Diaz H, Jiang Z, Rozengurt N, Wagner KU, Wu DC, Lane TF, Liu X, et al. Conditional loss of PTEN leads to precocious development and neoplasia in the mammary gland. *Development.* 2002;129(17):4159-70.

78. Mora A, Davies AM, Bertrand L, Sharif I, Budas GR, Jovanovic S, Mouton V, Kahn CR, Lucocq JM, Gray GA, et al. Deficiency of PDK1 in cardiac muscle results in heart failure and increased sensitivity to hypoxia. *The EMBO journal.* 2003;22(18):4666-76.

79. Falciatori I, Lillard-Wetherell K, Wu Z, Hamra FK, and Garbers DL. Deriving mouse spermatogonial stem cell lines. *Methods Mol Biol.* 2008;450(181-92.

80. Gallardo TD, John GB, Shirley L, Contreras CM, Akbay EA, Haynie JM, Ward SE, Shidler MJ, and Castrillon DH. Genomewide discovery and classification of candidate ovarian fertility genes in the mouse. *Genetics.* 2007;177(1):179-94.

81. Namekawa SH, Park PJ, Zhang LF, Shima JE, McCarrey JR, Griswold MD, and Lee JT. Postmeiotic sex chromatin in the male germline of mice. *Curr Biol.* 2006;16(7):660-7.

82. Naughton CK, Jain S, Strickland AM, Gupta A, and Milbrandt J. Glial cell-line derived neurotrophic factor-mediated RET signaling regulates spermatogonial stem cell fate. *Biol Reprod.* 2006;74(2):314-21.

83. Azzato EM, Driver KE, Lesueur F, Shah M, Greenberg D, Easton DF, Teschendorff AE, Caldas C, Caporaso NE, and Pharoah PD. Effects of common germline genetic variation in cell cycle control genes on breast cancer survival: results from a population-based cohort. *Breast cancer research : BCR.* 2008;10(3):R47.

84. Bergsagel PL, Kuehl WM, Zhan F, Sawyer J, Barlogie B, and Shaughnessy J, Jr. Cyclin D dysregulation: an early and unifying pathogenic event in multiple myeloma. *Blood.* 2005;106(1):296-303.

85. Lopez-Beltran A, Requena MJ, Luque RJ, Alvarez-Kindelan J, Quintero A, Blanca AM, Rodriguez ME, Siendones E, and Montironi R. Cyclin D3 expression in primary Ta/T1 bladder cancer. *J Pathol.* 2006;209(1):106-13.

86. Beumer TL, Roepers-Gajadien HL, Gademan IS, Kal HB, and de Rooij DG. Involvement of the D-type cyclins in germ cell proliferation and differentiation in the mouse. *Biol Reprod.* 2000;63(6):1893-8.

87. Zhang Q, Wang X, and Wolgemuth DJ. Developmentally regulated expression of cyclin D3 and its potential in vivo interacting proteins during murine gametogenesis. *Endocrinology.* 1999;140(6):2790-800.

88. Kang MJ, Kim MK, Terhune A, Park JK, Kim YH, and Koh GY. Cytoplasmic localization of cyclin D3 in seminiferous tubules during testicular development. *Exp Cell Res.* 1997;234(1):27-36.

89. Diehl JA. The cyclin D3 knockout: a pound of redundancy with a dash of tissue specificity. *Cancer biology & therapy.* 2004;3(2):162-4.

90. Gorry P, Lufkin T, Dierich A, Rochette-Egly C, Decimo D, Dolle P, Mark M, Durand B, and Chambon P. The cellular retinoic acid binding protein I is dispensable. *Proc Natl Acad Sci U S A.* 1994;91(19):9032-6.

91. Lampron C, Rochette-Egly C, Gorry P, Dolle P, Mark M, Lufkin T, LeMeur M, and Chambon P. Mice deficient in cellular retinoic acid binding protein II (CRABPII) or in both CRABPI and CRABPII are essentially normal. *Development.* 1995;121(2):539-48.

92. Gasi Tandefelt D, Boormans J, Hermans K, and Trapman J. ETS fusion genes in prostate cancer. *Endocrine-related cancer.* 2014;21(3):R143-52.

93. Wang S, Kollipara RK, Srivastava N, Li R, Ravindranathan P, Hernandez E, Freeman E, Humphries CG, Kapur P, Lotan Y, et al. Ablation of the oncogenic transcription factor ERG by deubiquitinase inhibition in prostate cancer. *Proc Natl Acad Sci U S A.* 2014;111(11):4251-6.

94. Kang HS, Beak JY, Kim YS, Herbert R, and Jetten AM. Glis3 is associated with primary cilia and Wwtr1/TAZ and implicated in polycystic kidney disease. *Molecular and cellular biology.* 2009;29(10):2556-69.

95. Kang HS, Kim YS, ZeRuth G, Beak JY, Gerrish K, Kilic G, Sosa-Pineda B, Jensen J, Pierreux CE, Lemaigre FP, et al. Transcription factor Glis3, a novel critical

player in the regulation of pancreatic beta-cell development and insulin gene expression. *Molecular and cellular biology.* 2009;29(24):6366-79.

96. Dimitri P, Warner JT, Minton JA, Patch AM, Ellard S, Hattersley AT, Barr S, Hawkes D, Wales JK, and Gregory JW. Novel GLIS3 mutations demonstrate an extended multisystem phenotype. *European journal of endocrinology / European Federation of Endocrine Societies.* 2011;164(3):437-43.

97. Hansen TV, Hammer NA, Nielsen J, Madsen M, Dalbaeck C, Wewer UM, Christiansen J, and Nielsen FC. Dwarfism and impaired gut development in insulin-like growth factor II mRNA-binding protein 1-deficient mice. *Molecular and cellular biology.* 2004;24(10):4448-64.

98. Hammer NA, Hansen TO, Byskov AG, Rajpert-De Meyts E, Grondahl ML, Bredkjaer HE, Wewer UM, Christiansen J, and Nielsen FC. Expression of IGF-II mRNA-binding proteins (IMPs) in gonads and testicular cancer. *Reproduction.* 2005;130(2):203-12.

99. Lu Y, Selvakumar P, Ali K, Shrivastav A, Bajaj G, Resch L, Griebel R, Fourney D, Meguro K, and Sharma RK. Expression of N-myristoyltransferase in human brain tumors. *Neurochemical research.* 2005;30(1):9-13.

100. Shrivastav A, Selvakumar P, Bajaj G, Lu Y, Dimmock JR, and Sharma RK. Regulation of N-myristoyltransferase by novel inhibitor proteins. *Cell biochemistry and biophysics.* 2005;43(1):189-202.

101. Quintero-Rivera F, Leach NT, de la Chapelle A, Gusella JF, Morton CC, and Harris DJ. Is the disruption of an N-myristoyltransferase (NMT2) associated

with hypoplastic testes? *American journal of medical genetics Part A.* 2007;143A(15):1796-8.

102. Goncalves V, Brannigan JA, Thinon E, Olaleye TO, Serwa R, Lanzarone S, Wilkinson AJ, Tate EW, and Leatherbarrow RJ. A fluorescence-based assay for N-myristoyltransferase activity. *Analytical biochemistry.* 2012;421(1):342-4.

103. Mukhopadhyay M, Teufel A, Yamashita T, Agulnick AD, Chen L, Downs KM, Schindler A, Grinberg A, Huang SP, Dorward D, et al. Functional ablation of the mouse Ldb1 gene results in severe patterning defects during gastrulation. *Development.* 2003;130(3):495-505.

104. Song SH, Kim A, Ragoczy T, Bender MA, Groudine M, and Dean A. Multiple functions of Ldb1 required for beta-globin activation during erythroid differentiation. *Blood.* 2010;116(13):2356-64.

105. Quintero-Rivera F, Xi QJ, Keppler-Noreuil KM, Lee JH, Higgins AW, Anchan RM, Roberts AE, Seong IS, Fan X, Lage K, et al. MATR3 disruption in human and mouse associated with bicuspid aortic valve, aortic coarctation and patent ductus arteriosus. *Hum Mol Genet.* 2015.

106. Fifita JA, Williams KL, McCann EP, O'Brien A, Bauer DC, Nicholson GA, and Blair IP. Mutation analysis of MATR3 in Australian familial amyotrophic lateral sclerosis. *Neurobiology of aging.* 2015;36(3):1602 e1-2.

107. Senderek J, Garvey SM, Krieger M, Guergueltcheva V, Urtizberea A, Roos A, Elbracht M, Stendel C, Tournev I, Mihailova V, et al. Autosomal-dominant distal myopathy associated with a recurrent missense mutation in the gene

encoding the nuclear matrix protein, matrin 3. *American journal of human genetics.* 2009;84(4):511-8.

108. Ozturk S. Telomerase activity and telomere length in male germ cells. *Biology of reproduction.* 2015;92(2):53.

109. Relaix F, and Zammit PS. Satellite cells are essential for skeletal muscle regeneration: the cell on the edge returns centre stage. *Development.* 2012;139(16):2845-56.

110. Yin H, Price F, and Rudnicki MA. Satellite cells and the muscle stem cell niche. *Physiological reviews.* 2013;93(1):23-67.

111. Tanaka SS, Toyooka Y, Akasu R, Katoh-Fukui Y, Nakahara Y, Suzuki R, Yokoyama M, and Noce T. The mouse homolog of Drosophila Vasa is required for the development of male germ cells. *Genes Dev.* 2000;14(7):841-53.

112. Vergouwen RP, Huiskamp R, Bas RJ, Roepers-Gajadien HL, Davids JA, and de Rooij DG. Postnatal development of testicular cell populations in mice. *Journal of reproduction and fertility.* 1993;99(2):479-85.

113. Lepper C, and Fan CM. Inducible lineage tracing of Pax7-descendant cells reveals embryonic origin of adult satellite cells. *Genesis.* 2010;48(7):424-36.

114. Franca LR, Avelar GF, and Almeida FF. Spermatogenesis and sperm transit through the epididymis in mammals with emphasis on pigs. *Theriogenology.* 2005;63(2):300-18.

115. Lian G, and Enders GC. Entactin ultrastructural immunolocalization in the basal laminae of mouse seminiferous tubules and with only subtle changes following hypophysectomy. *J Androl.* 1994;15(1):52-60.

116. Meistrich ML, and Shetty G. Suppression of testosterone stimulates recovery of spermatogenesis after cancer treatment. *International journal of andrology.* 2003;26(3):141-6.

117. van Keulen CJ, and de Rooij DG. Spermatogenetic clones developing from repopulating stem cells surviving a high dose of an alkylating agent. *Cell and tissue kinetics.* 1975;8(6):543-51.

118. Enders GC, and May JJ. Developmentally regulated expression of a mouse germ cell nuclear antigen examined from embryonic day 11 to adult in male and female mice. *Dev Biol.* 1994;163(2):331-40.

119. Lu CC, and Meistrich ML. Cytotoxic effects of chemotherapeutic drugs on mouse testis cells. *Cancer Res.* 1979;39(9):3575-82.

120. Goldfarb S, Mulhall J, Nelson C, Kelvin J, Dickler M, and Carter J. Sexual and reproductive health in cancer survivors. *Seminars in oncology.* 2013;40(6):726-44.

121. Withers HR, Hunter N, Barkley HT, Jr., and Reid BO. Radiation survival and regeneration characteristics of spermatogenic stem cells of mouse testis. *Radiation research.* 1974;57(1):88-103.

122. Castrillon DH, Gonczy P, Alexander S, Rawson R, Eberhart CG, Viswanathan S, DiNardo S, and Wasserman SA. Toward a molecular genetic analysis of spermatogenesis in Drosophila melanogaster: characterization of male-sterile mutants generated by single P element mutagenesis. *Genetics.* 1993;135(2):489-505.

123. Tarnawa ED, Baker MD, Aloisio GM, Carr BR, and Castrillon DH. Gonadal expression of foxo1, but not foxo3, is conserved in diverse Mammalian species. *Biol Reprod.* 2013;88(4):103.

124. Roosen-Runge EC. Comparative aspects of spermatogenesis. *Biol Reprod.* 1969;1(Suppl 1:24-31.

125. Fuller MT. Genetic control of cell proliferation and differentiation in Drosophila spermatogenesis. *Seminars in cell & developmental biology.* 1998;9(4):433-44.

126. Kawakami A, Kimura-Kawakami M, Nomura T, and Fujisawa H. Distributions of PAX6 and PAX7 proteins suggest their involvement in both early and late phases of chick brain development. *Mechanisms of development.* 1997;66(1-2):119-30.

127. Nagano MC, and Yeh JR. The identity and fate decision control of spermatogonial stem cells: where is the point of no return? *Current topics in developmental biology.* 2013;102(61-95.

128. Yoshida S. Elucidating the identity and behavior of spermatogenic stem cells in the mouse testis. *Reproduction.* 2012;144(3):293-302.

129. Nakagawa T, Sharma M, Nabeshima Y, Braun RE, and Yoshida S. Functional hierarchy and reversibility within the murine spermatogenic stem cell compartment. *Science.* 2010;328(5974):62-7.

130. Snippert HJ, and Clevers H. Tracking adult stem cells. *EMBO Rep.* 2011;12(2):113-22.

131. Zhang Z, Shao S, and Meistrich ML. The radiation-induced block in spermatogonial differentiation is due to damage to the somatic environment, not the germ cells. *J Cell Physiol.* 2007;211(1):149-58.

132. Rojas-Rios P, and Gonzalez-Reyes A. The plasticity of stem cell niches: A general property behind tissue homeostasis and repair. *Stem Cells.* 2013.

133. Barker N, van Es JH, Kuipers J, Kujala P, van den Born M, Cozijnsen M, Haegebarth A, Korving J, Begthel H, Peters PJ, et al. Identification of stem cells in small intestine and colon by marker gene Lgr5. *Nature.* 2007;449(7165):1003-7.

134. Kiel MJ, Yilmaz OH, Iwashita T, Yilmaz OH, Terhorst C, and Morrison SJ. SLAM family receptors distinguish hematopoietic stem and progenitor cells and reveal endothelial niches for stem cells. *Cell.* 2005;121(7):1109-21.

135. de Lau W, Barker N, Low TY, Koo BK, Li VS, Teunissen H, Kujala P, Haegebarth A, Peters PJ, van de Wetering M, et al. Lgr5 homologues associate with Wnt receptors and mediate R-spondin signalling. *Nature.* 2011;476(7360):293-7.

136. Wang N, Satoskar A, Faubion W, Howie D, Okamoto S, Feske S, Gullo C, Clarke K, Sosa MR, Sharpe AH, et al. The cell surface receptor SLAM controls T cell and macrophage functions. *The Journal of experimental medicine.* 2004;199(9):1255-64.

137. Drach J, Zhao S, Drach D, Korbling M, Engel H, and Andreeff M. Expression of MDR1 by normal bone marrow cells and its implication for leukemic hematopoiesis. *Leukemia & lymphoma.* 1995;16(5-6):419-24.

138. Petriz J. Flow cytometry of the side population (SP). *Current protocols in cytometry / editorial board, J Paul Robinson, managing editor [et al].* 2013;Chapter 9(Unit9 23.

139. Garcia TX, and Hofmann MC. NOTCH signaling in Sertoli cells regulates gonocyte fate. *Cell cycle.* 2013;12(16):2538-45.

140. Garcia TX, DeFalco T, Capel B, and Hofmann MC. Constitutive activation of NOTCH1 signaling in Sertoli cells causes gonocyte exit from quiescence. *Developmental biology.* 2013;377(1):188-201.

141. Shinohara T, Orwig KE, Avarbock MR, and Brinster RL. Spermatogonial stem cell enrichment by multiparameter selection of mouse testis cells. *Proc Natl Acad Sci U S A.* 2000;97(15):8346-51.

142. Zhou Q, Nie R, Li Y, Friel P, Mitchell D, Hess RA, Small C, and Griswold MD. Expression of stimulated by retinoic acid gene 8 (Stra8) in spermatogenic cells induced by retinoic acid: an in vivo study in vitamin A-sufficient postnatal murine testes. *Biol Reprod.* 2008;79(1):35-42.

143. Niedenberger BA, Busada JT, and Geyer CB. Marker expression reveals heterogeneity of spermatogonia in the neonatal mouse testis. *Reproduction.* 2015;149(4):329-38.

144. Dann CT, Alvarado AL, Molyneux LA, Denard BS, Garbers DL, and Porteus MH. Spermatogonial stem cell self-renewal requires OCT4, a factor downregulated during retinoic acid-induced differentiation. *Stem Cells.* 2008;26(11):2928-37.

145. Aponte PM, de Rooij DG, and Bastidas P. Testicular development in Brahman bulls. *Theriogenology.* 2005;64(6):1440-55.

146. Takashima S, Kanatsu-Shinohara M, Tanaka T, Morimoto H, Inoue K, Ogonuki N, Jijiwa M, Takahashi M, Ogura A, and Shinohara T. Functional Differences between GDNF-Dependent and FGF2-Dependent Mouse Spermatogonial Stem Cell Self-Renewal. *Stem cell reports.* 2015;4(3):489-502.